Journal Of Applied Chemistry

Vol. 24 No. 7

TREATING MANGANESE SLUDGES AND ORES WITH SULFUR DIOXIDE[1]

V. M. Kakabadze

The S. M. Kirov Polytechnic Institute of Georgia

Treating Manganese Carbonate Ores With Sulfur Dioxide

Manganese carbonates are lean ores, containing little metallic manganese. As a result they are of slight industrial importance. But their comparatively low manganese content cannot serve as an obstacle to the efficient utilization of these ores.

It should be noted that not much work has been done on the physicochemical investigation of manganese carbonate ores up to now. The reaction of manganese carbonate ores with sulfuric acid has been better explored [1]. It is considered certain that treating these ores in water with sulfur dioxide yields manganese sulfite to begin with, which is then converted into manganese sulfate by oxidation with atmospheric oxygen:

$$MnCO_3 + SO_2 \longrightarrow MnSO_3 + CO_2, \quad (1)$$

$$MnSO_3 + {}^1/_2\, O_2 \longrightarrow MnSO_4. \quad (2)$$

But the research work already done on the treatment of manganese carbonate ores with sulfur dioxide shows that this type of extraction of manganese is highly unsatisfactory (the rate being extremely low), and that the ore must be roasted first when this process is to be utilized industrially [2,3,4]. Some researchers believe, moreover, that the percentage of manganese that dissolves is only slightly dependent upon the coarseness of the ore grains.

We set as our objective a study of the conditions governing the extraction of manganese from manganese carbonate ores.

EXPERIMENTAL

Manganese carbonate ores Nos. 11 and 12, the per cent composition of which is given below, were used in the research.

Ore No. 11. Roasting losses: 34.08, SiO_2 4.16, Al_2O_3 2.66, Fe_2O_3 0.89, MnO 24.32, (ΣMn 18.86), CaO 30.81, MgO 1.77, SO_3 1.45, P_2O_5 0.55, moisture 1.68%.

Ore No. 12. Roasting losses: 29.78%, SiO_2 7.57, Al_2O_3 1.65, Fe_2O_3 1.33, MnO 21.49, (ΣMn 16.66), CaO 33.18, MgO 2.68, SO_3 1.60, P_2O_5 0.48, moisture 1.32%.

[1]) T. A. Ivanova assisted in the experimental work.

The apparatus described previously [5] was used in our experiments.

We began with tests of the carbonate ore No. 11. All the ore samples used in these tests weighed 10 g. The percentages of manganese dithionate and sulfate were calculated from the sum (ΣMn), taken as 100.

Effect of various factors upon the extraction of mangarese from manganese carbonate ores

The data illustrating the effect of fineness of grind upon the process are shown in Fig. 1.

The results of tests of the effect of time upon the process are shown in Fig. 2.

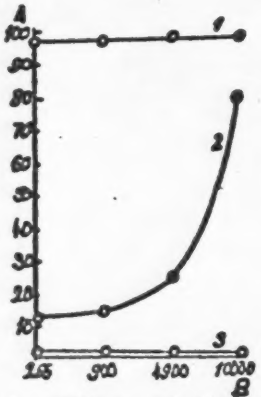

Fig. 1. Effect of fineness of grind upon the extraction of manganese from manganese carbonate ores. Temperature: 80 deg; time: 30 minutes; solid factor: 0.1; SO_2 concentration: 11.6—12%; SO_2 put through: 5 liters.
A —Per cent manganese dissolved;
B —fineness of grind (holes per sq cm). 1 - $MnSO_4$; 2 — ΣMn;
3 —MnS_2O_6.

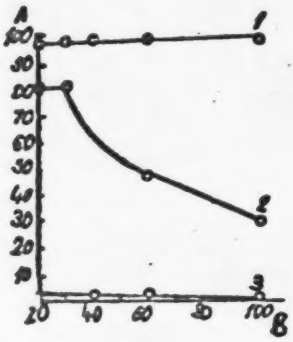

Fig. 2. Effect of time on the extraction of manganese from manganese carbonate ores. Temperature: 80 deg, fineness of grind: 10,000 holes per sq cm; solid factor: 0.1; SO_2 concentration: 12.72-14.97%; SO_2 put through: 5-5.5 liters.
A —Per cent manganese dissolved,
B —time, minutes. 1 — $MnSO_4$;
2 — ΣMn; 3 —MnS_2O_6.

We then ran tests to learn the variation of the lixiviation of manganese with the fineness of grind under the following conditions: temperature. 80 deg; SO_2 concentration: 13.0%; solid factor: 0.1; and SO_2 put through: 5 liters.

Our results are shown in Figs. 3 and 4.

The results of these tests indicate that more manganese is extracted as the fineness of grind is increased, the per cent extraction being substantial at a fineness of 10,000 holes per sq. cm. No more than 20-30 minutes is required for the lixiviation process under the conditions we have employed, so that the reaction rate is high.

It is typical that the per cent manganese dissolved falls off when the time is prolonged beyond 20-30 minutes. This evidently results in the formation of coordination compounds.

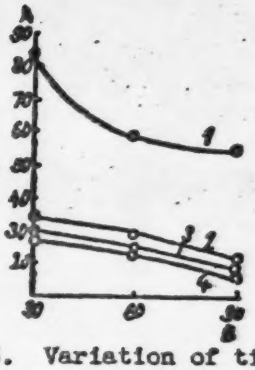

Fig. 3. Variation of time and per cent extraction of manganese from manganese carbonate ores with the fineness of grind. A - Per cent manganese dissolved; B - time, minutes. Fineness of grind (holes per sq cm): 1 - 10,000; 2 - 2500; 3 - 900; 4 - 400.

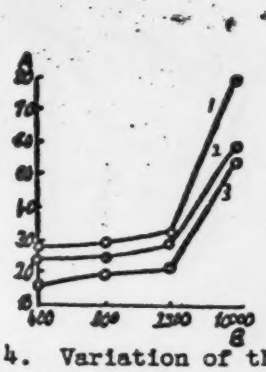

Fig. 4. Variation of the per cent extraction of manganese with the fineness of grind and the time.
A - Per cent manganese dissolved; B - fineness of grind (holes per sq cm). Time, minutes: 1 - 30; 2 - 60; 3 - 120.

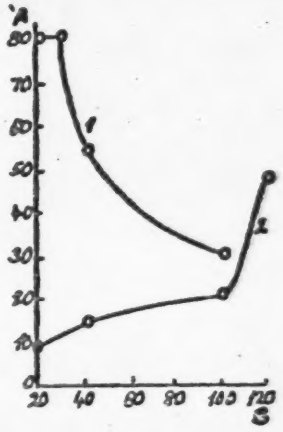

Fig. 5. Effect of time upon the extraction of manganese from various carbonate ores. A - Per cent manganese dissolved; B - time, minutes. 1 - Carbonate ore No. 11; 2 - carbonate ore No. 12.

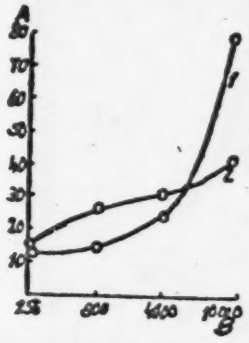

Fig. 6. Effect of fineness of grind upon the extraction of manganese from various carbonate ores.
A - Per cent manganese dissolved; B - fineness of grind (holes per sq cm). 1 - Carbonate ore No. 11; 2 - carbonate ore No. 12.

The data on the effect of temperature are listed in Table 1.

TABLE 1

Effect of Temperature Upon the Extraction of Manganese from Manganese Carbonate Ores

Time: 30 minutes; fineness of grind: 10,000 holes per sq cm; solid factor: 0.1; SO_2 concentration: 12.72-13.14%; SO_2 put through: 5 liters.

Temperature, (°C)	Grams dissolved			Per cent dissolved		
	ΣMn	Mn dithionate	Mn sulfate	ΣMn	Mn dithionate	Mn sulfate
20	1.4917	0.0683	1.4234	80.45	4.59	95.41
40	1.4917	0.0659	1.4358	80.45	4.42	95.58
60	1.4917	0.0476	1.4441	80.45	3.18	96.82
80	1.4917	0.0207	1.4710	80.45	1.38	98.62

TABLE 2

Effect of the Solid Factor Upon the Extraction of Manganese from Manganese Carbonate Ores

Temperature: 80°; Time: 30 minutes; fineness of grind: 10,000 holes per sq cm; SO_2 concentration: 10.5%; SO_2 put through: 5 liters.

Grams of ore	Ml of water	Grams dissolved			Per cent dissolved		
		ΣMn	Mn dithionate	Mn sulfate	ΣMn	Mn dithionate	Mn sulfate
10	25	0.3895	0.0108	0.3787	20.00	2.79	97.21
10	50	0.5908	0.0108	0.3787	31.86	1.83	98.17
10	75	0.7790	0.0170	0.7620	42.01	2.18	97.82
10	100	1.4917	0.0207	1.4710	80.45	1.38	98.62

As these figures show, raising the temperature from 20 to 80° does not increase the manganese extraction, the extraction being satisfactory even below 20°, which is an indication that the process is efficient even at low temperatures. As in the preceding tests, raising the temperature increases the percentage of manganese sulfate and diminishes the percentage of the manganese dithionate.

The results of our experiments on the effect of the solid factor are given in Table 2.

Varying the solid factor from 0.4. to 0.1, i.e., increasing the dilution, increases the percentage of manganese entering solution, the 1: 10 dilution yielding results that are satisfactory.

As the solution is diluted, the percentage of manganese sulfate rises, the percentage of manganese dithionate falling accordingly. In general, it should be noted that when manganese carbonate ores are processed with sulfur dioxide, the amount of manganese dithionate is too small to be accorded practical consideration.

When manganese carbonate ores are processed with sulfur dioxide, the dissolution of the manganese is accompanied by that of calcium as $CaSO_4$, which subsequently settles out as a white precipitate when the filtrate cools.

The dissolution of the $CaSO_4$ (and hence its subsequent precipitation) depends upon the amount of water used, more of the calcium sulfate entering solution at higher dilutions.

We then ran tests with samples of the No.12 ore to learn the effect of time and fineness of grind upon the process. The test results indicated that the percentage of manganese in the No.12 ore that entered solution increased with time, while the percentage of the manganese dithionate fell and that of the manganese sulfate rose.

As in the preceding cases, increasing the fineness of grind resulted in raising the percentage of manganese dithionate in the solution. Apparently, much more dithionate is formed as the fineness of grind of the ore is increased, i.e., the reation surface of the particles is increased, the subsequent process of its decomposition being less intense under the conditions employed in our experiments (determination of temperature, time, medium acidity, etc.) than that in the first process.

The findings of these latter tests are contrasted with those in the preceding ones (with No.11 ore) in Figs.5 and 6.

As we see in Figs. 5 and 6, the effect of time upon the extraction of manganese is different in the No.11 and No.12 ores. Fineness of grind has a favorable effect upon the extraction of manganese from carbonate ores, though the results of manganese extraction from the ore are much more satisfactory with the No.11 ore at a high fineness of grind (10,000 holes per sq cm).

As we see from a comparison of the findings secured in the processing of the No.11 and 12 manganese carbonate ores, they behave differently. Whereas No.11 ore is readily lixiviated by sulfur dioxide at a suitably fine grind, without preliminary roasting, the No.12 ore yields less satisfactory results under these same conditions.

We ran tests to determine the completeness of manganese extraction from the No.11 manganese carbonate ore. The ore was processed twice with sulfur dioxide, the latter being employed in excess (the Mn/SO_2 ratio being 1:2.6 in Test No.1.

The test results are listed in Table 3.

TABLE 3

Extraction of Manganese From No.11 Carbonate Ore by Treating it twice with an excess of Sulfur Dioxide.

Temperature: 80° solid factor:0.1; fineness of grind: 10,000 holes per sq cm; SO_2 concentration: 14-15%

Time, minutes.	Liters of SO_2 put through	Manganese dissolved.	
		Grams	per cent
30	13	1.4777	79.70
20	7	0.3688	19.89
			99.59

As we see from the figures in Table 3, treating this manganese carbonate ore with an excess of sulfur dioxide twice is quite adequate to secure a nearly 100% extraction of the manganese.

We then ran tests to determine the completeness of manganese extraction from the unroasted No.12 carbonate ore, at a comparatively coarse grind, by repeatedly processing the same 10 gram sample of ore. In one series of tests the concentration of sulfur dioxide was high (Table 4,) and in another low (Table 5).

TABLE 4

Extraction of Manganese From No.12 Carbonate Ore by Triple Processing with Sulfur Dioxide at High Concentration.

Temperature: 80°; fineness of grind: 900 holes per sq cm;, solid factor: 0.1; SO_2 concentration: 15.01%

Time, minutes.	Liters of SO_2 put through	Manganese dissolved.	
		Grams	per cent.
30	5	0.4237	26.22.
70	15	1.0832	67.40
70	15	0.0328	2.31
			95.93

TABLE 5

Extraction of Manganese from No.12 Carbonate Ore by Repeated Processing with Sulfur Dioxide at Low Concentration.

Temperature: 80°; fineness of grind: 900 holes per sq cm; solid factor: 0.1; SO_2 concentration: 4.22-5.0%

Time, minutes.	Liters of SO_2 put through	Manganese dissolved.	
		Grams	per cent.
30	5	0.1718	10.63
70	15	0.5018	31.05
70	15	0.4583	28.36
70	15	0.2411	14.63
70	15	0.1453	8.99
70	15	0.0312	1.93
			95.59

When a high concentration of sulfur dioxide is employed under laboratory conditions, 94-95% of the manganese is extracted within 1.5 hours. When a low gas concentration is used, approximately 5 hours are required for the same per cent extraction. In general, increasing the concentration of sulfur dioxide accelerates the process.

The extraction of manganese from manganese carbonate ores is also accelerated by increasing the fineness of grindand by preliminary roasting of the ore.

Extracting manganese from a mixture of manganese carbonate ores and pyrolusite sludges.

As we have shown above, the reaction of sulfur dioxide in the liquid phase with manganese dioxide coming from oxidized ores yields manganese sulfate and weak sulfuric acid. The resultant sulfuric acid reacts with the carbonate ore, so that manganese is extracted as manganese sulfate from both the oxidized and the carbonate ores.

Instead of an oxidized ore, we took a No.17 pyrolusite sludge [5] and mixed it with the No.12 carbonate ore in the proportions of 2 parts of the carbonate ore to 3 parts of the sludge. The above-mentioned ore is hardest to process chemically. An excess of sulfur dioxide was passed through a suspension of this mixture, the ΣMn, $MnSO_4$, and MnS_2O_6 being determined in the solution.

In the first set of tests separate 10-gram samples of the foregoing mixture were used in every run. The test results are listed in Table 6.

TABLE 6

Extraction of Manganese from a Mixture of Manganese Carbonate Ore and a Pyrolusite Sludge.
Temperature: 80°; fineness of grind; 256 holes per sq cm; solid factor: 0.1.

Time, Minutes.	SO_2 concentration. %	Liters of SO_2 put through	Per cent manganese dissolved.		
			ΣMn	Mn dithionate	Mn sulfate
60	12.8	15	62.21	38.00	62.00
110	13.5	30	87.80	17.95	82.05
110	18.9	30	93.52	15.49	84.51
120	19.1	30	95.40	13.76	86.24

Then we ran tests to determine the extraction of manganese by processing the same 10-g sample of the mixture repeatedly, using the same carbonate ore-sludge ratio as in the preceding series of tests. The results are given in Table7.

TABLE 7

Extraction of Manganese by Triple Processing with Sulfur Dioxide of a Mixture of Carbonate Ore and Pyrolusite Sludge.

Temperature: 80°; fineness of grind: 256 holes per sq.cm; solid factor: 0.1; SO_2 concentration: 12.9%

Time, Minutes.	Liters of SO_2 put through	Per cent manganese dissolved.		
		ΣMn	Mn dithionate	Mn sulfate
30	7	54.82	42.56	57.44
60	15	39.24	27.84	72.16
100	30	4.88	18.49	81.51
		98.94		

The results of these tests demonstrate that it is best to extract the manganese by repeatedly processing the same mixture, the process being rather rapid at first and then slowing down. More than 95% of the manganese can be extracted if enough time is allowed. It may therefore be uneconomical to extract the last few percentage points of the manganese.

Balance Sheet of Treating Manganese Sludges with Sulfur Dioxide.

In drawing up the balance sheet of treating manganese sludges with sulfur dioxide we used No.18 pyrolusite sludge, the analysis of which has been given in [5].

50 g of the sludge was taken, and 300 ml of water, so that the solid factor was 1/6. The other test conditions were as follows: temperature: 80°; time: 220 minutes; fineness of grind: 900 holes per sq cm; SO_2 concentration: 13.98%; amount of SO_2: 60 liters. Stirring was employed during the run.

The figures for the balance sheet are given in Table 8.

TABLE 8

Balance Sheet for the Treatment of Manganese Sludges with Sulfur Dioxide.

No.	Constituents	Intake			Outgo				
		Sludge	Gas	Total	Precipitate	Solution	Gas	Discrepancy	Total
		1	2	3	4	5	6	7	8
1	SiO_2	18.344	-	18.344	18.024	0.336	-	-0.016	18.344
2	Al_2O_3	4.193	-	4.193	3.752	0.365	-	+0.076	4.193
3	Fe_2O_3	1.585	-	1.585	1.370	0.296	-	-0.081	1.585
4	CaO	1.218	-	1.218	0.932	0.238	-	+0.048	1.218
5	MgO	0.406	-	0.406	0.425	0.077	-	-0.096	0.406
6	SO_3	0.129	24.215	24.344	1.351	22.493	0.500[1]	-	24.344
7	P_2O_5	0.325	-	0.325	0.036	0.239	-	+0.050	0.325
8	BaO	1.199	-	1.199	1.132	-	-	+0.067	1.199
9	ΣMn	11.620	-	11.620	0.588	11.028	-	+0.004	11.620
10	Moisture and impurities	10.981	-	10.981	1.242	9.739[2]	-	-	10.981
	TOTAL	50.000	24.215	74.215	28.852	44.811	0.500	+0.052	74.215

No. 1 to 9 in column 1 show an incoming total of 39.0192 g; with 24.215 g in Column 2, for a total (in column 3) of 63.234 g. Under the outgoing items we have: 27.610 g in Column 4, 35.072 g in Column 5, and 0.500 g in Col.6 for a total of 63.182 g.

The quantity unaccounted for between the intake and outgo is negligible (Col.7), 0.052 g.

The figures in this balance sheet indicate that the manganese

1) Assumed (taking losses as 2%)
2) By difference.

extraction is 95%, based on the total manganese in the sludge. As we saw in the previous tests, we managed to extract some 96% of the manganese by double lixiviation from the same sludge.

In general, the extraction of manganese from oxidized ores and sluiges by means of sulfur dioxide is quite satisfactory.

The analysis data indicate that the solution contained 23.99 grams of $MnSO_4$ and 7.88 grams of MnS_2O_6. Thus there is 8.74 grams of manganese sulfate, or approximately 81%, and 2.01 grams of manganese dithionate, or approximately 19%.

Since the formation of manganese dithionate during the lixiviation of the ore with sulfur dioxide involves a number of difficulties, steps must be taken to eliminate it, and, as indicated above, the solution should be boiled thoroughly at the end of the extraction process to achieve this objective.

An excess of SO_2 must be used to achieve complete extraction. In counterflow lixiviation this excess of SO_2 will circulate in the system, but only the quantity of the gas will be consumed that is required for the reaction, except for negligible losses.

On the basis of the ΣMn contained in 1 kg of the sludge we used, 0.27 g of the gas would be required theoretically. In actuality, however, 1 kg of the sludge reconsumed 0.387 kg of sulfur dioxide in our experiments (recomputing the SO_3 as SO_2). Thus, the useful consumption of SO_2, i.e.. the percentage used in extracting the manganese, was some 69%.

The balance sheet indicates that the gas losses and the gas unaccounted for (based on SO_2) total 1.6% . Hence, some 29-30% of the SO_2 was consumed in reactions with other constituents.

We believe that the losses of sulfur dioxide should not exceed 1% in an apparatus of suitable design, appropriately gastight, with repeated lixiviation.

The consumption factor of sulfur dioxide is taken to be 0.40, i.e., 0.40 kg is used up per kg of the sludge (or an ore of similar composition).

A large amount of precipitate is thrown down when manganese sludge is processed with sulfur dioxide, totalling some 58% of the original material. The per cent composition of this precipitate is as follows:

SiO_2 65.76, Al_2O_3 12.96, Fe_2O_3 4.98, CaO 3.39, MgO 1.55, BaO 4.13, MnO 2.29, P_2O_5 0.13, SO_3 4.93.

Siliceous and clayey substances predominate in the precipitate, together with sulfates (barium, calcium, etc.,). Part of the manganese apparently did not decompose, while another part may remain in the unextracted form. This precipitate should find appropriate utilization.

Under our experimental conditions Ba does not enter solution, while extremely little of the SiO_2 dissolves.

Much of the phosphorus enters solution, although its total percentage is not high. Iron also enters solution rather readily. It should be noted that the conversion of these elements into a soluble state depends upon the dilution, much higher percentages (particulary of the phosphorus) being lixiviated in more dilute solutions.

Under our experimental conditions about 19% of the CaO and MgO dissolve. It should be borne in mind that part of these oxides enter solution as a result of the washing of the precipitate.

SUMMARY

1. Some types of manganese carbonate ores are readily processed with sulfur dioxide, and extremely short period of time being required for extracting the manganese from finely crushed ore.

2. A more or less satisfactory extraction of the manganese may be achieved from other types of manganese carbonate ores that are relatively hard to process even without a particularly great fineness of grind, provided a high concentration of sulfur dioxide or prolonged roasting is employed.

3. Manganese carbonate ores may also be treated by a combined process: a) treating the manganese dioxide contained in pyrolusite sludges or lean manganese ores with sulfur dioxide, and b) using the sulfuric acid produced during treatment to decompose the carbonates in the ore.

LITERATURE CITED

[1] V.Kakabadze, The chemical concentration of manganese ores by decomposition with sulfuric acid, Sep. Polytech. Inst. Georgia 2 (16), 34 (1945).

[2] E.Davis, Dissol.of various Manganese Mineraibs. U.S. Bureau of Mines, 3024 (1930).

[3] E.Leaver. Hydrometallurgy of Manganese. U.S. Bureau of Mines, 6770 (1934).

[4] Yu.Klimenko and A.Kvaskov. The chemical concentration of Manganese ores. Metallurgy Press (1943).

[5] V.Kakabadze, J.Appl. Chem.24, 3 (1951).[1]

Received April 8, 1948.
Resubmitted May 15, 1950.

---

[1]) See Consultants Bureau translation, p. 279.

THE EQUILIBRIUM PRESSURE OF NITROGEN OXIDES ABOVE NITROSES IN THE PRESENCE OF FREE NITRIC ACID

M.L. Varlamov.

In our previous paper [1] on the equilibrium pressure of nitrogen oxides above nitroses we compared and analyzed the published experimental data on a system in which there was no free nitric acid (H_2SO_4, H_2O, N_2O_3).

The equations derived were utilized in the construction of an alignment chart [2] for calculating the equilibrium pressure of nitrogen oxides in such a system.

We were interested in considering a more complicated system (H_2SO_4, H_2O, N_2O_3, HNO_3) containing free nitric acid. Starting out with the special features of the nitrose sulfuric acid process, let us consider the possible acid concentrations and temperatures in this process.

The sparse published experimental papers on this topic should be borne in mind; they are insufficiently generalized and occasionally contradictory.

Sanfourche and Rondier [3] have measured the equilibrium pressure of nitrogen oxides, working with nitroses with an initial strength of 56-93% H_2SO_4, containing 1.10-6.36% N_2O_3 and 0.03-3.4% HNO_3, combined and separately. The tests were run at temperatures ranging from 0 to 40°C, with individual measurements made up to 60° C. The nitrogen oxides were converted into the gas phase and then analyzed by the colorimetric method. The results cited are equivalent to dissociated N_2O_3 molecules in the gas phase.

They found that the total equilibrium pressure of the nitrogen oxides ($P_{HNSO_5} + HNO_3$) rose sharply when HNO_3 and N_2O_3 were simultaneously present in the nitrose above the sum of the individual pressure p_{HNSO_5} and p_{HNO_3}.

This was most evident in the percentage of H_2SO_4 of the strong acids, as is shown in Table 1 for acids at 30° C.

TABLE 1

Variation of $\underline{n}$ With Per Cent of H_2SO_4 in the Acid

Acid strength, per cent H_2SO_4	92.97	78	73.2
Note. $\underline{n} = \frac{P_{HNSO_5 + HNO_3}}{p_{HNSO_5} + p_{HNO_3}}$	105	9	7.4

Berl and Saenger [4] investigated three nitroses at 30 to 130° C, with initial strengths of 67, 75.65, and 78.04% of H_2SO_4 and containing 0.1 mole/liter of HNO_3 and 0.1 mole/liter of $HNSO_5$, combined and separately.

They also found that the total equilibrium pressure $P_{HNSO_5} + HNO_3$ increased for acids whose strength exceeded 70% H_2SO_4. The values of $\underline{n}$ they secured were, however, much below those found by Sanfourche and Rondier; this was particularly noticeable for the strong acids. In the case of 78% H_2SO_4, for example, they found $\underline{n}$ = 2.2 (mean value).

Kudryavtsev [5] determined the equilibrium pressure of nitrogen oxides above nitroses with an initial strength of 90% H_2SO_4, containing 0.5. to 6% N_2O_3 and 0.4% HNO_3 at temperatures ranging from 30 to 150° C, and for an acid strength of 90% H_2SO_4, containing 4.5% N_2O_3 and 0.2 to 2% HNO_3 for the same temperature range. In both cases it was found that a linear equation held good for calculating the equilibrium pressure. He also found that the combined equilibrium pressure rose substantially when HNO_3 was present in the nitrose. When the nitrose contained 0.5% N_2O_3 and 0.4% HNO_3, the equilibrium pressure was 2.16 times higher than when there was no HNO_3 in the solution.

Unfortunately his paper contains no information on the method of analysis and calculation he employed in his study of the system (H_2SO_4, H_2O, N_2O_3, HNO_3).

Kuzminykh reports [6] that Kudryavtsev determined the percentage of nitrogen oxides blown off by titrating the nitrose formed by further absorption of the oxides with permanganate, and recalculating the result in terms of N_2O_3. In view of the fact that the nitrose contains free HNO_3, an excess of NO_2 (over the equimolecular proportion to NO) and HNO_3 vapor will be in equilibrium above the liquid, HNO_3 being formed in the solution (and not determined by the permanganate) during the subsequent absorption of nitrogen oxides. This is all the more palpable, since concentrated acids were employed in the research.

Hence, the results of these determinations had to be too low.

Kuzminykh [6] investigated an acid containing 75.6% H_2SO_4, with a nitrosity of 0.5-2% of N_2O_3, containing 0 07-0.8% of HNO_3, at temperatures of 30, 45 and 60° C. He showed that adding the initial batch of HNO_3 to the nitrose resulted in a marked increase in the total equilibrium pressure. The ensuing batches of HNO_3 produced a smaller rise in pressure <u>i.e.,</u> there is no straight-line relationship, as Kudryavtsev had asserted.

Cherepkov [7] measured the equilibrium pressure of nitroses with an initial strength of 75, 80 85, and 92% H_2SO_4, a nitrosity of 0.5 to 4% N_2O_3, and containing 0.5 to 4% HNO_3 at temperatures ranging from 30 to 90° C. For the acid containing 92% H_2SO_4 he also secured results for nitrosities of 1% and 7% N_2O_3, with up to 9% HNO_3 in the nitrose. He found a substantial rise in the total equilibrium pressure of the nitrogen oxides due to the pressure of HNO_3 in the nitrose.

Pozin and Flerinskaya [8] also confirm the appreciable increase in the equilibrium pressure of nitrogen oxides above this system, on the basis of isolated measurements.

Malin [9] in his research on the desorption of nitrogen oxides from the nitrose in a sprayed wall tube, showed that when even minute quantities of free HNO_3 were present, the rate of desorption increased substantially. He tested a nitrose containing 70.85% H_2SO_4, 3.6% N_2O_3, and 0-0.8% HNO_3 at 50° C and a nitrose containing 77% H_2SO_4, 3.65% N_2O_3, and 0-1.1% HNO_3 at 80° C.

These tests may be regarded as qualitatively characterizing the process as far as the equilibrium pressure of nitrogen oxides above nitroses is concerned. The practically linear relationship between the coefficients of desorption and the percentages of HNO_3 in the nitrose for the acid containing 70.85% H_2SO_4 is worthy of note.

In the acid containing 77% H_2SO_4, on the other hand, the coefficients rise more than proportionally to the percentage of HNO_3 in the nitrose.

According to the researches of Lunge and Weintraub [10], the increase in the total equilibrium nitric-nitrous pressure $P_{HNSO_5 + HNO_3}$ above the sums of the individual pressures p_{HNSO_5} and p_{HNO_3} is due to the general trend of Reaction (1), resulting in the formation of the more volatile, less soluble N_2O_4:

$$SO_3NH+HNO_3 \rightleftharpoons H_2SO_4+N_2O_4. \qquad (1)$$

In the sense of the formation of N_2O_4, a similar result is secured when nitrous anhydride or an equimolecular mixture of $NO + NO_2$ acts on nitric acid, a reaction that has been investigated by Sanfourche [11].

Nitrous acid behaves toward weak nitric acid as if the latter were water, and dissolution is accompanied by decomposition:

$$3HNO_2 \rightleftharpoons HNO_3+2NO+H_2O. \qquad (2)$$

There is less decomposition with a strong nitric acid (>50%), and the reaction involves formation of N_2O_4:

$$N_2O_3+2HNO_3 \rightleftharpoons 2N_2O_4+H_2O. \qquad (3)$$

According to Lunge, the evolution of N_2O_4 ceases when there is no more HNO_3 in the solution containing the acid mixture.

In his time Sorel asserted that the solution was a stable one in nitroses prepared from acids with a high percentage of H_2SO_4 and low concentrations of HNO_3, no action of the HNO_3 upon the nitrosylsulfuric acid being apparent. Sanfourche and Rondier, on the other hand, have shown that the higher the nitrose's H_2SO_4 content, the greater the difference between the total equilibrium pressure and the individual pressures. This is corroborated by the data of other research workers.

The equilibrium pressure of nitrous acid falls as the H_2SO_4 strength increases. According to Sanfourche and Rondier, the equilibrium pressure of nitric acid rises up to an acid strength of 78% H_2SO_4, after which it likewise falls.

The researches of Sapozhnikov [12] on the properties of mixtures of nitric and sulfuric acids are not applicable to our case, since the HNO_3 concentrations in the solution were different. These researches indicate that as the concentration of the initial HNO_3 falls, the maximum equilibrium vapor pressure is shifted toward a lower percentage of HNO_3 in the acid mixture. Kudryavtsev cites a single measurement of the pressure above a mixture of the same acids with the initial H_2SO_4 percentage of 95.6% [5].

It follows from all of this that the increased values of $\underline{n}$ for strong acids are due principally to the course of Reaction (1) when N_2O_3 and HNO_3 are both present in the nitrose.

Now let us turn to an analysis of the experimental data on the equilibrium pressure of nitrogen oxides for the (H_2SO_4, H_2O, N_2O_3, HNO_3) system.

The results of our working up the Berl and Saenger experimental findings are shown in Figure 1 in ($\log p_{H_2O}$-$\log P_{NO, NO_2}$) coordinates, with the logarithms of the equilibrium pressure of dry, saturated water vapor laid off along the axis of abscissas for temperatures from 0 to 150 degree C, and with the equilibrium pressure of the nitrogen oxides for the same temperatures laid off along the axis of ordinates.

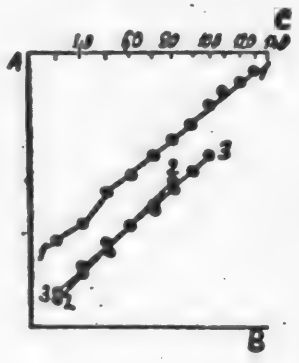

Fig.1. Results of working up the experimental findings of Berl and Saenger.
A) $\log P_{NO, NO_2}$; B) $\log p_{H_2O}$; C) temperature, °C. Acid strength (% H_2SO_4): 1) 67; 2) 75.65; 3) 78.0. The mixture contained 0.1 mole of $HNSO_5$ per liter and 0.1 mole of HNO_3 per liter in all three cases.

Fig.2. Results of working up the experimental findings of Sanfourche and Rondier.
A) $\log P_{NO, NO_2}$; B) $\log p_{H_2O}$; C) temperature, °C. Acid strength (% H_2SO_4) and percentages of N_2O_3 and HNO_3, respectively: 1) 93, 6.37 and 0.106; 2) 93, 84 and 0.106; 3) 73, 0.08 and 0.136; 4) 73, 0.082 and 0.014; 5) 65.5, 0.05 and 0.32; 6) 65.5, 0.05 and 0.013.

All the points for the acids containing 75.65% and 78.04% H_2SO_4 lie along straight lines. The same is true for the acids containg 67% H_2SO_4, with the exception of the points for 30 and 40 °C.

The results of our working up the experimental data of Sanfourche and Rondier in the same coordinates are given in Figure 2. Practically all the points lie along straight lines. The points corresponding to the upper half of the explored temperature range have a tendency to lie on straight lines with a different slope. Part of the graph is omitted for the sake of saving space.

Practically all the experimental points reported by Kudryavtsev lie on the straight lines 1 and 2, as we see in Figure 3. The points are displaced substantially to one side at the low temperatures of 30 and 40 °C. The results of working up the findings of Kuzminykh are given in the same diagram by Curves 3-6. Owing to the author's failure to give the numerical data in his paper, the equilibrium pressure was found from the graphs reproduced in his article, which diminished the accurancy of the cited results somewhat.

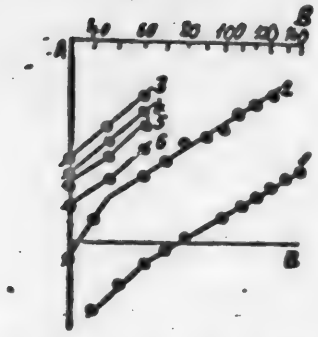

Fig.3. Results of working up the experimental findings of Kudryavtsev (Curves 1 and 2) and Kuzminykh (Curves 3–6). A) log P_{NO}, NO_2; B) log pH_2O; C) temperature, °C. Acid strength (% H_2SO_4) and percentages of N_2O_3 and HNO_3, respectively: 1) 90, 1 and 0.4; 2) 90, 4.5 and 1; 3) 75.6, 1.5 and 1; 4) 75.6, 1.5 and 0.8; 5) 75.6, 1.5 and 0.4; 6) 75.6, 1.5 and 0.2.

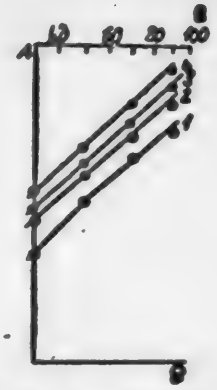

Fig.4. Results of working up the experimental findings of Cherepkov. A) log P_{NO}, NO_2; B) log pH_2O; C) temperature, °C. Acid strength (% H_2SO_4) and percentages of N_2O_3 and HNO_3, respectively: 1) 75, 4 and 0.5; 2) 75, 4 and 1; 3) 75.4 and 2; 4) 75, 4 and 4.

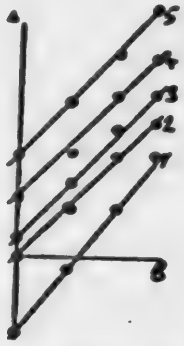

Fig.5. Results of working up the experimental findings of Cherepkov. A) log P_{NO}, NO_2; B) log pH_2O; C) temperature, °C. Acid strength (% H_2SO_4) and percentages of N_2O_3 and HNO_3, respectively: 1) 92, 1 and 0.5; 2) 92, 1 and 1; 3) 72, 1 and 2; 4) 92, 1 and 4; 5) 92, 1 and 9.

The results of our working up the experimental findings of Cherepkov are shown, in part, in Figures 4 and 5.

Practically all the points for an acid with a strength of 75% H_2SO_4 lie on straight lines (Figure 4). The points for 90 °C exhibit somewhat low values.

For the acid containing 80% H_2SO_4 the deviation of the points for 30 °C and for 2% of HNO_3 in the nitrose at 70 °C is worthy of note.

The figures for an acid containing 85% H_2SO_4 are essentially different from those for all the other acids, it being impossible to draw straight lines through the points covering the entire temperature range.

The points corresponding to 4% HNO_3 at 50 °C. 1% HNO_3 at 70 °C, and 2% HNO_3 at 70 °C lie somewhat off the straight lines for the acid containing 92% H_2SO_4 (Figure 5), 1% N_2O_3, and 0.5 to 9% HNO_3.

The points representing 0.5% HNO_3 at 70°C and 1, 2, and 4% HNO_3 at 30 °C lie off the line for the same acid, but containing 4% N_2O_3 and 0.5 to 9% HNO_3.

All the points lie off the curve at 30 °C for the same acid, but containing 7% N_2O_3 and 0.5 to 9% HNO_3, as well as the points representing 0.5% HNO_3 at 90° and 2% HNO_3 at 70 °C.

Therefore, the properties of the system containing H_2SO_4, H_2O, N_2O_3, and HNO_3 change during the transition from the low temperatures of 30-40 °C to higher temperatures, as was the case for the nitrose that contained no free nitric acid, apparently as the result of the disintegration of the hydrates, which leads to a change in the equilibrium pressure and, hence, in the slope of the straight lines in the graphs ($\log p_{H_2O} - \log P_{NO, NO_2}$).

The higher the percentage of H_2SO_4 in the original acid, the higher the temperature at which the break in the straight lines occurs in the graphs, i.e., the more stable are the hydrates and the higher the temperatures required to break them down.

The slopes of the straight lines, $\tan \alpha = \varrho$ (Figures 1-5) are given in Figure 6 as functions of the H_2SO_4 concentration in the original acid.

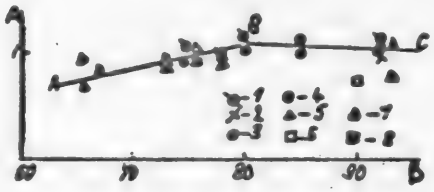

Fig.6. Slopes of the straight lines represented in Figs. 1-5. $\varrho = \tan \alpha = (C_{H_2SO_4})$.
A) $\tan \alpha$; B) Per cent concentration of H_2SO_4. Cherepkov's figures on the percentages of N_2O_3 and HNO_3, respectively: 1) 4 and 0.5; 2) 4 and 1; 3) 4 and 2; 4) 4 and 4; 5) figures of Gerl and Saenger; 6) Kudryavtsev's figures; 7) Sanfourche's and Rondier's figures; 8) Kuzminykh's figures.

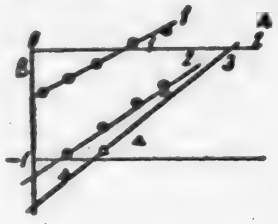

Fig.7. Coordinate system $\log [C_{HNO_3} C_{N_2O_3}] - B$.
A) $\log [C_{N_2O_3} C_{HNO_3}]$ B) B. Acid strength (% H_2SO_4) and percentages of N_2O_3 and HNO_3, respectively: 1) 75, 4 and 0.5 ÷ 4; 2) 80, 4 and 0.5 ÷ 4; 3) 85, 4 and 0.5 ÷ 4.

All the points lie satisfactorily near two straight lines, AB and BC, for the interval 65-93% H_2SO_4, which meet at an acid strength of 80% H_2SO_4.

In all the experiments the values of ϱ were taken for temperatures above 30-40 °C, inasmuch as other patterns of behavior apply at low temperatures. It should be noted that the value of ϱ hardly changes at acid strengths in excess of 80% H_2SO_4. If we start from Equation (1) and apply the law of mass action, we find:

$$[N_2O_4] = K [HNSO_5] [HNO_3]. \qquad (4)$$

for the given H_2SO_4 strength.

Therefore we ought to expect the total equilibrium pressure of the nitrogen oxides, $P_{HNSO_5} + HNO_3$, to be proportional to:

$$[HNO_3]^{0.5} [N_2O_3]^{0.5}.$$

for acid strengths for which Reaction (1) plays an essential role.

Actually, the process is much more complicated, the equilibrium pressure of HNO_3, in particular, making itself felt.

The points of $\log[C_{HNO_3}C_{N_2O_3}] - \underline{B}$ lie fairly well along straight lines when plotted in logaritmic coordinates, as shown in Figures 7 and 8, each straight line corresponding to a certain acid strength ($\underline{B}$ = the intercepts on the axis of ordinates of the prolonged straight lines in Figures 1-5).

The absence of adequate experimental data makes it impossible to follow up this relationship for acid strengths below 75% H_2SO_4. Sanfourche's experiments with an acid containing 65% H_2SO_4 were run at low temperatures and must be discarded in the light of the foregoing. The tests made by Berl and Saenger with a 67% acid yield only a single point.

The separate points of the various research workers are plotted in the same graph with a certain amount of scattering. For the acid with a strength of 78.04% H_2SO_4 (Berl, Saenger), for instance, the points are somewhat low, while they are somewhat high for the acid containing 75.85% H_2SO_4. When we continue the straight lines in Figures 7 and 8, they intersect the ordinate at a point where $\log[C_{N_2O_3}C_{HNO_3}] = 0$, i.e., $C_{N_2O_3}C_{HNO_3} = 1$.

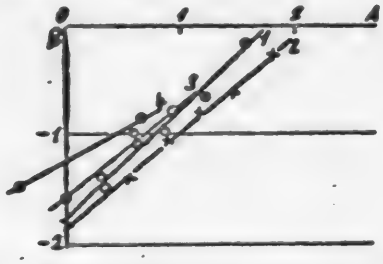

Fig.8. Cordinate system $\log[C_{HNO_3}C_{N_2O_3}]-\underline{B}$ for acids with strengths of 90% and 92% H_2SO_4.
A) $\log[C_{HNO_3}C_{N_2O_3}]$, B) B. Acid strength (% H_2SO_4) and percentages of N_2O_3 and HNO_3, respectively, from Cherepkov's findings: 1) 92, 4 and 0.5 ÷ 9; 2) 92, 7 and 0.5 ÷ 9; 3) 92, 1 and 0.5 ÷ 9; from Kudryavtsev's findings: 4) 90%.

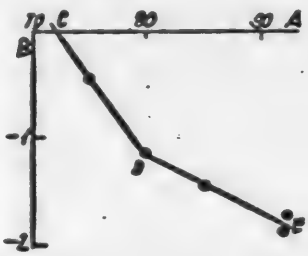

Fig. 9. Value of $\underline{B}$(at $C_{N_2O_3}C_{HNO_3} = 1$) as a function of acid strength.
A) % H_2SO_4; B) $\underline{B}$.

Figure 9 gives the intercepts $\underline{B}_o$ on the ordinates axis at $C_{N_2O_3}C_{HNO_3} = 1$ as a function of the acid strength. The points lie along two straight lines $\underline{CD}$ and $\underline{DE}$, which meet at an acid strength of 80% H_2SO_4.

The equation for these straight lines looks like this in B_o - % H_2SO_4 coordinates:

1) At $C_{H_2SO_4} \leqslant 80\%$ H_2SO_4 $B_o = 10.64 - 0.1475\ C_{H_2SO_4}$; (5)

2) At $C_{H_2SO_4} \geqslant 80\%$ H_2SO_4 $B_o = 2.84 - 0.05\ C_{H_2SO_4}$. (6)

On the other hand, $-\underline{B} = -\underline{B}_o + m \log[C_{N_2O_3}C_{HNO_3}]$, (7)
where $\underline{m}$ is the tangent of the straight lines in Figures 7 and 8. The values of $\underline{m}$ are given in Table 2.

When we find the equations for the straight lines in the Q - % H_2SO_4 coordinates (Figure 6) and insert them in (8) together with (5 and 6):

$$\log P_{NO,\ NO_2} = Q \log p_{H_2O} + B, \quad (8)$$

the final equation for the total equilibrium pressure (mm of Hg) above the nitrose when the latter contains free nitric acid will be:

Table 2

Variation of m with H_2SO_4 Strength

Acid Strength (% H_2SO_4)	75	80	85	92
m	0.5	0.7	0.8	0.87

1) At $C_{H_2SO_4} < 80\%$ H_2SO_4 $P_{NO, NO_2} = 10^{D_1}$ (9

where:

$$D_1 = (0.02284\ C_{H_2SO_4} - 0.7572) \log p_{H_2O} + 10.64 - 0.1475\ C_{H_2SO_4} + m \log [C_{N_2O_3} C_{HNO_3}];$$

2) At $C_{H_2SO_4} > 80\%$ H_2SO_4 $P_{NO, NO_2} = 10^{D_2}$ (10)

where

$$D_2 = (1.4 - 0.0041\ C_{H_2SO_4}) \log p_{H_2O} + 2.84 - 0.05\ C_{H_2SO_4} + m \log [C_{N_2O_3} C_{HNO_3}].$$

In these equations $C_{H_2SO_4}$, $C_{N_2O_3}$, C_{HNO_3} - are the per cent by weight of H_2SO_4, N_2O_3, and HNO_3; P_{H_2O} - is the equilibrium pressure of dry saturated water vapor at the temperature at which the equilibrium pressure of the nitrogen oxides above the nitrose was measured; and m is found as a function of the H_2SO_4 strength by plotting a curve from the data in Table 2.

Table 3 compares the data calculated from Equations (9) and (10) with the experimental findings of the several research workers. The agreement is satisfactory as we see. These equations should be regarded as a first approximation to the solution of the problem facing us. As experimental material accumulates the equations will have to be corrected accordingly.

If we bear in mind the conditions of the experiments, we will apply the following restrictions on the use of these equations:

1) Acid strength: 75 - 92% H_2SO_4.
2) Temperature: 40 - 120° C.
3) Nitrosity: up to approx. 7-8% N_2O_3 and up to approximately 4-6% HNO_3.

Equations (9) and (10) may be represented as alignment charts; we have not reproduced these charts here in order to simplify the computations.

SUMMARY

1. The experimental data on the total equilibri m pressure of nitrogen oxides above nitroses in the presence of free HNO_3 have been analyzed.

2. The functional relationship between the total equilibrium pressure of the nitrogen oxides in the presence of HNO_3 and the concentration of the system's components and the temperature has been established.

3. It has been found that the system's properties change during the transition from temperatures of 30-40° C to higher temperatures, as is manifested by the change in the slope of the straight lines plotted in log P_{NO, NO_2} - log p_{H_2O} coordinates.

LITERATURE CITED

(1) M.L. Varlamov, J.Appl. Chem. 23, 8, 816 (1950). [1]

(2) M.L. Varlamov, J.Appl. Chem. XXII, 9, 938 (1949).

(3) A. Sanfourche, L. Rondier, Bull., 43, 815 (1928).

(4) E. Berl, Saenger, Z.allg. anorg. Chem. 202, 1 (1931).

(5) A. Kudryavtsev, J Appl.Chem. 10 (1941).

[1]) See Consultants Bureau translation, p. 863.

TABLE 3

Comparison of the Calculated and Experimental Figures for the Total Equilibrium Pressure of Nitrogen Oxides above Nitroses with Free Nitric Acid Present

Per cent			Temperature, (°C)	Pressure, (mm Hg)		Author
H_2SO_4	N_2O_3	HNO_3		From the equation	Experimental	
1	2	3	4	5	6	
90	1	0.4	50	1.06	0.86	Kudryavtsev [1]
90	1	0.4	70	2.75	1.87	
90	4.5	0.2	50	2.1	2	
90	4.5	0.2	70	5.5	4.1	
78	0.9	0.114	40	1.92	1.96	Sanfourche and Rondier
78	0.057	0.9	40	1.25	1.42	
78	0.225	0.114	40	0.79	0.92	
92.9	0.84	0 106	40	0.11	0.17	
75.6	0.224	0.374	40	4.2	3.1	Berl and Saenger
75.6	0.224	0.374	70	17	13.4	
78	0.22	0.368	40	1.6	3.6	
78	0.22	0.368	70	7	13	
75	4	0.5	50	36	37	Cherepkov
75	4	1	50	54	53	
75	4	2	50	76	74	
75	4	4	50	101	104	
75	4	0.5	70	78	90	
75	4	1	70	110	127	
75	4	2	70	157	180	
75	4	4	70	240	255	
92	4	0.5	50	3.3	3.8	
92	4	1	50	6	7.3	
92	4	2	50	11	12.1	
92	4	0.5	70	7.7	7.5	
92	4	1	70	15.1	17.2	
92	4	2	70	28	33	
92	4	4	70	51.3	56	
92	4	9	70	104	116	
80	4	0.5	50	14.5	18	
80	4	1	50	23.6	24	
80	4	2	50	38	36	
80	4	4	50	62	52	
80	4	0.5	70	39	55	
80	4	1	70	63.5	65	
80	4	2	70	103	85	
80	4	4	70	167	138	

LITERATURE CITED (Continued)

[6] I.N. Kuzminykh, J.Chem.Ind. 1945, 3.
[7] I. Cherepkov, J. Chem. Ind.1950, 5.
[8] M Pozin and E. Flerinskaya, J.Appl. Chem. 1948, 7.
[9] K. M. Malin, J. Appl.Chem., 1938, 6.
[10] G. Lunge, Weintraub, Z. ang. Chem. 393, 417 (1899).
[11] A. Sanfourche, Ann. de Chemie, 1, 67 (1924)
[12] A. Sapozhnikov, Z. phys. Chem. 4, 9, 6 (1904);51, 5 (1905); 53, 53 225(1905).

Received November 17, 1949.

[1] Kudryavtsev's experimental figures have been multiplied by two to convert them into dissociated molecules.

BLANK
PAGE

THE PARTIAL PRESSURES OF AMMONIA AND CARBON DIOXIDE ABOVE THE NH_4NO_3-NH_3-CO_2-H_2O SYSTEM

B.I.Levi and N.A.Vasilenko

Strong aqua ammonia, containing ammonia, carbon dioxide, and hydrogen chloride, is recovered in the manufacture of coke. The hydrogen sulfide is separated from these gases by various industrial methods when this solution is distilled. The suggestion has been made that solutions of ammonium nitrate, which lower the vapor pressure of ammonia and increase that of carbon dioxide when they are dissolved, be employed to separate the ammonia from the carbon dioxide.

The same method of separating NH_3 from CO_2 by using ammonium nitrate may be employed in the utilization of the waste gases in urea synthesis, these gases totalling as much as 40% of the initial amount. This requires that we know the pressures of NH_3 and CO_2 above solutions of ammonium nitrate that contain ammonia and carbon dioxide.

Many research workers have dealt with this problem [1-8]. However, their findings apply principally to solutions with a molar ratio of $NH_3:CO_2 = 2:1$, corresponding to ammonium carbonate.

Inasmuch as the ammonia--carbon dioxide ratio in the waste gases varies widely in the production processes mentioned above, these figures proved to be inadequate for developing a technological plan for separating these gases.

In the present research we have measured the total and partial pressures of NH_3, CO_2, and H_2O at 25, 40 60, and 80° above aqueous solutions of ammonium nitrate than contained ammonia and carbon dioxide in various molar ratios. Inasmuch as the total pressure above the system varied from 40 to 1500 mm in our tests, we employed the static method of measurement.

In our research we utilized the test flask I (Fig.1), with a capacity of 1200 ml, fitted with two vacuum stopcocks a and b, a funnel c for drawing in the test solutions, a tube d, a mercury seal e, an outlet tube f to remove the liquid phase from the flask, and two branches g and h connecting to a manometer and an evacuated flask or pipet to take gas samples.

The test flask was evacuated to 10^{-3} mm Hg, and then 250 ml of the test solution were drawn in from the funnel c, plus 2-3 drops of mercury to fill the seal e. Then the flask was placed in a thermostat adjusted to the desired temperature. A manometer fitted with a mirror scale (Fig.1) a stopcock k and a bottle l for mercury, was connected to the branch pipe g. The branch pipes g and h were filled with mercury by raising the bottle l the pipes being interconnected by turning the stopcock a to the appropriate position. Then the stopcock k was closed, the test flask was connected to the manometer, and the manometer was read. The total pressure in the flask

was found by measuring the atmospheric pressure and reading the manometer. When the total pressure reached a constant level, it was taken as proof that the system had reached a state of equilibrium. After the total pressure had been measured, a gas sample was taken from the flask for analysis. At high temperatures and pressures the equilibrium composition of the liquid phase changed whenever a gas sample was taken in the presence of a liquid phase.

That is why the liquid phase was removed from the test flask via the seal d and the tubes d and f before taking a gas sample in these tests. This distortion was not observed at pressures below 400 mm Hg (25,40 and even 60°), the gas sample then being taken without first removing the liquid phase. The gas sample for analysis was transferred to the evacuated flask, the tube connecting the test flask with the evacuated one first being heated to prevent any condensation of water vapor. Then the flask containing the gas sample was connected to a series of weighed absorbers, consisting of two potash bulbs containing concentrated H_2SO_4 to absorb the ammonia and water vapor, and three U-tubes filled with asbestos wool soaked with a dilute caustic alkali to absorb the CO_2.

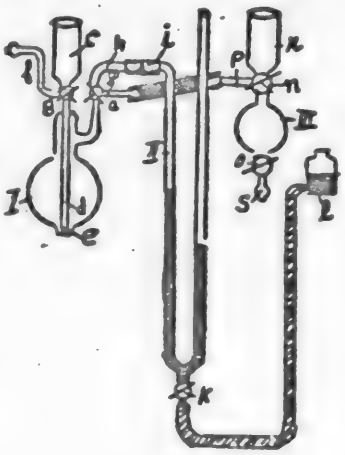

Fig.1. Layout of the aparatus for analyzing a gas by the evacuated flask method. See the text for explanations of the notation.

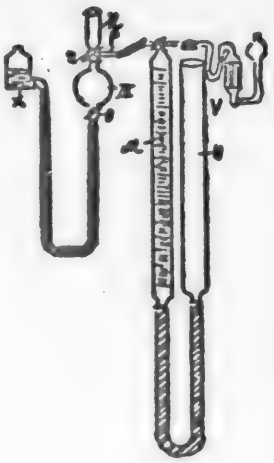

Fig.2. Layout for gas analysis by the pipet method. See the text for explanations of the notations.

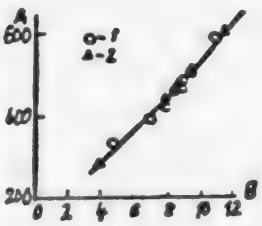

Fig.3. Vapor pressure above a NH_3-H2O system at 60° with the NH_3 concentration in water ranging from 4 to 16%. A - Vapor pressure, mm Hg; B - Per cent NH_3. 1 - The present author' findings; 2 - Perman's findings.

The fourth U-tube was filled with $CaCl_2$. After the potash bulbs had been weighed, the ammonia was determined by the Kjeldahl method. The NH_3, CO_2 and H_2O content was expressed in per cent by volume, thus making it possible to calculate the partial pressure of each component. Analyzing the gas in the evacuated flask takes a long time.

To speed up the analysis we worked out a method of determining the composition of the gas by means of a 200-ml gas pipet (Figs 1 and 2). To take a gas sample the pipet III was evacuated to 10^{-3} mm Hg, placed in the thermostat, and connected to the test flask I and the manometer II as shown in Fig.1.

The manometer was connected to the funnel r by turning the stopcocks a and n, and the branch pipe g, h, and p and part of the funnel r were filled with mercury by raising the bottle l. Then the manometer stopcock k was closed and the manometer was connected to the test flask I by turning stopcock a. After the total pressure had been measured and the branch pipes g and p had been warmed up, the stopcocks n and a were turned to connect the pipet first to the test flask to take a gas sample and then, by turning stopcock a to the manometer to read the pressure of the gas sample in the pipet.

The gas in the pipet was analyzed as follows: A definite excess of a 0.1N solution of H_2SO_4 was drawn into the pipet III from funnel r to absorb the NH_3, the acid being back-titrated after the CO_2 in the gas had been determined. Then the pipet was connected to a device for determining the CO_2 Fig 2.) Raising the bottle x caused mercury to drive the gas from the pipet into the buret m, after which a certain amount of air was drawn into the pipet by turning the stopcock n and lowering the bottle x. Then the pipet was again connected to the buret m, and the liquid in the pipet was cautiously heated to boiling to drive out any dissolved CO_2. After boiling was over, the residual gas in the pipet was forced into the buret m by mercury pressure and then analyzed for CO_2 by absorption in alkali. Knowing the volume, temperature, and pressure of the gas taken for analysis and its ammonia and carbon dioxide content, we were able to calculate its water vapor. Pipet analysis took 1.5 to 2 hours.

Comparison of the gas analysis using the pipet with that using the evacuated bottle yielded satisfactory agreement of the results at temperatures below 60°. At higher temperatures the pipet did not afford the required precision of analysis owing to partial condensation of the gas in the manometer. This was extremely useful at low pressures, as it enabled us to determine small percentages of ammonia and carbon dioxide in the gas without increasing the volume of the test flask.

This method of determining total pressure and the partial pressures of the gas was tested in the NH_3-H_2O system, which has been investigated by several researchers.

Perman's figures [9] for a temperature of 60° and concentrations of ammonia in water that ranged from 4 to 16% are shown in Fig.3 for the sake of comparison with our findings.

The method described above was employed to determine the total and partial pressures at 80, 60, 40 and 25° of aqueous solutions of ammonium nitrate containing ammonia and carbon dioxide. The weight ratio of the water to the ammonium nitrate was about 2.6 in all our tests.

The NH_4NO_3 per liter of solution varied from 2.0 to 250 grams, depending upon the concentrations of NH_3 and CO_2, thus approximating 25-27%.

The NH_3 concentration was kept constant in these tests (120,100 85, 50, and 35 grams of NH_3 per liter), while the CO_2 concentration was varied from 0 to 110 grams per liter.

The composition of the liquid phase once the system had reached equilibrium was determined from the composition of the initial solution, allowing for the percentages of ammonia and carbon dioxide that had passed to the gas phase. The experimental data are listed in Tables 1-5 and shown graphically in Figs 4 and 5.

TABLE 1

Total and Partial Pressures above Solutions Containing 32-35 grams of NH_3 per liter

Test No.	Liquid phase.							Gas phase						
	Original solution			Equilibrium solution				Per cent by volume			Partial pressures, mm			Total pressure
	Specific gravity, g/ml	Concentration, (grams/liter)		Concentration (Grams/liter)		(Moles/liter)								
		NH_3	CO_2	NH_3	CO_2	NH_3	CO_2	NH_3	CO_2	H_2O	P_{NH_3}	P_{CO_2}	P_{H_2O}	P_{total}
60° Temperature.														
100	1.0874	33.0	-	32.5	-	1.91	-	54.95	-	45.05	147	-	121	268
101	1.0983	34.5	14.4	34.1	14.2	2.01	0.32	48.64	7.72	43.64	125	20	111	256
102	1.1060	33.8	24.3	33.5	23.7	1.97	0.54	37.12	24.65	38.23	100	67	104	271
103	1.1128	33.7	31.3	33.5	30.3	1.97	0.69	24.88	39.24	35.88	76	120	111	307
104	1.1235	34.8	41.8	34.6	40.0	2.03	0.91	17.16	54.58	28.26	66	209	108	383
105	1.1391	33.5	55.1	33.4	50.1	1.97	1.25	4.97	78.47	16.56	38	598	126	762
40° Temperature														
106	1.0874	33.0	-	32.8	-	1.93	-	53.99	-	46.01	58	-	49	107
107	1.0967	33.8	11.8	33.7	11.8	1.98	0.27	43.14	2.85	54.01	41	3	52	96
108	1.1078	33.4	22.2	33.3	22.1	1.96	0.50	36.92	10.11	52.97	38	11	54	103
109	1.1162	33.2	31.4	33.1	31.2	1.95	0.71	30.17	23.14	46.69	30	23	46	99
110	1.1276	34.5	40.8	33.3	40.4	1.96	0.92	21.64	38.88	39.48	24	44	45	113
111	1.1375	32.1	54.2	32.0	52.6	1.89	1.20	6.48	70.45	23.07	17	180	59	256
112	1.1420	33.1	59.8	33.1	57.0	1.95	1.30	2.79	81.86	15.35	10	308	58	376
25° Temperature														
116	1.0874	33.0	-	32.9	-	1.94	-	56.5	-	43.2	29.4	-	22.6	52
118	1.0967	33.8	11.8	33.7	11.8	1.98	0.27	50.61	5.29	44.1	24.8	2.6	21.6	49
117	1.1078	33.4	22.2	33.3	22.2	1.96	0.50	38.09	6.75	55.16	15.6	2.8	22.6	41
119	1.1162	33.2	31.4	33.2	31.3	1.95	0.71	34.99	15.64	49.37	13.6	6.1	19.3	39
121	1.1275	34.5	40.8	34.5	40.7	2.03	0.93	25.14	26.92	47.94	11.3	12.1	21.6	45
120	1.1375	32.1	54.2	32.1	53.6	1.89	1.22	5.23	70.57	24.20	4.6	62.1	21.3	88
122	1.1420	33.1	59.8	33.1	58.6	1.95	1.33	1.71	84.14	14.15	2.7	130.4	21.9	155

Tables 1-5 and Figs 4 and 5 show the variation of the total and partial pressures as functions of the temperature and the changes in the CO_2 content of the solution above aqueous solutions of NH_4NO_3 containing a constant percentage of NH_3. They indicate that the water vapor pressure is greatly affected by the temperature. At a constant temperature the water vapor pressure above solutions of ammonium nitrate containing various amounts of NH_3 and CO_2 changes negligibly.

As we see from the tables and figures, the total pressure above a system drops at first as the percentage of CO_2 in the solution rises, then passes through a certain maximum value, and begins to drop off again. When the

TABLE 2

Total and Partial Pressures Above Solutions Containing 50-53 grams NH_3 per liter

Test No	Liquid phase							Gas phase						
	Original solution			Equilibrium solution				Per cent by volume			Partial pressures, mm			Total pressure
	Specific gravity, g/ml	Concentration, (grams/liter)		Concentration (Grams/liter)		(Moles/liter)								
		NH_3	CO_2	NH_3	CO_2	NH_3	CO_2	NH_3	CO_2	H_2O	P_{NH_3}	P_{CO_2}	P_{H_2O}	P_{total}
80° Temperature														
133	1.0741	51.8	-	50.5	-	2.97	-	59.28	-	40.72	423	-	291	714
134	1.0896	52.5	17.8	51.5	17.0	3.03	0.39	46.18	14.56	39.26	319	100	271	690
135	1.1030	52.2	29.3	51.4	27.8	3.02	0.63	36.90	26.88	36.22	265	193	261	719
136	1.1140	52.8	41.6	52.1	39.4	3.06	0.90	28.49	33.98	37.53	236	281	311	828
137	1.1323	50.8	55.2	50.2	50.6	2.95	1.15	17.02	53.66	29.31	181	572	313	1066
80	1.1297	50.9	56.7	50.3	52.3	2.96	1.19	18.39	50.59	31.02	201	552	339	1092
60° Temperature														
138	1.0741	51.8	-	51.1	-	3.00	-	64.77	-	35.23	220	-	119	338
139	1.0896	52.5	17.8	51.9	17.7	3.05	0.40	57.86	4.74	37.40	180	15	116	311
140	1.1030	52.2	29.3	51.7	29.0	3.04	0.66	48.80	12.30	38.90	145	36	115	297
141	1.1140	52.8	41.6	51.4	41.0	3.02	0.93	37.66	25.27	37.07	113	76	112	301
142	1.1371	50.6	60.3	50.4	58.6	2.96	1.33	19.19	50.62	30.19	75	198	118	391
40° Temperature														
147	1.0741	51.8	-	51.5	-	3.03	-	64.70	-	35.30	98	-	54	152
146	1.0896	52.5	17.8	52.3	17.8	3.08	0.40	53.24	2.10	44.66	73	3	60	136
143	1.1030	52.2	29.3	52.0	29.3	3.06	0.67	53.28	5.00	41.72	64	6	50	120
144	1.1140	52.8	41.6	52.6	41.5	3.09	0.94	50.60	10.70	38.70	58	12	44	114
145	1.1371	50.6	60.3	50.6	59.9	2.98	1.36	21.00	40.00	39.00	24	45	44	113

percentages of CO_2 and NH_3 in the solution approach the molar proportions of NH_3: CO_2 = 2: 1 or 3: 1, the rise in the total pressure is particularly striking. The rise in the P_{total} at the left of the maximum is due to the high partial pressure of the ammonia, and at the right to the high partial pressure of the carbon dioxide.

It should be noted that the minimum on the curve of total pressure is somewhat shifted toward a high CO_2 content as the temperature is lowered in solutions containing the same percentage of NH_3. As the CO_2 content of the solution is increased, the P_{NH_3} pressure drops, the relationship being nearly linear. The slope of the P_{NH_3} curves to the axis of abscissas shows that the higher the

TABLE 3

Total and Partial Pressures Above Solutions Containing 79.7-86.2 grams NH_3 per liter

Test No	Liquid phase							Gas phase						
	Original solution			Equilibrium solution				Per cent by volume			Partial pressures, mm			Total pressure
	Specific gravity, g/ml	Concentration, (grams/liter)		Concentration (Grams/liter)		(Moles/liter)								
		NH_3	CO_2	NH_3	CO_2	NH_3	CO_2	NH_3	CO_2	H_2O	P_{NH_3}	P_{CO_2}	P_{H_2O}	P_{total}
80° Temperature														
69	1.0548	88.5	-	86.2	-	5.07	-	73.43	-	26.57	740	-	268	1008
74	1.0679	83.7	14.6	81.7	14.2	4.81	0.32	66.16	5.78	28.06	638	56	271	965
75	1.0892	84.3	28.6	82.6	28.1	4.86	0.64	60.28	7.45	32.27	547	68	293	908
70	1.0859	87.5	41.3	86.0	40.3	5.06	0.92	54.33	13.91	31.76	490	126	287	903
76	1.1024	81.0	55.8	79.7	54.4	4.69	1.24	45.23	20.10	34.67	405	180	311	896
71	1.1316	86.0	73.2	84.8	70.5	4.99	1.60	38.17	35.57	27.26	375	340	267	982
72	1.1425	86.0	84.1	85.0	80.8	5.00	1.84	31.83	38.88	29.29	338	413	310	1061
73	1.1491	86.2	97.2	85.3	92.2	5.02	2.10	24.71	50.70	24.59	306	628	304	1238
60° Temperature														
58	1.0567	83.6	-	82.4	-	4.85	-	74.83	-	25.17	358	-	121	479
60	1.0676	82.3	14.1	81.2	14.0	4.78	0.32	72.87	1.53	25.60	333	7	117	457
89	1.0755	83.4	24.1	82.5	24.0	4.85	0.55	69.28	4.16	26.56	290	17	111	418
57	1.1044	84.9	42.0	84.1	41.7	4.95	0.95	57.59	9.05	33.36	222	35	128	385
62	1.1020	83.5	54.2	82.8	53.9	4.87	1.23	59.13	10.96	29.91	220	41	111	372
61	1.1344	84.5	73.4	84.0	72.7	4.94	1.65	I 43.38	25.40	31.22	157	92	113	362
								II 45.27	26.03	28.70	165	95	106	366
59	1.1416	83.7	83.9	83.2	82.9	4.89	1.88	35.03	31.96	33.01	136	124	129	389
63	1.1549	85.5	98.0	85.2	96.1	5.01	2.18	I 23.53	50.85	25.62	105	228	115	448
								II 27.28	48.80	23.92	120	215	106	441
40° Temperature														
83	1.0529	83.1	-	82.5	-	4.85	-	77.79	-	22.21	168		48	216
85	1.0634	84.2	13.0	83.6	13.0	4.91	0.30	78.89	0.52	20.59	163	1	42	206
82	1.0755	83.4	24.1	83.0	24.1	4.88	0.55	70.07	1.20	28.73	123	2	51	176
84	1 0909	84.0	44.0	83.6	44.0	4.92	1.00	69.80	2.05	28.15	116	3	47	166
88	1.1020	83.5	54.2	83.1	54.2	4.89	1.23	68.70	3.20	28.10	106	5	43	154
86	1.1169	84.0	70.3	83.7	70.2	4.92	1.60	63.38	5.92	30.70	90	8	44	142
87	1.1277	84.0	80.8	83.8	80.7	4.93	1.83	53.77	10.68	35.55	72	14	47	133
88	1.1488	83.8	106.0	83.7	105.5	4.92	2.40	29.84	37.70	32.46	42	54	46	142

TABLE 4

Total and Partial Pressures Above Solutions Containing 98.1-104.8 grams NH_3 per liter

Test No.	Liquid phase.							Gas phase						
	Original solution			Equilibrium solution				Per cent by volume			Partial pressures, mm			Total pressure
	Specific gravity,	Concentration, (grams/liter)		Concentration (Grams/liter		(Moles/liter)								
	g/ml	NH_3	CO_2	NH_3	CO_2	NH_3	CO_2	NH_3	CO_2	H_2O	P_{NH_3}	P_{CO_2}	P_{H_2O}	P_{total}
80° Temperature														
129	1.0386	101.9	-	99.1	-	5.83	-	75.65	-	24.38	912	-	294	1206
130	1.0553	100.6	19.2	98.1	18.8	5.77	0.43	71.74	4.2	24.06	797	47	267	1111
131	1.0763	100.6	37.2	98.5	36.6	5.79	0.83	64.83	7.07	28.10	685	75	297	1057
132	1.0928	101.1	56.2	99.3	55.2	5.84	1.25	57.09	12.09	26.36	581	128	306	1017
60° Temperature														
150	1.0468	103.0	-	101.4	-	5.96	-	80.7	-	19 3	485	-	116	601
151	1.0609	103.4	20.0	102.0	19.8	6.00	0.45	76.13	3.40	20.47	424	19	114	557
152	1.0814	103.4	38.8	102.3	38.5	6.01	0.88	70.63	7.05	22.32	348	35	110	493
153	1.0882	105.9	53.7	104.8	53.4	6.17	1.21	68.41	6.89	24.70	321	32	116	469
40° Temperature														
146	1.0468	103.0	-	102.2	-	6.01	-	84.40	-	15.60	238	-	44	282
147	1.0609	103.4	20.0	102.7	20.0	6.04	0.45	84.00	1.30	14.70	213	3	37	253
148	1.0814	103.4	38.8	102.8	38.8	6.04	0.88	81.30	1.80	16.90	187	4	39	230
149	1.0906	105.4	53.7	104.8	53.6	6.16	1.22	74.00	6.12	19.88	162	13	44	219

temperature, the steeper will be the drop in the partial pressure of NH_3 with the increase in the CO_2 concentration in the solution.

The variation of $\frac{P}{-}CO_2$ with the concentration of CO_2 in the solution is exponential: as the concentration of CO_2 in the solution increases, the partial pressure of the carbon dioxide rises, the rate of rise increasing as the CO_2 concentration in the solution approaches the molar NH_3: CO_2 ratio of 2:1 or 3:1. The higher the temperature, the steeper the rise of the CO_2 pressure.

Evaluation of Results

We have been able to establish certain patterns of behavior for the NH_4NO_3-NH_3-H_2O system. To shed light on them we began with a consideration of a simpler system: NH_3-H_2O, using Perman's data for this purpose [9].

We know that when the ammonia concentration in aqueous solutions exceeds 0.1 mole per liter, the latter is in an undissociated state, as molecules of NH_4OH [10].

TABLE 5

Total and Partial Pressures Above Solutions Containing 118.6-123.0 Grams NH_3 per liter

Test No.	Liquid phase							Gas phase						
	Original solution			Equilibrium solution				Per cent by volume			Partial pressures, mm			Total pressure
	Specific gravity,	Concentration, (grams/liter)		Concentration (Grams/liter)		(Moles/liter)								
	g/ml	NH_3	CO_2	NH_3	CO_2	NH_3	CO_2	NH_3	CO_2	H_2O	P_{NH_3}	P_{CO_2}	P_{H_2O}	P_{total}
80° Temperature														
124	1.0377	124.9	-	121.2	-	7.13	-	80.00	-	20.00	1197	-	299	1496
126	1.0367	126.4	19.9	123.0	19.8	7.24	0.45	77.11	0.95	21.94	1100	13.5	312.5	1426
127	1.0572	125.4	37.6	122.4	37.3	7.20	0.85	72.28	3.09	24.63	960	41.0	327	1328
128	1.0776	123.0	55.6	120.4	54.6	7.08	1.24	67.90	9.01	23.09	835	111	284	1230
60° Temperature														
154	1.0485	121.4	-	119.3	-	7.02	-	85.15	-	14.85	625	-	109	734
155	1.0437	122.1	18.5	120.3	18.3	7.08	0.42	81.21	2.90	15.89	548	19	107	674
156	1.0667	121.1	36.4	119.5	36.1	7.03	0.82	76.58	5.45	17.97	477	34	112	623
157	1.0798	122.1	50.6	120.7	50.3	7.09	1.14	73.26	5.34	20.40	433	38	121	592
40° Temperature														
113	1.0464	120.8	-	119.8	-	7.05	-	87.77	-	12.23	293	-	41	334
114	1.0450	119.6	19.6	118.7	19.6	6.98	0.45	86.24	0.28	13.48	261	1.0	41	303
115	1.0638	121.4	38.0	120.5	38.0	7.09	0.86	86.21	0.59	13.20	245	2.0	38	285
125	1.0810	119.3	55.6	118.6	55.6	6.98	1.26	78.44	1.69	19.87	195	5.0	49	249

When we express Perman's figures (Table 6) for the liquid phase as mole fractions of NH_4OH and H_2O, we find that the water vapor pressure above this system obeys Raoult's law exactly.

$$P_{H_2O} = \pi(1 - \alpha), \tag{1}$$

where P_{H_2O} is the water vapor pressure above the system at the temperature of $t°$: π - is the vapor pressure of pure water at the temperature $t°$: $(1 - \alpha)$ is the mole fraction of water.

The ammonia pressure obeys the formula:

$$K = \frac{P_{NH_3} \cdot P_{H_2O}}{\alpha}$$

or

$$P_{NH_3} = \frac{K\alpha}{P_{H_2O}} = \frac{K}{\pi} \frac{\alpha}{(1 - \alpha)} \tag{2}$$

where P_{NH_3} is the ammonia vapor pressure above the system at the temperature $t°$: K is a constant for the given temperature; and α - is the mole fraction of NH_4OH.

TABLE 6

Partial Pressures of Ammonia and Water Above NH_3-H_2O Solutions

Perman's figures for $NH_3 - H_2O$			Liquid phase				Gas Phase					
NH_3 in solution, %	P_{NH_3} (mm)	P_{H_2O} (mm)	Content, in moles per 100 grams of solution of: NH_4OH	H_2O	Mole fraction of NH_4OH,	Mole fraction of H_2O, $(1-\alpha)$	P_{NH_3} (atm.)	P_{H_2O} (atm.)	$K = \frac{P_{NH_3} \cdot P_{H_2O}}{\alpha}$	$\pi = \frac{P_{H_2O}}{(1-\alpha)}$ (atm.)	$\pi = \frac{P_{H_2O}}{(1-\alpha)}$ (mm)	π, mm water vapor, in mm Hg
Temperature 60°												
3.86	136.9	144.1	0.227	5.114	0.0425	0.9575	0.1801	0.1896	0.8034	0.198	150.5	149.38
7.78	300.4	138.5	0.458	4.665	0.0894	0.9106	0.3953	0.1822	0.8056	0.200	152.0	
9.37	375.7	135.5	0.551	4.484	0.1094	0.8906	0.4943	0.1783	0.8056	0.200	152.1	
11.31	475.8	130.4	0.665	4.263	0.1349	0.8651	0.6261	0.1716	0.7965	0.198	150.7	
Mean value 0.8028												
Temperature 50°												
3.29	79.1	89.6	0.1935	5.1793	0.0360	0.964	0.1041	0.1179	0.3409	0.122	93.0	92.51
5.90	151.3	87.1	0.347	4.881	0.0663	0.9337	0.1991	0.1146	0.3441	0.122	93.3	
8.91	246.6	83.0	0.524	4.537	0.1035	0.8965	0.3245	0.1092	0.3423	0.121	92.6	
11.57	341.7	80.6	0.681	4.231	0.1386	0.8614	0.4496	0.1061	0.3442	0.123	93.6	
14.15	451.4	77.0	0.832	3.938	0.1744	0.8256	0.5939	0.1013	0.3449	0.122	93.2	
14.94	487.1	75.2	0.8788	3.847	0.1860	0.8440	0.6409	0.0990	0.3411	0.121	92.4	
Mean value 0.3429												
Temperature 40°												
3.79	61.1	53.5	0.223	5.122	0.0417	0.9583	0.0804	0.0704	0.1357	0.0734	55.8	55.3
7.36	133.0	50.7	0.433	4.714	0.0841	0.9159	0.175	0.0667	0.1382	0.0728	55.3	
11.06	218.5	49.1	0.6506	4.2905	0.1317	0.8683	0.2875	0.0646	0.1410	0.0743	56.6	
15.55	353.6	44.1	0.9147	3.777	0.195	0.8050	0.4652	0.0580	0.1384	0.0720	54.8	
20.85	576.1	37.8	1.2265	3.1707	0.2789	0.7211	0.758	0.0497	0.1351	0.0689	52.4	
Mean value 0.1377												
Temperature 30.09°												
3.93	41.2	31.1	0.231	5.1064	0.0433	0.9567	0.0542	0.0409	0.0512	0.0427	32.5	33.5
7.43	86.3	29.2	0.437	4.706	0.0850	0.915	0.1136	0.0384	0.0513	0.0419	31.9	
9.75	120.0	28.5	0.5735	4.4404	0.1144	0.8856	0.158	0.0375	0.05179	0.0423	32.2	
12.77	175.0	26.6	0.751	4.095	0.155	0.845	0.2303	0.035	0.0520	0.0414	31.5	
17.76	290.2	24.8	1.0447	3.5242	0.2286	0.7714	0.3818	0.0326	0.05444	0.0422	32.1	
17.84	291.1	24.3	1.0494	3.515	0.23	0.77	0.383	0.032	0.05329	0.0415	31.5	
21.47	404.6	22.1	1.2630	3.1	0.2895	0.7105	0.5324	0.0291	0.05351	0.0409	31.1	
Mean value 0.05251												
Temperature 19.9°												
4.18	27.4	16.4	0.2459	5.0774	0.046	0.954	0.0361	0.0216	0.01691	0.0226	17.2	17.4
6.50	45.8	16.1	0.3824	4.812	0.0736	0.9264	0.0603	0.0212	0.01737	0.0228	17.4	
6.55	46.0	16.0	0.3853	4.8064	0.0742	0.9258	0.0605	0.0210	0.01712	0.0226	17.3	
7.72	56.2	15.6	0.454	4.673	0.0885	0.9115	0.074	0.0205	0.01723	0.0224	17.1	
10.15	80.6	15.1	0.597	4.395	0.1196	0.8804	0.106	0.0198	0.01764	0.0224	17.1	
10.75	86.3	14.7	0.6206	4.349	0.1249	0.8751	0.1135	0.0193	0.01754	0.0220	16.8	
16.64	166.1	12.9	0.9788	3.6523	0.2113	0.7887	0.2185	0.0170	0.01758	0.0215	16.3	
19.40	215.6	12.3	1.1412	3.337	0.2548	0.7452	0.2837	0.0162	0.01804	0.0217	16.5	
23.37	302.4	10.3	1.3747	2.675	0.3396	0.6604	0.398	0.0136	0.01594	0.0205	15.5	
Mean value 0.01743												

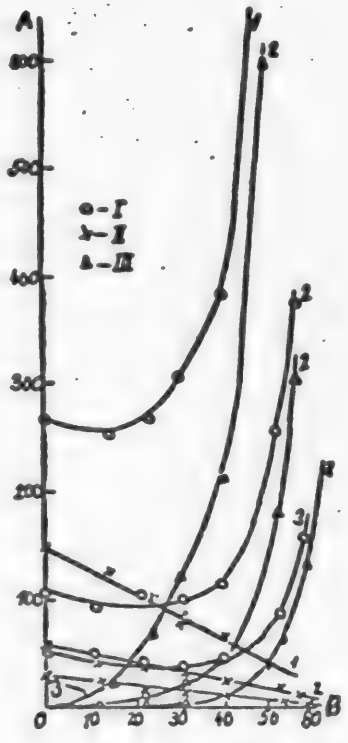

Fig.4. Total and partial pressures above solutions containing 32-35 grams of NH_3 per liter. A vapor pressure, mm Hg; B CO_2 content, grams per liter of solution. 1 Total pressure; 2 NH_3 partial pressure; 3 CO_2 partial pressure. Temperature, °C: 1 60; 2 40; 3 25.

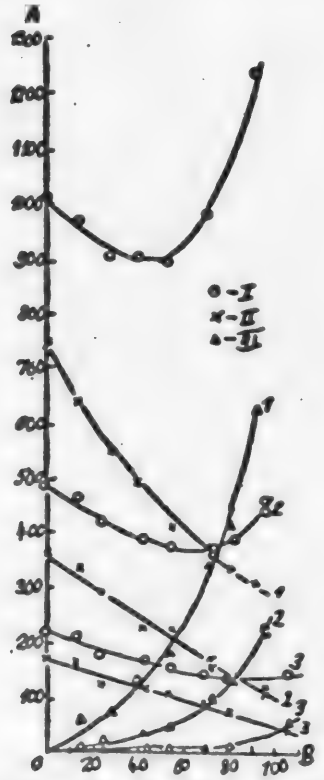

Fig.5. Total and partial pressures above solutions containing 79.7-86.2 grams of NH_3 per liter. A - vapor pressure, mm Hg; B - CO_2 content, grams per liter of solution. 1 Total pressure, 2 NH_3 partial pressure; 3 CO_2 partial pressure. Temperature, °C 1 - 80, 2 - 60, 3 - 40.

The values of π and K, as calculated from these formulas and cited in Table 6, Cols.10,11 and 12 remain constant at any given temperature and change with the ammonia concentrations.

We see from Cols.12 and 13 that the values of π (Col.12) calculated from the formula $\pi = \frac{P_{H_2O}}{(1-\alpha)}$ agree with the figures for the vapor pressure above pure water (Col.13). Perman's data go no higher than 23% of ammonia in the solution, stopping at as low as 11% NH_3 for 60°.

We were interested in finding out the limits within which the NH_3-H_2O system obeys the foregoing pattern of behavior. We did this by calculating the values of P_{NH_3} and P_{H_2O} from Equations 1) and 2) for various concentrations of NH_3 in the solution at 20, 30, 40, 50 and 60°.

The experimental data agree with the calculated figures within the following limits: up to 20% of NH_3 in the solution at 60°, up to 25% of NH_3 in the solution at 50°, up to 30% of NH_3 at 40°, up to 30% of NH_3 at 30°, and up to 35% of NH_3 at 20°. Equations (1) and (2) become unusable for these temperatures at higher NH_3 concentrations. Evidently, above these limits the solution contains other molecules, such as (NH_3), H_2O, NH_3, and others, in addition to the molecules of NH_4OH.

We examined the NH_4NO_3-NH_3-H_2O system in this light, allowing for the NH_4^+ and NO_3^- ions in computing the mole fractions of ammonia and water. In the solution of Test 154 (Table 5), for instance, which contained 119.3 grams of NH_3 per liter, 255 grams of NH_4NO_3 per liter, and 671 grams of H_2O per liter, the mole fraction of NH_4OH was 0.1607 and the mole fraction of water was 0.6928. Let us substitute our experimental values in the formula:

$$K = \frac{P_{NH_3} \cdot \pi \cdot \text{Mole fraction of } H_2O}{\text{Mole fraction of } NH_4OH} \qquad (3)$$

We calculated the value of the coefficient $\underline{K}$ for the NH_4NO_3-NH_3-H_2O system, the results being tabulated in Table 7.

TABLE 7

Test No.	Composition of the liquid phase, grams/liter.			Mole fraction		P_{NH_3} (atm)	K
	NH_3	NH_4NO_3	H_2O	NH_4OH	H_2O		
			Temperature 80°				
124	121.2	252.2	660.6	0.1658	0.6877	1.575	3.055
129	99.1	258.8	677.9	0.1321	0.7214	1.200	3.062
59	86.2	266.9	699.2	0.1114	0.7419	0.9737	3.030
133	50.5	282.4	739.9	0.0617	0.7919	0.5566	3.338
			Mean value				3.12
			Temperature 60°				
154	119.3	256.1	671	0.1607	0.6928	0.822	0.6949
150	101.4	260.7	683.1	0.1340	0.7360	0.638	0.6872
58	82.44	268.8	704.3	0.1058	0.7476	0.471	0.6528
138	51.1	282.4	739.8	0.0622	0.7911	0.289	0.7218
			Mean value				0.689
			Temperature 40°				
113	119.8	255.7	670	0.1616	0.6916	0.3855	0.119
146	102.2	260.7	683.2	0.135	0.718	0.3130	0.120
83	82.52	267.9	702	0.106	0.747	0.221	0.112
147	51.5	282.4	739.9	0.0629	0.790	0.129	0.117
106	32.8	291.6	762.8	0.0388	0.834	0.076	0.118
			Mean value				0.111

We see in Table 7 that K is constant in the temperature and concentration ranges we investigated, which bears out the applicability of Equation (3) in calculating the partial pressure of ammonia above the NH_4NO_3-NH_3-H_2O system.

We see in Table 6 and 7 that the value of $\underline{K}$ is lower in the NH_4NO_3-NH_3-H_2O system than in the NH_3-H_2O system, so that adding ammonium nitrate to the aqueous solution of ammonia ought to lower the partial pressure of the ammonia. The experimental findings bear this out.

It is obvious that the magnitude of $\underline{K}$ will depend upon the concentration of NH_4NO_3. Its numerical values will be somewhat different for concentrations of ammonium nitrate that are above or below 25-27%.

An endeavor to establish a relationship between the partial pressures of ammonia and carbon dioxide in the gas and their concentrations in the solution for the NH_4NO_3-NH_3-CO_2-H_2O system did not yield meaningful enough results. This is due to the fact that adding carbon dioxide results in the formation of new compounds in the solution (ammonium carbamate, ammonium bicarbonate, etc.), making the system much more complicated. Additional data, which we did not have, would be needed to ascertain the behavior patterns that prevail here.

SUMMARY

1] The curves of total pressure above the NH_4NO_3-NH_3-CO_2-H_2O system exhibit a minimum, to the left of which ammonia predominates in the gas, with carbon dioxide predominating at the right of the minimum.

2] The partial pressure of ammonia falls as the concentration of CO_2 in the solution is increased, the relationship being nearly linear.

3] The relationship between the CO_2 partial pressure and the concentration of carbon dioxide in the solution is an exponential one.

4] The water vapor pressure above the NH_3-H_2O and NH_4NO_3-NH_3-H_2O systems obeys Raoult's law.

5] A relationship has been found linking the ammonia partial pressure to the mole fractions of water and NH_4OH in the solution for the NH_3-H_2O and NH_4NO_3-NH_3-H_2O systems.

6] The derived patterns of behavior are evidence that ammonia is present in solution as molecules of NH_4OH or $NH_3 \cdot H_2O$ in the NH_3-H_2O and NH_4NO_3-NH_3-H_2O systems within the limits we have explored.

LITERATURE CITED

[1] Terres, Weiser, J. Gasbel., 63 705 (1920).

[2] Neumann, Domke, Altmann, Z. angew. Chemie, 42 275 (1929)

[3] Pexton, Bedger, J.Soc Chem. Ind., 57, 106 (1938)

[4] Clark, Krese, Ind. Eng.Chem., 19, 2, 205 (1927).

[5] Shabalin and Udintsova, Jour. Chem. Ind.(1950), 3, 165.

[6] Belopolsky, Shpunt, and Palkina, Jour.Chem. Ind. 14, 10, 717 (1937).

[7] Bolotov and Tugai, Jour.Chem. Ind. 14, 11-12, 799 (1937).

[8] Yushkevich, Shokin, Avdeyeva, and others, Jour.Chem. Ind. 6, 20, 1483 (1929).

[9] Perman, J.Chem. Soc. (London), 83, 2, 1186 (1903).

[10] Brodsky. The modern theory of electrolytes, 7. (1934).

Received June 15, 1950.

THE EFFECTIVE IONIC RADII OF ELEMENTS IN MELTS AND IN SOLIDS AT HIGH TEMPERATURE

S. I. Sobol

The development of theories of some metallurgical processes and phenomena, such as the diffusion theory of the refining of steel, the electrolytic theory of molten slags, the theory of solid solutions, and the like, required knowledge of the effective radii of the atoms and ions of the elements in melts and at high temperatures in general. Up to the present time the effective ionic radii (R_I) and atomic radii (R_A) that have been employed in calculations of the formulas involved in these theories have been calculated from the findings of the X-ray analysis of crystal lattice structure and from quantum-mechanics data that again refer to a substance's solid state. In both cases the values of $R_{I,A}$ refer to room temperatures, far from the temperatures at which the vast majority of metallurgical processess occur. This is what Samarin and Shvartsman [1] do in their calculations of the diffusion of impurities from the Einstein equation:

$$D = \frac{RT}{N} \cdot \frac{1}{6\pi\eta r}, \qquad (1)$$

where N is the Avogadro number; R is the gas constant; T is the absolute temperature; η is the viscosity of the medium; and r is the mean radius of the diffused particles.

These authors took as the value of the last variable the values of R_I given by Goldschmidt. Comparing the diffusion coefficients of various metals with the values calculated from Equation (1), Samarin and Shvartsman found that "the agreement of the calculated and experimental values was better than could have been expected, especially when the substantial errors involved in the experimental measurements of viscosity and the diffusion coefficients are considered" and concluded: "We may therefore assert that the Stokes-Einstein equation yields approximately correct values of the diffusion coefficients of metals in the liquid state at low as well as high temperatures." It should be borne in mind that the values of the diffusion coefficients calculated by Samarin and Shvartsman for a temperature of about 500 °C differ from the experimental values by at least 25–35% in most instances.

Though we agree with Samarin and Shvartsman when they say that the experimental data on diffusion in molten media are still very sparse, we cannot accept their proposal to employ the Goldschmidt values of R_I and R_A in high-temperature calculations based on Equation (1). As a matter of fact, the values of R_I and R_A in crystal lattices of the same element vary considerably with changes in the coordination number and the composition of the compound.

A mere change in the coordination number from 4 to 12 is enough to change the ionic or atomic radii by 12–15%. The magnitude and nature of coordination changes radically during the transition from the solid to the liquid state: the definite value for the given type and composition of space lattice turns into an indeterminate value, largely dependent upon the random thermal motion

of the ions in the melt. It is obvious that the change in the values of R_i and R_A in the molten state is governed by other rules than those holding in crystal lattices, and that the higher the temperature of the melt, the greater will be this difference. That is why the values of R_i and R_A calculated for solid bodies at room temperature must result in serious errors when used to secure any data on phenomena that occur at temperatures of 1000-1600° and upward.

An attempt has been made in the present paper to estimate the values of R_i and R_A in melts from the figures on the diffusion coefficients of various elements in molten metals and salts and the viscosity of these melts, as published at various times. Equation (1) was used in our calculations. The values we secured in this manner are listed in Tables 1 and 2. These tables also give the values of the diffusion coefficients and the viscosities of the melts at the temperatures for which the calculations were made. The diffusion coefficients have been recomputed from cm^2 per day to cm^2 per second.

Variation of ionic radii with temperature. The data in Tables 1 and 2 and in Figure 1 are evidence of the substantial change in the ionic radii of the elements as the temperature of the melts is raised. As we see, the size of the element varies directly with the temperature in any given melt. Tables 3 and 4 give the calculated temperature gradients of change of the ionic radii when the temperature of the melts is raised 1°.

Analysis of the magnitude of the gradient

$$a = \frac{\Delta R_i}{\Delta t} \qquad (2)$$

indicates that the order of magnitude of the numerical values remains the same (except for the individual cases denoted by a footnote) in molten metals as well as molten salts. The arithmetical mean values of the gradient are found to be:

For molten metals: 0.00250 A per degree.

For molten salts: 0.00303 A per degree.

These values are of the same order of magnitude and extremely close together. Inasmuch as the mean deviations are smaller in Table 3, we shall henceforth use the value of $\underline{a} = 0.0025$.

This is a figure of some magnitude, and the part it plays is particularly in evidence at the high temperatures of most molten slags and metals.

Let us calculate the value of R_i for manganese and silicon in molten iron at a temperature of 1600 °C by way of an example of the use of Equation (2).

Taking the values found by Goldschmidt [4] and Pauling, 0.91 and 0.80 A, respectively, as the R_i of Mn^{+2} at room temperature, and 0.39 and 0.41 A, respectively, as its values for Si^{+4}, we find that when the temperature rises to about 1580 °, the ionic radii should increase by about 3.92 A, so that the value of R_i should be of the order of 4.72-4.83 A for manganese and of the order of 4.32 A for silicon.

This estimate of the order of magnitude of R_i involves a certain simplification, inasmuch as, first of all, Goldschmidt gives his value of R_i as applying to a lattice of the sodium chloride type with a coordination number of 6. If we recompute these figures for coordination numbers of, say, 4 or 12, the initial values will be more or less changed accordingly, this change being

of the order of ±10%, i.e., about ±(0.08--0.09)A for Mn^{+2} and ±0.04 A for silicon. Second, and this is extremely important in the given case, we do not know the valency of the manganese and silicon ions in an alloy with iron at 1600 °C. It should be noted that the R_i of manganese has the following values at higher valencies (in A):

Goldschmidt's values:

+3	+4	+6
0.70	0.52	

Third and last, we make no allowance for the fact that the R_i of an element in a solid lattice and in solution must differ somewhat even at the same temperature.

In the light of all these assumptions and reservations it is highly interesting to calculate the ionic radii of manganese and silicon in molten iron at 1600 °C from Equation (1). We take as our initial data the diffusion coefficient of manganese in molten iron, as determined in the experiments of Paschke and Hautmann, and the diffusion coefficient of silicon as given by Samarin and Shvartsman, at 1600 °C.

D_{Mn}=9.6 cm^2 per day or $1.11 \cdot 10^{-4}$ cm^2 per second.

D_{Si}=7.39 cm^2 per day or $0.86 \cdot 10^{-4}$ cm^2 per second.

The viscosity of iron at this temperature is estimated to be about 0.028 poise [5]. Calculation yields the following values:

TABLE 1

Ionic Radii of Metal Elements in Molten Metals

Diffusing metal	Metal medium	Temp. of the melt, °C	Expt. diffusion coeff., $cm^2/sec \cdot 10^{-4}$	Viscosity of the metal medium at the expt. temp poises	Ionic radius of the diffusing metal, Angströms
Pb	Hg	9.4	1.74	0.0162	0.72
Pb	Hg	15.6	1.59	0.0159	0.84
Pb	Hg	99.2	2.22	0.0121	1.02
Pb	Sn	500	3.68	0.0120	1.32
Pb	Sn	555	3.70	0.0112	1.47
Au	Hg	11	0.834	0.0161	1.55
Au	Pb	490	3.51	0.0190	0.84
Au	Pb	500	3.69	0.0188	0.84
Au	Bi	500	5.24	0.0118	0.94
Au	Bi	555	5.2	0.0107	1.09
Au	Sn	500	5.38	0.0120	0.90
Au	Sn	555	5.4	0.0112	1.00
Au	Pb	555	3.7	0.0170	0.96
Pt	Pb	490	1.96	0.0190	1.50
Rh	Pb	500	3.52	0.0188	0.86
Rh	Pb	550	3.50	0.0170	1.01
Ag	Sn	500	4.79	0.0120	0.99
Ag	Sn	555	4.8	0.0112	1.12
Li	Hg	8.2	0.77	0.0162	1.65
Na	Hg	9.6	0.74	0.0162	1.73
K	Hg	10.5	0.61	0.0161	2.12
Rb	Hg	7.3	0.53	0.0163	2.37
Cs	Hg	7.3	0.52	0.0163	2.42
Ca	Hg	10.2	0.63	0.0161	2.04
Sr	Hg	9.4	0.55	0.0162	2.32
Ba	Hg	7.8	0.60	0.0163	2.10
Tl	Hg	11.5	1.01	0.0161	1.28
Sn	Hg	10.7	1.77	0.0161	0.73
Th-B	Pb	340	2.5	0.025	0.72
Cd	Hg	8.7	1.68[1]	0.0162	0.76
Cd	Hg	15.0	1.81[1]	0.0159	0.73
Cd	Hg	99.1	3.43[1]	0.0121	0.66
Cd	Hg	20.0	1.52	0.0155	0.91
Cd	Hg	20.0	1.44[2]	0.0155[3]	0.96
Zn	Hg	11.5	2.52	0.0161	0.51
Zn	Hg	15.0	2.42	0.0159	0.55
Zn	Hg	99.2	3.36	0.0121	0.67
Mg	Al	670	6.08	0.0635	1.79
Mg	Al	700	7.55	0.0289	3.17

[1]) Diffusion coefficient from Bogau's data; these figures differ greatly from those obtained by other researchers and contain an error, the R_i decreasing with rising temperature.

[2]) The diffusion coefficient was determined at a pressure of 1500 atm.

[3]) A nominal value of viscosity was used.

TABLE 2

Ionic Radii of Metals in Molten Salts

Diffusing metal	Diffusing salt	Salt medium	Temperature, °C	Experimental diffusion coeff.[2] $cm^2/sec \cdot 10^{-4}$	Viscosity [3a] of the salt medium at the given temp, poises	Effective ionic radius R_i of the diffusing metal, Angstroms
Ag	$AgNO_3$	KNO_3	360	4.57	0.027	0.35
Ag	$AgNO_3$	KNO_3	390	4.86	0.022	0.45
Ag	$AgNO_3$	$NaNO_3$	330	4.57	0.027	0.36
Ag	$AgNO_3$	$NaNO_3$	360	5.06	0.0235	0.39
Ag	AgCl	KCl, LiCl	480	4.61	0.035	0.34
Ag	AgCl	KCl, LiCl	500	4.65	0.0308	0.40
Ag	AgCl	KCl, LiCl	520	4.63	0.0275	0.46
Ag	AgCl	KCl, LiCl	600	5.30	0.0184	0.66
Ag	AgCl	KCl, LiCl	740	6.67	0.0100	1.11
Ag	AgBr	KBr	780	4.92	0.0130	1.21
Ag	AgI	KI	780	5.09	0.0165	0.92
Ag	AgI	KI	720	4.63	0.0215	0.73
Tl	$TlNO_3$	KNO_3	380	3.36	0.023	0.62
Tl	$TlNO_3$	KNO_3	365	3.28	0.026	0.55
Tl	$TlNO_3$	KNO_3	345	3.17	0.028	0.51
Tl	$TlNO_3$	$NaNO_3$	360	4.31	0.0235	0.46
Tl	$TlNO_3$	$NaNO_3$	330	3.92	0.027	0.42
Tl	$TlNO_3$	$NaNO_3$	320	3.94	0.028	0.39
Tl	TlCl	KCl, LiCl	580	3.47	0.020	0.70
Tl	TlCl	KCl, LiCl	520	3.10	0.0275	0.68
Tl	TlCl	KCl, LiCl	600	3.36	0.0184	1.03
Tl	TlBr	KBr	780	3.78	0.0130	1.57
Tl	TlBr	KBr	770	4.28	0.0135	1.32
Tl	TlI	KI	720	3.14	0.0215	1.08
Tl	TlI	KI	780	3.30	0.0165	1.41
Na	$NaNO_3$	KNO_3	360	5.21	0.027	0.33
Br	KBr	KNO_3	360	3.01	0.027	0.57
Br	KBr	KNO_3	380	2.94	0.023	0.71
Br	KBr	KNO_3	360	2.96	0.027	0.58
Ba	$Ba(NO_3)_2$	KNO_3	370	2.08	0.0244	0.93
Ba	$Ba(NO_3)_2$	$NaNO_3$	360	3.72	0.0235	0.52
Sr	$Sr(NO_3)_2$	KNO_3	370	3.06	0.0244	0.63
Sr	$Sr(NO_3)_2$	KNO_3	360	2.82	0.027	0.61
Sr	$Sr(NO_3)_2$	$NaNO_3$	345	4.17	0.0255	0.43
Sr	$Sr(NO_3)_2$	$NaNO_3$	360	4.40	0.0235	0.45
Pb	$PbCl_2$	KCl, LiCl	530	2.02	0.0260	1.12
Pb	$PbCl_2$	KCl, LiCl	720	4.40	0.0107	1.55
Cu	CuI	AgI	480	3.7—4	(0.045)	(0.42)

R_i of manganese. . . . . 4.43 A

R_i of silicon. . . . . 5.7 A

Notwithstanding the exceptional difficulties of determining the diffusion coefficients and the viscosities experimentally at such high temperatures, we note the satisfactory agreement between the experimental and calculated values of R_i,

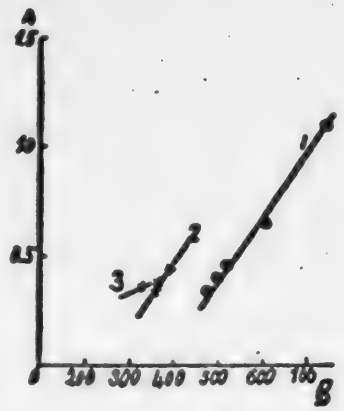

Fig.1. Variation of the ionic radius of silver with temperature in various melts. A) Ionic radii, A; B) temperature, °C. Ionic radii of silver: 1) in KCl + LiCl; 2) in KNO_3; 3) in $NaNO_3$.

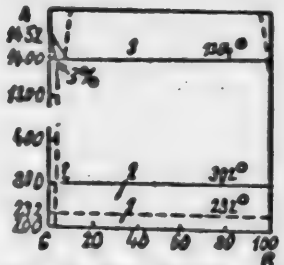

Fig.2. The Ni–Tl system. A) Temperature, °C; B) per cent of Tl by weight. 1) α + αTl; 2) α + βTl; 3) two liquid layers.

differing by no more than 0-2%, and the feasibility of employing the Einstein equation for these calculations at any temperatures.

If we use Goldschmidt's figures for the R_i of Mn^{+2} and Si^{+4} at such high temperatures without applying any corrections, i.e., as Samarin and Shvartsman [1] recommend, and compute the diffusion coefficients of these impurities in molten iron, we get figures that are 5 to 8 times higher than the experimental values.

Nor can we ignore the fact that the ionic radii of nitrogen, carbon, and sulfur in iron at 1600 °, as computed from the diffusion coefficients of these elements calculated by Samarin and Shvartsman [6] and from the viscosity or iron as 0.028 poise, are extremely high (Table 5).

TABLE 3

Temperature Gradients of the Change of the Effective Radii of Elements in Molten Metals.

Element	Metal medium	Δt	ΔR_i (B A)	Gradient, $a = \frac{\Delta R_i}{\Delta t}$
Ag	Sn	50	0.13	0.00260
Au	Sn	55	0.10	0.00182
Au	Pb	55	0.12	0.00218
Au	Bi	55	0.15	0.00272
Zn	Hg	87.7	0.16	0.00183
Pb	Hg	88.8	0.30	0.00338
Pb	Hg	83.6	0.18	0.00215
Pb	Sn	55	0.15	0.00273
Rh	Pb	50	0.15	0.00300
	Mean value			0.00250

It must be supposed that the diffusion coefficient of silicon should not be smaller, as found by Samarin and Shvartsman, but larger than the respective values for manganese. If we assume that the molten iron contains N^{-3}, C^{-4}, and S^{-2} ions, the ionic radii of which are given by Goldschmidt as 2.12, 2.60, and 1.74 A, respectively, their ionic radii at 1600°C should be of the order of magnitude given in Column 4 in Table 5 The discrepancy is nearly 2 in the case of nitrogen and carbon, and 4.5 for sulfur, which indicates that the absolute values of the diffusion coefficients of these elements in molten iron found by Samarin and Shvartsman must be approached with a certain amount of caution.

The ionic radius of magnesium has been calculated from its diffusion coefficient in

TABLE 4

Temperature Gradients of the Change of the Ionic Radii of Elements in Molten Salts

Element	Molten medium	Δt	ΔR_i (B A)	Gradient, $a = \frac{\Delta R_i}{\Delta t}$
Ag·	KNO_3	30	0.10	0.00333
Ag·	$NaNO_3$	30	0.03	0.00100
Ag·	KCl, LiCl	260	0.77	0.00296
Ag·	KI	60	0.19	0.00317
Tl·	KNO_3	35	0.11	0.00314
Tl·	$NaNO_3$	40	0.07	0.00175
Tl·	KCl, LiCl	80	0.45	0.00437
Tl·	KBr	10	0.25	0.025*
Tl·	KI	60	0.33	0.055*
Br'	KNO_3	20	0.14	0.00700
Sr··	KNO_3	10	0.02	0.00200
Sr··	$NaNO_3$	15	0.02	0.00133
Pb··	KCl, LiCl	190	0.43	0.00226
	Mean value			0.00303

molten aluminum (measured by Belozersky and Barzakovsky [3b]). The viscosity of molten aluminum is not yet known with sufficient accuracy [7]. Starting with the experimental values of D and η, we find the R_i of magnesium in aluminum to be 1.79 A at 67°C and 317 A at 700°C. The ionic radius of the Mg^{+2} ion should be about 2.39 - 2.47 A at 670 - 700°C, according to Equation (2) (Goldschmidt gives R_A = 0.78 A). Here, again, Equation (2) enables us to secure values that approach those calculated from Equation (1).

Variation of R_i with the qualitative composition of melts. We see from Tables 6 and 7 that the effective radius of a given ion at a given temperature is different in different melts. This is obviously attributable to the fact that the dimensions of the ions and their probable distribution throughout the molten mass, which sets up some image of the coordination number for the impurity ion, will be different in different melts. In gold, for example, the value of R_i rises 0.1 A at 500°C when we shift from an alloy with lead, the atomic radius of which is R_A = 1.74 A to an alloy with bismuth, for which R_A = 1.46A(both of these figures being taken from the crystal lattices of these metals). The changes in the ionic radii of the elements in molten salts are no less substantial when the composition of the latter is changed.

Variation of the R_i of an element with its concentration in the melt. Changing the concentration of an element in a melt must affect its effective radius, if all other conditions remain the same. As a matter of fact, the energy of a given element's interaction with the constituents of the melt changes insofar as the ions of the melt change the geometry of the surroundings of the element's ion. This is particularly true when the valency of an element changes in the given melt: in the Co - Si system, for example, the compounds Co_3Si, Co_2Si, CoSi, $CoSi_2$ and $CoSi_3$ have been found. Although these compounds are formed when the melt crystallizes, it must be assumed that considerable changes occur in the dimensions of the ions even in the liquid state as a result of changes in the quantitative proportions of the melt's constituents.

Only extremely sparse material is available at the present time to illustrate this general postulate. The data we possess are Weisstedel's findings [8] on the diffusion of zinc in mercury and Weisstedel's and Bogau's findings [9] on the diffusion of cadmium in mercury. All these experiments were run at 20°C. As we see from their findings (Table 8), the diffusion coeffients fall systematically as the concentration of zinc and cadmium is increased in the amalgams from which these elements diffuse into the mercury, and, since there is but little change in the viscosity involved in such changes in the composition of the liquid metal, the change in the diffusion coefficients must be attributed to a change in the ionic radii of the diffusing elements.

TABLE 5

Ionic Radii of Nitrogen, Carbon, and Sulfur

Element	Diffusion coefficient D, cm^2 per day	Ionic radius at 1600° from Equation (1), Angstroms	Ionic radius at 1600°, as given by Goldschmidt, corrected for temp. from Equation (2)
N....	3.26	12.9	7.0
C....	2.83	14.9	8.5
S....	1.66	25.8	5.7

Application of the behavior patterns to explain certain phenomena observed in solid solutions. Hume-Rothery [10] has found that solid solutions are formed in binary alloys whenever the ionic or atomic radii of the elements comprising the alloys do not differ by more than 15%. This rule, however, cannot explain the finding of solid solutions in several alloys of elements whose R_A differ by 20-30 per cent and more.

The variation of the effective radii of ions and atoms with temperature discovered above indicates that the relative difference between the dimensions of all ions (or atoms) diminishes as the temperature is raised. Hence, elements whose dimensions differ substantially at room temperature (the difference between their R_A exceeding 15%) may form solid solutions as the temperature rises, due to the decrease in the relative difference between their effective radii, these solutions decomposing at a certain instant during cooling, when the relative difference between their dimensions attains some critical value.

In the Ni-Tl system, for example, the atoms of the constituents have radii of 1.24 and 1.71 A, respectively, at room temperature, i.e., they differ by 38% (Figure 2).

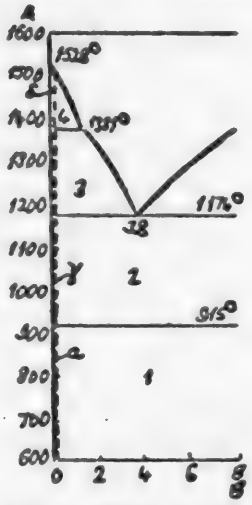

Fig.3. Part of the Fe-B system.
A) Temperature, °C; B) per cent of Tl by weight. 1) α + Fe_2B; 2) γ + Fe_2B; 3) liquid + γ; 4) liquid + δ.

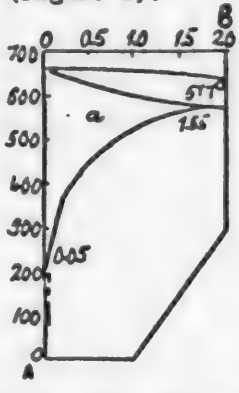

Fig.4. Part of the Al-Si system.
A) Temperature, °C; B) per cent Si by weight.

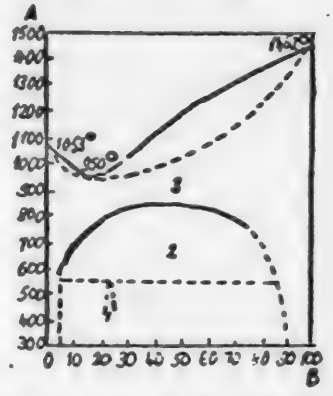

Fig.5. The Au-Ni system.
A) Temperature, °C; B) per cent Ni. 1) AuNi; 2) saturated Au - solid solution + saturated Ni - solid solution; 3) solid solution.

Nevertheless there is a limited solid solution in this system, with up to 3% of Tl, at 1387°. The boundaries of this solid solution at room temperature have not been determined, but they are extremely small. The appearance of this solid solution at a high temperature becomes comprehensible in view of the fact that the radii of both atoms are increased by some 3 50 A when the temperature is raised some 1400°C, thus diminishing the difference between them to 11%.

In the iron-boron system (Figure 3), the atoms of which have radii of 1.27 and 0.97 A, respectively, representing a difference of 31% between the two at room temperature, while a δ solid solution may exist at about 1400°C as the result of the difference between the two values of R_A dropping to 6.7%. A gamma solid solution exists between the temperatures of 915 and 1381°, being transformed into an α-solid solution at 915°. The latter transformation occurs at a difference of 9% between the R_A for the two elements.

In the aluminum - silicon system (Figure 4) the difference between the atomic radii is 22% at room temperature, the solid solution of Si in Al decomposing nearly completely at this temperature. As the temperature is raised, a solid solution appears in the vicinity of the pure Al constituent, increasing rapidly as the temperature rises, in accordance with a decrease in the difference between the atomic radii. Thus, at a temperature of about 250°C, when the solubility of Si in Al is 0.05%, the difference between the R_A values is 15%, while at 577°, when the solubility totals 1.65% of Si, the difference between the atomic radii has fallen to 10%.

In the gold-nickel system (Figure 5), the difference between the atomic radii is 16% at room temperature, i.e., their difference is at the critical limit, according to Hume-Rothery. None the less, this system exhibits an unbroken series of solid solutions at high temperature, thoughout the concentration range. This is quite understandable, inasmuch as the difference between the R_A of gold and nickel is less than 6% at about 850°C. The decomposition of the initial solid solution into two other solid solutions in this system occurs at a difference between the values of R_A totaling 6 to 9%.

The origin of introduction solid solutions. The foregoing enables us to advance some hypothesis on the origin of introduction solid solutions. It is thought [10] that if the dimensions of the atoms of the two constituents are not too far apart, so-called substitution solid solutions (in which the atoms of one constituent replace the atoms (or ions) of the other constituent in its space lattice) are produced, without distorting (or else distorting only negligibly) the lattice parameters. It is held that introduction solid solutions [10, 11] are formed by the "introduction" of atoms or ions of one constituent into the space lattice of the other constituent, the two constituents differing substantially in atomic radius (Hagg's theory) thus causing an appreciable deformation of the space lattice parameters.

The concept of a change in the effective atomic and ionic radii with temperature and of a decrease in the relative differences between the dimensions of all atoms and ions as the temperature is raised enables us to outline the following process of formation of solid solutions.

At high temperatures the primary solid solutions are formed, these being substitution solid solutions, as may be readily calculated for the most diversified pairs of components.

The wolfram atom has an R_A = 1.41 A, while the R_A of the carbon atom is 0.77 A, i.e., they differ by 83%. A solid solution is formed in the W-C system at about 3360° (containing about 3 atomic per cent of carbon); this is quite comprehensible, since at that temperature, the atomic radii of both constituents have increased by 8.40 A over the respective values for room temperature, which diminishes the difference between the R_A of these constituents to 7%.

Two possible cases may arise during the cooling of a substitution solid solution:

a) When the ratio between the dimensions of the atoms (or ions) of the constituents varies within a narrow range throughout the temperature range from the melting point to room temperature, the solid solution will still be a substitution solid solution in the cold state.

b) When the ratio between the dimensions of the atoms (or ions) of the constituents varies over a wide range as the temperature of the solid solution changes from the melting point to room temperature, the primary substitution solid solution will have to be transformed into an introduction solid solution in the cold state.

The decomposition of introduction solid solutions is governed by several factors and may take place at different rates at various temperatures. Intermediate phases, such as are actually observed in many instances (as, for instance, in Figure 3), may be formed depending upon the limits within which the ratio of the atomic dimensions of the components in the solid solution and the rate of decomposition of primary solid solutions during cooling vary.

Hence, introduction solid solutions are formed from substitution solid solutions as the latter cool, provided the ratio of the components' atomic dimensions varies widely as the melt cools.

TABLE 6

Effect of the Nature of the Molten Metal Upon the Ionic Radius of Gold at 500 °C.

Melt		Ionic radius of gold, A	Goldschmidt's value for the atomic radius of the metal medium, A
Gold	in lead	0.84	1.74
	in tin	0.90	1.58
	in bismth	0.94	1.46

TABLE 7

Effect of the Composition of the Molten Salts Upon the Ionic Radius of an Element

Temp. °C	Melt		Ionic radius of the metal, A
360	Silver in	KNO_3....	0.35
360		$NaNO_3$...	0.39
780		KBr.....	1.21
780		KI.....	0.92
365	Thallium in	KNO_3....	0.55
360		$NaNO_3$...	0.46
780		KBr.....	1.57
780		KI.....	1.41
360	Strontium in	KNO_3....	0.64
360		$NaNO_3$...	0.45

Note. The R_i of potassium is 1.33 A, of sodium 0.98 A, of bromine 1.96 A, and of iodine 2.20 A.

SUMMARY

1. It has been shown that the dimensions of the ions of elements in molten metals and salts vary with their temperature and composition, as well as with the concentration of the elements in the melts.

2. In the general case the dimensions of ions of any one element at any one temperature are different in liquid phases that are in contact with each other, as in the metal-slag, metal-matte, slag-matte systems, and the like.

3. It has been shown that the Einstein equation for the diffusion coefficient of colloidal particles in a liquid may be employed to determine the sizes of ions in melts, provided the diffusion coefficient of the element and the viscosity of the melt are known.

4. It has been shown that Samarin's and Shvartsman's conclusion that the ionic radii of elements calculated by Goldschmidt for space lattices at room temperature may be used to calculate the diffusion coefficients in melts at high temperatures is erroneous.

5. It has been shown that in melts in which there is a great difference between the atomic or ionic radii of the components at room temperature, solid solutions are regularly formed at high temperatures, since at these temperatures there is a relative decrease in the differences between the R_I or R_A of the elements.

TABLE 8

Effect of the Concentration of Zinc and Cadmium in a Mercury Amalgam Upon Their Effective Radii

Element	Concentration of element by weight in amalgam	Diffusion coefficient, cm^2 per day	Ionic radius of the element, A
Zinc	0.1	2.22	0.54
	0.2345	1.44	0.828
	0.475	1.39	0.860
	0.675	1.35	0.884
	0.850	1.315	0.91
	0.900	1.265	0.94
Cadmium	0.9 - 1.5	1.32	0.91
	0.1	1.65*	0.73

Note. The 2.22 value is extrapolated.

6. A hypothesis is advanced regarding the origin of introduction solid solutions during the cooling of substitution solid solutions whenever the ratio of the components' atomic (or ionic) dimensions varies greatly during the cooling of the melt.

Literature Cited

[1] A. M. Samarin and L. A. Shvartsman, Bull USSR Acad. Sci., Div. Tech. Sci. 1948, 12, 1649. [2] Landolt-Börnstein Tables, Vol. 1, 2nd ed, 199-200. [3] Antipin, Alabyshev, and others. The electrochemistry of molten salts. a) Par. 14; b) p. 105 (1937). [4] A. E. Fersman. Geochemistry, I, 96-98 (1934). [5] A. M. Samarin and L. A. Shvartsman, Bull. USSR Acad. Sci., Div. Tech. Sci. 1949, 6, 893. [6] A. M. Samarin and L. A. Shvartsman, Jour. Phys, Chem. 22, 5, 573 (1948). [7] E. V. Polack and S.V.Sergeiev, Compts Rendues, USSR Acad. Sci. 30, 2, 137 (1941). [8] Landolt-Börnstein Tables, Vol. 1, 3rd. enlarg. ed., 239 (1935). [9] Landolt-Börnstein Tables, Vol. 1, prin. ed., 249. [10] Hume-Rothery, Electrons and metals (Russ. ed.), 267 (1948). [11] Ya. S. Umansky. Carbides of solid solutions, 86ff (1947).

Received December 9, 1949.

THE EFFECT OF AMMONIUM SALTS UPON THE CORROSION OF COPPER POWDER

A. V. Pomosov, T.N. Rogatkina, and A. I. Levin

As we know, copper powder is acted upon readily by various corroding agents. The presence of ammonium salts or other chemicals in the room where copper powder is stored accelerates the latter's corrosion.

The hypothesis had been advanced earlier [1] that the corrosion activity of ammonium salts in atmospheric corrosion, in the absence of any direct contact with the corroded surface, must be related to the volatility of the acid formed by this salt. This hypothesis was put forward on the basis of a study of the corrosive action of only two salts: ammonium chloride and carbonate. It was therefore felt to be advisable to check the correctness of this notion on a large number of objects. In the present research we have investigated the corrosive action of chemically pure ammonium halides and of the carbonate, nitrate, acetate, sulfate, and disubstituted phosphate of ammonium. Common copper powder produced industrially, containing 99.92% copper and with a specific gravity of the dry, granular material of 0.9, was used in our tests.

The corrosion tests were run as follows. Weighed samples of the powder were placed in porcelain beakers inside 2.5-liter jars, with the ammonium salt and water placed in separate porcelain beakers. The sample of copper powder was always the same – 2.5 g. As for the salts, their samples were dimensioned so as to contain 1 g of ammonium [NH_4^+]. Then the jars were closed tight with paraffined cork stoppers, sealed with parrafin, and placed in a thermostat. The corrosion tests lasted 12 hours at 40±0.5° . After the test was over, the samples were transferred to a dessicator containing calcium chloride, chilled, and weighed until their weight was constant. The rate of corrosion was expressed in milligrams per gram of sample per day [mg/ g/ day].

The effect of the corrosive action of the ammonium salt was defined as the per cent increase of weight of the sample over the original weight.

The test results are listed in Table 1. The data listed in this table are the means of fours measurements, the deviation never exceeding 10-15%.

We see in Table 1 that the corrosive action differs for various ammonium salts, depending upon the nature of the acid constituting the salt.

Inasmuch as this is a case of atmospheric corrosion, its velocity will be determined by the thickness of the liquid adsorption layer on the surface of the metal and the amount of vapor and gas dissolved in it [2]. In this case the formation of the liquid adsorption film is the same for every salt tested and, hence, the thickness of the layer is likewise the same. Hence, the observed difference in the rate of corrosion depends solely upon the quantity and nature of the vapors and gases dissolved in the liquid adsorption layer. These vapors and gases are formed in the reaction space as a

result of the partial decomposition of the ammonium salts, due to the latter's thermal instability. Therefore, the corrosive action of an ammonium salt will, in the general case, vary inversely with its thermal stability.

The nature of the thermal decomposition of ammonium salts is governed by the properties of the resultant acid anion, its volatility. The salts consituted by nonvolatile acids [H_2SO_4, H_3PO_4] yield nothing but ammonia when they are decomposed, whereas the ammonium salts of volatile acids [HCl, H_2CO_3] yield acid vapors in addition. That is why the corrosive action of the ammonium salts of volatile acids is usually much greater than that of salts that are formed from nonvolatile compounds. This is borne out by the data in Table 2, in which we have tabulated the corrosion effect of various ammonium salts and the boiling points of the acids that form these salts.

TABLE 1

Corrosive Action of Ammonium Salts upon Copper Powder
[12 hours exposure; temperature: 40 ±0.5° C]

Salt		Grams of Copper	Added weight after test, mg	Corrosion rate mg/g/day	% corrosive action
Ammonium	Chloride	2.5	53.2	42.56	2.12
	bromide	2.5	42.9	34.03	1.71
	iodide	2.5	43.4	34.72	1.73
	fluoride	2.5	21.4	17.12	0.84
	acetate	2.5	90.0	72.00	3.60
	nitrate	2.5	11.1	8.88	0.44
	carbonate	2.5	299.9	239.12	12.00
	sulfate	2.5	9.3	7.44	0.37
	biphosphate	2.5	14.6	11.68	0.58

Table 2

Variation of the Corrosive Action of Ammonium Salts with the Volatility of the Acids Forming these Salts

Phenomenon tested	NH_4Cl	NH_4Br	$[NH_4]_2CO_3$	NH_4NO_3	$[NH_4]_2SO_4$	$[NH_4]_2HPO_4$
% Corrosion	2.12	1.71	11.10	0.44	0.37	0.58
Acid's b.p.,°C	-85	-68.7	-65	84	338 (1)	250(1) [Decomposition]

(1) B.p. of a 98.3% mixture.

In ammonium salts of the same structural type the thermal stability rises with an increase in the strength of the acid of which the salt is a derivative.

In the acid series; HI--HBr--HCl--HF, the thermal stability diminishes from HI to HF /3/. This would lead one to expect that the aggressive action

of these salts would rise in the same sequence. Ammonium fluoride exhibits a discrepancy, however, due, no doubt, to the fact that the volatility of HF is lower than that of the other hydrohalides (the boiling point of HF is 19.5°C and that of hydrogen chloride is -85°C.

Thus, the volatility of the acid that constitutes the anion of the ammonium salt is the principal factor determining the corrosive action of ammonium salts upon copper powder.

The presence of water vapor promotes the decomposition of ammonium salts. Apparently, the higher the per cent hydrolysis of a given salt, the more active will be the decomposing effect of the water. The per cent hydrolysis of ammonium carbonate, for example, is 80%, and its corrosive action is 11.10% whereas the per cent hydrolysis of ammonium chloride is 0.14%, and its corrosive action 2.12%.

It stands to reason that these factors-- acid volatility, thermal stability of the salts, and their hydrolytic cleavage--do not exhaust the diversity and complexity of the phenomenon discussed here. There is no doubt that the hygroscopicity of the salts and the solubility of the acid vapors in the liquid adsorption film are likewise essential factors that must be taken into account.

SUMMARY

It has been shown that the volatility of the acid constituting the anion of a salt is the principal factor affecting the corrosive action of the salt.

LITERATURE CITED

[1] A.I.Levin and A. V. Pomosov, J. Appl. Chem. 22, 6, 592 (1949).
[2] B. Akimov. Theory and research methods of metallic corrosion, 148-150. USSR Acad. Sci. Press (1945).
[3] B. V. Nekrasov. Treatise of General Chemistry, 364. State Chemical Press(1948).

Received May 15, 1950.

BLANK
PAGE

THE ATMOSPHERIC CORROSION OF COPPER POWDER

A. V. Pomosov and A. I. Levin.

In the literature of the past few years atmospheric corrosion has been considered to be a special case of electrochemical corrosion, it being assumed that the corrosion processes take place beneath a film of moisture, at the boundary between the metal surface and the liquid phase [1].

The temperature range of atmospheric corrosion is ordinarily confined to the region in which water exists in the liquid state. The corrosive action of dry vapors and gases upon metals (chemical corrosion) is held to be possible at temperatures that are much higher than the boiling point of water, above 200°C for chlorine, above 300°C for hydrogen chloride, and above 450-500°C for sulfur dioxide and hydrogen sulfide [2]. But even when corrosion occurs in an atmosphere of dry vapors and gases (such as hydrogen sulfide), it is usually stated that the process also involves the action of moisture formed during the action of the aggressor upon the metal or upon the latter's oxide film.

Thus, the presence of moisture is considered to be an indispensable condition for atmospheric corrosion.

In Kistyakovsky's film theory, atmospheric corrosion is regarded as a region in between purely chemical and electrochemical corrosion. The corrosion process is divided into three periods:

1) The reaction of the metal with moist oxygen, giving rise to films of metallic oxides.
2) Solidation of the films (coagulation, formation of crystallites).
3) Sorption of gases, condensation of liquids, and colloido-electrochemical processes.

The rupture of the initial film (the appearance of solidation centers) may be produced by particles suspended in the air, by vapors, and by gases. It is readily seen that a decisive role is assigned to the influence of water in this theory, too, though the process of corrosion as a whole is not reduced solely to the electrochemical reactions that occur at the boundary between the metal surface and the film of moisture.

Research on the corrosion of metal powders, in which atmospheric corrosion is of a specific nature, while some of its aspects are shown in greater relief than in dense metals, enables us to examine the mechanism involved in atmospheric corrosion more closely.

The previous corrosion tests of copper powder in various aggressive gases have shown that moisture is the basic factor governing the corrosion process [4]. In view of this, we have developed a novel method of stabilizing copper powders against corrosion, involving the hydrophobization of the surface of the metal particles [5].

The formation of chemisorbed hydrophobic films prevents the adsorption of water vapor at the surface of the metal particles, thus completely elimin-

ating any possibility of the formation of liquid adsorbed films of moisture on these particles.

This increases the anticorrosion properties of the metal powder several hundred per cent; it increased 50 to 70 times, for instance, in carbon dioxide saturated with water vapor at 40°. This high resistance to atmospheric corrosion is understandable, inasmuch as electrochemical reactions cannot occur in the stabilized powders.

The present research is an endeavour to make a comparative study of the corrosion behavior of hydrophobized and ordinary copper powder.

EXPERIMENTAL[1]

The method used in the corrosion tests was basically the same as the one employed previously [4]. To ensure that the conditions were identical in the tests, two samples of powder, one hydrophobized and the other the ordinary powder, were placed in each dessicator, The tests were run in atmospheres of hydrogen sulfide, hydrogen chloride, ammonia and carbon dioxide. The gases were dehydrated by passing them through bottles filled with calcium chloride and sulfuric acid, bottles containing soda lime being added in some instances. The same amount of test gas was used in filling the desiccators every time, and the same procedure was followed. Copper powder produced industrially was employed in the tests, the extent of corrosion being determined by the gain in weight.

The test results are shown in Tables 1 and 2.

TABLE 1

Corrosion of Copper Powder in Atmospheres of Hydrogen Sulfide and Carbon Dioxide
(Exposure 8 hours; temperature: 40 ± 1°C.

Kind of powder	Corrosion atmosphere				
	Hydrogen sulfide		Carbon dioxide		
	Anhydrous	Saturated with water vapor	Anhydrous	Saturated with water vapor	Water vapor
Ordinary...	7.72	28.22	0.05	0.72	0.33
Hydrophobized	4.21	6.56	0.05	0.04	0.002

Note. The gain in weight is expressed as per cent of the original weight in Table 1 and the following tables.

As we see in Tables 1 and 2, the hydrophobized powders resist corrosion much better than do the ordinary powders in every instance. The corrosion of ordinary copper powder increases substantially in a moist atmosphere of hydrogen sulfide or carbon dioxide, whereas it either does not change at all (in CO_2) or changes negligibly (in H_2S) in the case of the hydrophobized metal. The copper powder behaved anomalously in the hydrogen chloride atmosphere. The metal corrosion is greater in the anhydrous gas than when water vapor is present. We shall return to an explanation of this anomaly later on.

[1]) The laboratory assistants T. A. Tkachenko and K. V. Mityshina assisted in the experimental work.

TABLE 2

Corrosion of Copper Powder in Atmospheres of Hydrogen Chloride and Ammonia (Exposure: 4 hours; temperature: 40°C)

Kind of powder	Corrosion atmosphere		
	Hydrogen chloride		Ammonia
	Anhydrous	Saturated with water vapor	
Ordinary	3.01	2.09	4.00
Hydrophobized	1.90	1.02	0.73

Note. The ammonia atmosphere was produced by placing a beaker containing a 25% solution of ammonia in the desiccator.

TABLE 3

Corrosion of Copper Powder in an Atmosphere of Hydrogen Sulfide as a Function of the Exposure Time (Temperature: + 16 ± 2°C)

Test No.	Kind of powder	Corrosion atmosphere	Exposure, hours		
			24	48	264
1	Ordinary	Anhydrous hydrogen sulfide	16.1	16.2	20.5
2	Hydrophobized		6.5	6.9	15.2
3	Ordinary	Hydrogen sulfide saturated with water vapor	18.8	18.1	20.0
4	Hydrophobized		12.2	10.0	17.6
5	Ordinary	Hydrogen sulfide saturated with water vapor, and water saturated with hydrogen sulfide	—	20.6	—
6	Hydrophobized		—	12.2	—

We then ran corrosion tests of the powder in hydrogen sulfide for longer periods of time, the results being tabulated in Table 3.

Apparently most of the unhydrophobized copper is corroded at once during the initial period, the corrosion penetrating deeper into the sample during the rest of the process. Table 3 likewise shows that hydrophobized copper is corroded much more slowly than the ordinary copper, but corrosion increases with time in this case, however. The concentration of gas in the reaction space is of basic importance. In Tests 5 and 6 (Table 3), for example, we placed beakers of water that had first been saturated with hydrogen sulfide in the desiccators, while beakers containing ordinary distilled water were used in Tests 3 and 4. This caused a decrease in the gas concentration, due to the partial absorption of the hydrogen sulfide by the water, in Tests 3 and 4, so that the extent of corrosion fell.

As we know, metal powders that have been stabilized with soap cannot be wetted with water at all. But even more interesting were the results secured in tests of the wettability of samples that had been tested for corrosion. It was found that copper powders that had been first hydrophobozed were not wetted by water even after prolonged atmospheric corrosion.

It was also noted that the powder samples caked after the corrosion tests, the ordinary powders caking more than the hydrophobized ones. The caking of unhydrophobized powders was particularly marked when water vapor was present. But when corrosion was carried out in a moist atmosphere at higher temperatures (90°C), the corroded powder samples caked much less than at lower temperatures.

No difference was found in the degree of caking of ordinary and hydrophobized powders at these high temperatures, however. Hence, water has

a marked effect upon caking at ordinary processes, apparently promoting closer contact and bonds between the metal particles.

The corrosion tests of hydrophobized copper powder in hydrogen sulfide, hydrogen chloride, and ammonia are indubitable evidence of the presence of atmospheric corrosion even when there is no film of moisture on the surface of the highly dispersed metal particles. Apparently, the corrosion process is the result of direct chemical action of the gases and vapors with the metal's surface.

The higher corrosion of ordinary copper powder than that of the hydrophobized powder in anhydrous hydrogen sulfide may be explained as follows: first, the entire surface of the particles is accessible to the action of the gas in unprotected powders, whereas the gas must overcome a certain resistance of the protective film to get into direct contact with the metal when the metal surface is covered with hydrophobic films; second, the water formed in the reaction of hydrogen sulfide with the metal will be adsorbed at an ordinary powder, thus promoting the rise of electrochemical corrosion, in addition to the chemical corrosion. It is a matter of course that this cannot happen in hydrophobized powders. The same holds true in an even greater degree when the reaction space is saturated with water vapor, the corrosion of the unhydrophobized metal increasing very sharply in this latter case. Then a film of moisture is formed on the surface not only because of the chemical reaction between the hydrogen sulfide and the metal, but also as the result of adsorption and capillary condensation of the water on the highly dispersed metal particles. It is quite understandable that then the chemical corrosion is supplemented by extremely intense electrochemical corrosion.

As we see from the experimental data, the corrosion of hydrophobized copper powder either is wholly unaffected under these conditions or changes very negligibly. A certain increase in the corrosion of hydrophobized metal powders in the presence of water vapor is attributable to the disintegrating effect of the vapor on the film formed by the products of the metal's reaction with the hydrogen sulfide. The lower corrosion of copper powder in hydrogen chloride saturated with water vapor than in the anhydrous gas is due to the decrease in the concentration of the aggressive gas caused by its partial absorption in the water.

SUMMARY

1. It has been shown that atmospheric corrosion can take place in hydrophobized copper even when there is no film of moisture on the surface being corroded. In this connection it is asserted that the unqualified view of atmospheric corrosion as a special case of electrochemical corrosion is false.

2. At temperatures at which water is a liquid purely chemical-gaseous corrosion also plays an important part, alongside electrochemical corrosion.

LITERATURE CITED

[1] G.V.Akimov. Theory and research methods of metallic corrosion, Vol. IV. USSR Acad. Sci. Press (1945).

[2] V.K.Pershke and I.Ya. Klinov. Chemical resistance of metals. Moscow-Leningrad: State Chemical Press (1940).

[3] V.A.Kistyakovsky, Trans. First Conf. on Metallic Corrosion. USSR Acad. Sci. Press (1935).

[4] A.I.Levin and A.V.Pomosov, J.Appl. Chem.22, 592 (1949); A.I.Levin and A.V.Pomosov, Proc. USSR Acad. Sci. 1950, 6, 1075.

Received May 15, 1950.

THE THERMAL CHLORINATION OF NORMAL BUTANE

B. A. Krentsel and N. A. Pokotilo

Science is indebted to the researches of Russian chemists for the theoretical foundations of the chlorination of paraffin hydrocarbons. The major patterns of behavior in the chlorination of the paraffins were explored in the well-known paper by Markovnikov [1], dealing with the reciprocal influences between atoms in a molecule of an organic compound. The rules discovered by Markovnikov for the substitution of chlorine for hydrogen atoms in a paraffin still hold in the exploration of the chlorination reactions of hydrocarbons. The chlorination of the paraffins has been studied in detail by Semenov [2], who demonstrated that this is a chain process and elaborated the theoretical views of chlorination reactions in the light of modern concepts in the theory of free radicals.

Numerous papers and patents have appeared since then on the experimental study of the chlorination of the paraffins, dealing with the thermal, catalytic, and photochemical chlorination of hydrocarbons [3]. These publications contain only brief references to the results of chlorinating n-butane [4], on which no systematic research has been done. And yet the chlorination of butane is of theoretical as well as practical interest, since the monochloro derivatives of butane are very important in organic synthesis as intermediates for the production of many individual hydrocarbons [5].

In the present research we had as our objective an investigation of the conditions governing the thermal chlorination of n-butane to monochlorobutanes.

EXPERIMENTAL[1]

The raw material we used was n-butane, prepared by rectifying a technical butane-isobutane mixture. Analysis in a Podbielniak column of the n-butane thus prepared indicated that it contained 98-98.5% of n-butane, the impurity being a negligible quantity of isobutane.

The chlorine was secured in cylinders of liquid chlorine, 99.8% pure. The butane was chlorinated in a circulating system.

From a gasholder the butane passed through a scrubber containing a sodium hydroxide solution, a drying column filled with calcined calcium chloride, and a flowmeter to the mixer. The mixer was painted black and protected by a black screen against direct light. The gaseous chlorine entered the mixer through a glass tube from the cylinder, via a Tishchenko bottle filled with sulfuric acid and a flowmeter. The amounts of hydrocarbon and chloride entering the mixer were regulated by appropriate stopcocks according to the flowmeter readings.

From the mixer the reaction mixture traveled to the reaction tube of Pyrex filled with broken pieces of glass tubing. The reaction tube was placed in an electric furnace equipped with a thermoregulator, which made it possible to keep the temperature constant with ±5° in the reaction zone. The diameter of

[1]) The laboratory assistant A. C. Popova took part in the experimental work for this report.

the tube was 28 mm, its volume totaling 332 ml. From the reaction tube the reaction products entered a special trap, placed in a cooler chilled with running water, from which they passed to an auxiliary trap of the coil type, located in a vessel filled with a freezing mixture (temperatures of 0 to -10°). The butyl chlorides condensed in these traps, especially in the first one in line, the unreacted butane and the hydrogen chloride formed in the reaction passing through an intermediate vessel into two absorbers in series, filled with water to absorb the hydrogen chloride. From these absorbers the butane, freed of its hydrogen chloride, passed through a control washer, filled with water and containing methylorange, to check on whether all the hydrogen chloride had been scrubbed out of the gas, and then into a coil trap immersed in a Dewar flask containing liquid air. Almost all the butane condensed in this trap, the negligible quantity of untrapped butane and the inert gases being collected in a gasholder. After the run was over the butane was evaporated from the trap into a separate gasometer, where the amount of unreacted butane was measured, the measured figure later being corrected according to the analysis of the gas.

The liquid chlorination products collected in the traps were transferred to a separatory funnel and washed with water until their reaction was neutral. The wash waters were combined and added to the water from the hydrogen-chloride absorbers. The amount of hydrogen chloride evolved during the chlorination of n-butane was then determined by titrating these waters. The neutralized product was dried above calcium chloride and then fractionated into a glass-packed column with an efficiency of 16 theoretical plates. This fractionation indicated the amount of monochlorides produced.

The percentage of butane in the waste gases was determined by combustion, the percentage of unsaturated hydrocarbons being determined by the customary sulfuric-acid method in the apparatus designed by the All-Union Institute of Heat Engineering. Two Tishchenko bottles, filled with a 20% aqueous solution of potassium iodide and chilled with ice, were inserted in the line ahead of the absorbers in a series of tests designed to determined the optimum reaction temperature. After each run was over, the amount of free iodine evolved was determined by titration with a hyposulfite solution, the per cent of chlorine conversion being calculated from the iodine recovered.

The principal process variables in chlorination are the temperature in the reaction zone, the chlorine-butane ratio, and the space velocity of the reacting gases, i.e., the liters of gas per liter of reaction space.

Variation of the chlorine utilization factor with temperature. The experiments to determine how the chlorine utilization factor varied with temperature were run in a tube that was first empty and then filled with bits of broken glass tubing. The tube was filled in order to ensure a more uniform distribution of heat throughout the reaction space [6]. The tests were made with three to four times the amount of butane required and at a space velocity of the reacting gases approximating 70.

The results of this test series are listed in Table 1 and shown as curves in the figure.

As we see from the tabulated figures, 100% utilization of the chlorine is attained at temperatures approaching 300°. The fact that the reaction sets in at a lower temperature in the reaction tube filled with bits of glass tubing, with the per cent conversion of chlorine remaining higher in that tube than in the empty reactor up to a certain temperature (about 250°), is extremely

interesting. Above this transitional temperature the chlorine utilization factor becomes higher in the empty reaction tube than in the filled one, though 100% conversion of the chlorine is reached at 300° in both reaction tubes.

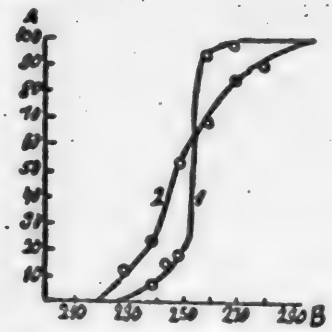

Variation of the chlorine utilization factor with temperature.
A) Chlorine utilization factor, per cent; B) temperature, °C.
1) Empty tube; 2) tube filled with bits of glass tubing.

These observations lead us to assume that the process is heterogeneous at temperatures below 250°, turning into a homogeneous process at higher temperatures.

Thus, n-butane must be chlorinated at 300° to secure 100% conversion of the chlorine, and this was the temperature employed in our subsequent experiments.

Chlorine-butane ratio in the initial mixture, space velocity of the reacting gases, and monochloride yield. As we have stated above, the literature indicates that the chlorine-butane ratio is the decisive process variable in the formation of monochloro derivatives in the chlorination of the paraffins, an increase in the excess of the hydrocarbon tending to raise the percentage of monochloro derivatives. Accordingly, we chlorinated normal butane, using a substantial excess of the hydrocarbon in an effort to secure the maximum percentage of monochlorobutanes. We ran a series of tests of the effect of the excess of butane upon the yield of the monochlorides at 300° and at a space velocity of 12-15. The results of these tests are tabulated in Table 2.

The results of these tests show that a 100% yield of monochloro derivatives cannot be achieved under these conditions, while a substantial excess of butane must be maintained in the reaction mixture to secure an 83% yield of monochlorides, making the per cent conversion of the butane extremely low; moreover, there is a perceptible entraining of the reaction products with the unreacted butane.

In the light of this, we explored the feasibility of raising the yield of monochlorides by increasing the space velocity of the reacting gases. The results of this series of tests are given in Table 3.

TABLE 1

Chlorine Utilization Factor as a Function of Temperature.

Temp.	Chlorine	Temp.	Chlorine
Tube empty		Tube filled	
225	0.0	220	< 1.0
240	7.5	230	12.4
245	15.3	240	24.3
250	17.5	250	53.5
260	94.0	260	70.0
270	99.7	270	85.5
300	100.0	300	100.0

These results indicate that a 100% yield of monochloro derivatives cannot be achieved by merely increasing the space velocity within the limits we have explored, the securing of this yield requiring a certain excess of the hydrocarbon, totaling about 4.5 for space velocities of 32 and above, which is equivalent to approximately 22-23% conversion of butane per single pass. At a maximum space velocity of 500-530, the yield of monochlorides exceeded 3000 grams per hour per liter of reaction space.

TABLE 2

Variation of the Yield of Monochloro Derivatives with the Excess of Butane in the Reaction Mixture.

Test No.	Molar excess of Butane	Conversion of butane, in % of throughput	Monochloride yield, % of total chlorides
5	5	16.6	58.2
22	4.4	19.0	
20	8	9.6	60.6
11	13	6.55	
15	13	7.1	83.25
10	13	6.6	

TABLE 3

Yield of Monochlorides as a Function of the Excess of Butane and the Space Velocity

Test No.	Space Velocity	Molar excess of butane	Monochloride yield, % of total chlorides
52	37.2	2.55	72.2
53	31.8	5.5	100.0
55	31.8	5.5	100.0
56	35.0	4.5	100.0
70	32.0	3.2	81.0
73	35.0	1.95	72.4
63	48.0	1.94	71.2
66	67.0	3.5	78.8
67	67.0	6.8	100.0
54	68.2	4.5	100.0
68	75.0	3.3	76.7
58	92.7	3.7	82.0
57	75.2	6.2	100.0
61	104.0	1.93	78.0
62	181.0	2.74	81.1
39a	500.0	4.7	100.0
43a	530.0	3.5	84.9

Complete utilization of the chlorine was observed in all the tests, the waste gases containing no unsaturated compounds in the runs using a four- or fivefold excess of butane.

Composition of the liquid chlorination products. Two isomers of 1-chlorobutane must be expected during the chlorination of n-butane and the resulting formation of monochlorobutanes. The proportions of these isomers were determined by double fractionation of the monochlorides into a column such as described above, which yielded the following percentages of fractions: 1 - 3.9%; Fraction 2 (67.3-69°): 59.6%; and Fraction 3(73-76.5°): 35.5%.

The mixture was fractionated at 750 mm Hg. The fractions had the following refractive indexes:

	Refractive Index n_D^{20}		Refractive Index of the monochlorobutanes according to the literature
Fraction 2	1.3953	n_D^{25}	of 2-chlorobutane = 1.3953
Fraction 3	1.3994	n_D^{25}	of 1-chlorobutane = 1.4035

The discrepancy between the refractive indexes for 1-chlorobutane is due to the inadequate efficiency of the rectifying column. Hence, approximate ratio of the primary normal and the secondary chlorides is 59.6:36.5 = 1.64:1.

In the experiments run with an excess of butane below 450%, the percentage of chlorine was determined by the Carius method in the monochlorides and in the residue left after the distillation of the monochlorides, the results being as follows:

Sample	% Chlorine by the Carius method
Dichlorobutanes, from the appropriate formula	57.5
Found in the residues after distillation of the monochlorides:	
Sample 1	54.3
Sample 2	54.09
Monochlorobutanes, from the appropriate formula	38.3
Found in the monochlorides:	
Sample 1	37.50
Sample 2	37.43

These results indicate that in those tests in which the chlorination products contained chlorides whose boiling points were higher than those of the monochlorides the residue consisted of dichlorobutanes.

Utilization of catalysts in the chlorination of butane. We ran tests of the use of catalysts to lower the chlorination temperature and to determine the effect of catalysts upon the yield of monochlorobutanes.

The following catalysts were tested: activated charcoal; activated charcoal impregnated with a solution of cupric chloride (5, 10, and 15% of the charcoal by weight); and an aluminosilicate: askarite, likewise impregnated with a cupric chloride solution. The n-butane was chlorinated under the same conditions as those used in the foregoing tests. As the tests showed, these catalysts did not lower the chlorination temperature, while the complete utilization of the chlorine was achieved at 300°, exactly as in purely thermal chlorination. The products obtained when n-butane was chlorinated with the catalysts specified consisted entirely of dichlorobutanes, no attempt having been made to determine the proportions of the various isomers in the reaction products. These results substantiate the feasibility of utilizing a catalyst with a highly developed surface to secure more highly chlorinated products in the chlorination of the paraffins.

Chlorination of propane. Since technical n-butane often contains some propane, we were interested in testing the chlorination of propane under the same conditions as those chosen for our chlorination of butane. The raw material we used was the propane fraction of the cracking gas produced in one of the cracking plants, containing 86.5% propane, 12% propylene, and 1.5% CO_2+H_2S. The gas was washed with a rapid current of concentrated sulfuric acid and then with a 20% solution of sodium hydroxide before being chlorinated to free it of the unsaturated compounds and the hydrogen sulfide. With this exception the experimental procedure was the same as that used for the chlorination of the butane. A 98% utilization of the chlorine was secured at a temperature of 300°, a 450 to 500% molar excess of propane, and a space velocity of about 100. The chlorination products were a mixture of normal propyl chloride and isopropyl chloride; we did not try to determine the proportions of the two in the product.

These tests show that propane is effectively chlorinated under the same conditions as those used to chlorinate n-butane.

SUMMARY

1. 100% utilization of the chlorine is attained at 300° when n-butane is chlorinated. Utilizing an inert packing in the reaction tube lowers the initial

chlorination temperature, but does not lower the temperature at which all the chlorine is utilized.

2. The chlorination products consist entirely of monochlorides when the space velocity of the reacting gases ranges from 32 to 500 and when the molar excess of the butane is 450% and higher. The yield of monochlorides does not exceed 80% when a smaller excess of the hydrocarbon is employed.

3. The high-boiling products formed when butane is chlorinated with an insufficient excess of the hydrocarbon are dichlorobutanes, which were not analysed.

4. The monochlorides consist of 1-chlorobutane and 2-chlorobutane in the proportions of 1:1.64, respectively.

5. The use of catalysts such as activated charcoal and askanite, either pure or impregnated with cupric chloride, results in a 100% yield of dichlorobutanes.

6. Propane is successfully chlorinated under the conditions worked out for the chlorination of n-butane, yielding a mixture of normal propyl chloride and isopropyl chloride.

In conclusion, we wish to express our profound gratitude to Academician S.S. Nametkin and to A.L.Eglin for their invaluable advice and unflagging interest in our research.

LITERATURE CITED

[1] V.V.Markovnikov. Data on the problem of the mutual interactions between atoms in chemical compounds (1869).

[2] N. N. Semenov, Chem. Prog. 5, 321 (1936)

[3] L. S. Solodar and V. V. Markin, Chem. Prog.16, 83 (1947).

[4] H. B. Hass, E. T. McBee, P. Weber, Ind.Eng.Chem ,28,333 (1936)

[5] C. E. Board, A. L. Henne, K. W. Grenlee, Ind.Eng.Chem., 41, 609 (1949)

[6] M. M. Ketslakh, D. M. Pudkovsky, and I. F. Sukhnevich, J.Appl Chem.23, 2,215 [1] 1950.

Received June 9, 1950.

---

[1]) See Consultants Bureau English Translation, p. 221.

POTENTIOMETRIC INVESTIGATIONS OF CUPRAMMONIUM CELLULOSE SOLUTIONS(1)

M. I. Arkhipov and V. P. Kharitonova

Chair of Synthetic Fibers, Ivanovo Institute of Chemical Engineering

In one of our preceding papers [1] we stated that the problem of the nature of the bond between copper and cellulose in the copper-cellulose compound formed in a cuprammonium solution is still unsolved, notwithstanding the large number of research papers dealing with cuprammonium cellulose solutions.

We still do not know exactly whether the compound of copper with cellulose and other polyhydroxyl compounds involves the ordinary chemical bonds, yielding compounds of the alcoholate type, or coordination bonds between copper and the cellulose, or hydrogen bonds, yielding a molecular compound.

Opinions differ as to the nature of the bond between copper and cellulose in a copper-cellulose compound [2,3].

There is as yet no information in the literature on potentiometric investigations of the process of dissolving cellulose or other polyhydroxyl compounds in a cuprammonium solution.

Our potentiometric investigations had as their objective a study of the reaction between the cuprammonium base and polyhydroxyl compounds, including cellulose and particularly the nature of the copper-cellulose bond.

We reasoned as follows: if the reaction between the cuprammonium base and the polyhydroxyl compounds entails the formation of a compound that involves ordinary chemical bonds or hydrogen bonds, the concentration of OH ions ought to decrease substantially, whereas if the copper compounds formed entail coordination bonds, the concentration of OH bonds ought not to manifest any appreciable change. As we had thought, these investigations definitely indicate that the chemical reaction involves a decrease in the concentration of OH ions, i.e., the formation of an alcoholate-like compound or a compound of the molecular type, but not the formation of a compound as the result of coordination of the cellulose and the other polyhydroxyl compounds with the copper atom into a complex cation.

EXPERIMENTAL

Method of measuring the pH. We employed a vacuum-tube voltmeter in measuring the pH of aqueous ammonia and cuprammonium solutions.

Glass electrodes prepared from the glass ordinarily employed for this purpose were used in this determination. The glass electrodes were filled with mercury that had first been freed of its impurities with a chromic acid mixture, washed with distilled water, carefully dried, and steeped in a 0.1N solution of HCl for 10 to 15 days.

Before measuring the pH of the test solutions, the electrodes were washed and calibrated in buffer solutions whose pH had previously been determined with a hydrogen electrode. The buffer solutions employed had the following pH values:

(1)Report III of a series on cuprammonium solutions of cellulose

9.93, 10.70, 11.49, 11.78, 12.03, 12.70, and 12.98. A Weston cell was used as the standard cell.

A calomel electrode was coupled with the glass electrode as a half-cell.

Preliminary measurements of the pH of cuprammonium solutions indicated that a glass electrode ceases to react normally to changes in the concentration of OH ions at high NH_3 concentrations in a highly alkaline medium. The linear variation of the glass-electrode potential with the solution pH no longer applies, the straight line representing the potential as a function of the concentration of OH ions diverging towards the axis of abscissas at a pH >12.8.

Hence, it is impossible to measure the pH very accurately with a glass electrode made of ordinary glass at high concentrations of ammonia and copper in aqueous ammonia and cuprammonium solutions.

We therefore succeeded in making accurate measurements of the pH of cuprammonium solutions only at comparatively low NH_3 and Cu concentrations (up to 50 g NH_3 per liter and up to 0.81 g Cu per liter), while the pH determinations of ammonia solutions were accurate only up to 100 g NH_3 per liter. The accuracy of our pH determinations was inferior, unfortunately, at higher concentrations of NH_3 in aqueous ammonia and at higher concentrations of Cu and NH_3 in cuprammonium solutions.

The glass electrodes were calibrated more frequently than usually at high values of pH, in view of the fact that the potential of a glass electrode varies appreciably with time in highly alkaline solutions.

We employed the following method of measurement to increase the accuracy of our measurements of the pH of the test solutions.

Before use, the glass electrode was calibrated in three buffer solutions whose pH range included the pH of the solution under test, and then its potential was measured in 3 to 5 test solutions, after which it was recalibrated in the same three buffer solutions.

The resultant data were used to plot curves showing the variation of the electrode potential with the pH of the buffer solutions before and after measuring the pH of the test ammonia and cuprammonium solutions.

Knowing the electrode potential in each test solution, we found the respective pH on the assumption that the straight line along which the pH values of the test solutions are located passes halfway between the calibration lines for the electrode in the buffer solutions before and after the measurement of the electrode potential in the test solutions.

Whenever we had to measure the pH of cuprammonium solutions with a high Cu concentration and the electrode's calibration curve bending down toward the axis of abscissas at pH >12.8, we used a large number of buffer solutions for calibration and plotted the corresponding straight line, which bent downward at its end, before and after measuring the electrode potential in the test solutions. We found the pH of the test solution by a method resembling the one described above.

This measurement procedure yielded pH values that were less accurate than in the first method.

The temperature of the solutions was always 18° during the potential measurements.

Determining the pH of ammonia and cuprammonium solutions. We made parallel measurements of the pH of ammonia solutions at various concentrations with hydrogen and glass electrodes in order to compare them and to learn the degree of

accuracy involved. The results of these measurements are given by Curve I in Fig.1.

These results exhibit a fairly satisfactory agreement of the pH values secured with glass and hydrogen electrodes.

The cuprammonium solution was prepared by dissolving $Cu(OH)_2$ in an NH_3 solution, and then diluting with distilled water, or with an NH_3 solution, or with a combination of the two, depending upon the desired concentration of Cu and NH_3 in the working solution. The Cu concentration in the working solution was no more than 0.81 grams per liter before any polyhydroxy compounds had been added.

The $Cu(OH)_2$ was dissolved in the NH_3 solution in such a manner as not to leave any air in the flask in which dissolution was effected, so as to prevent the oxidation of the NH_3 to HNO_2 by atmospheric oxidation. The percentage of Cu in the cuprammonium solutions was determined iodometrically by the Bruhns method [4]. The percentage of NH_3 was determined by back-titration with an H_2SO_4 solution.

The results of our measurements of the pH of cuprammonium solutions containing 0.27, 0.41, and 0.81 grams of Cu per liter, at various NH_3 concentrations up to 3N are shown by the Curves II and III in Fig.1. The curves for the cuprammonium solutions lie far above the curve for the pH as a function of the NH_3 concentration in an ammonia solution, the greater the Cu concentration, the higher being the curve.

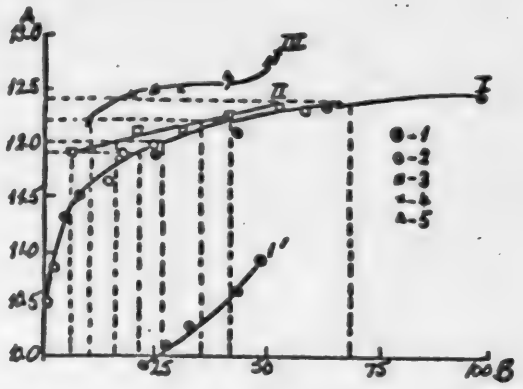

Fig.1. Change in the pH of agueous ammonia and cuprammonium solutions with the NH_3 and Cu in solution. A - Hydrogen ion concentration; B - NH_3 concentration, grams/liter; I - Aqueous ammonia; 1 - measured with a hydrogen electrode; 2 - measured with a glass electrode; I'- aqueous ammonia after part of the NH_3 had been neutralized; II - cuprammonium solution; 3 - Cu concentration = 0.27 grams/liter; III - cuprammonium solutions with the following Cu concentrations in grams/liter: 4 - 0.41, and 5 - 0.81

Determining the pH of cuprammonium solutions of dulcitol. To facilitate our experimental procedure, we used pure dulcitol and sucrose in our investigations.

A cuprammonium solution, prepared as described above, was diluted by adding an accurately weighed quantity of chemically pure dulcitol, the pH of the solution being measured after 2 hours had elapsed (the time required for the establishment of equilibrium in the reaction between the dulcitol and the cuprammonium base). Dulcitol was chosen as the additive to the cuprammonium solution because it has a higher resistance than aldose to oxidation in a cuprammonium solution. Since dulcitol combines with part of the copper, thus lowering the concentration of the free cuprammonium base, the concentration of Cu in the cuprammonium solution may be made much higher than when the pH of cuprammonium solutions is measured without adding any polyhydroxy compounds

(2.33-6.035 grams of Cu per liter, as against 0.27-0.81 grams per liter). Various amounts of dulcitol were added: ranging from 0.020 to 0.250 moles per liter, but always using more or less of an excess over the stoichiometric proportions.

The results of our pH determinations at various Cu concentrations and various Cu: dulcitol proportions in the solution are given in Table 1.

TABLE 1

Change in the pH of Cuprammonium Solutions of Dulcitol as Functions of the Cu Concentration and of the Cu: Dulcitol Ratio.

Solution Composition			Cu: $C_6H_{14}O_6$ ratio, moles/mole	Solution pH
NH_3 grams/liter	Cu Moles/liter	$C_6H_{14}O_6$, moles/liter		
54.4	0.0949	0	-	13.15
		0.200	0.4745	12.60
		0.250	0.3796	12.56
60.37	0.0899	0	-	-
		0.067	1.342	13.00
		0.100	0.899	12.95
		0.125	0.719	12.88
		0.143	0.629	12.87
		0.200	0.499	12.70
42.41	0.0366	0.020	1.830	12.70
		0.025	1.464	12.47
		0.033	1.109	12.40
		0.050	0.734	12.35
		0.100	0.366	12.05
50.56	0.0366	0	-	13.10
		0.020	1.830	13.05

Potentiometric titration of ammonia and cuprammonium solutions, with and without the addition of polyhydroxy compounds. These solutions were titrated with 1.0N and 0.5N solutions of H_2SO_4 as follows.

The given quantity of dulcitol was added to the cuprammonium solution to prepare a working solution by means of dilution, and after two hours had elapsed, the amount of titrated H_2SO_4 calculated to be necessary for neutralization was added, together with an NH_3 solution or distilled water.

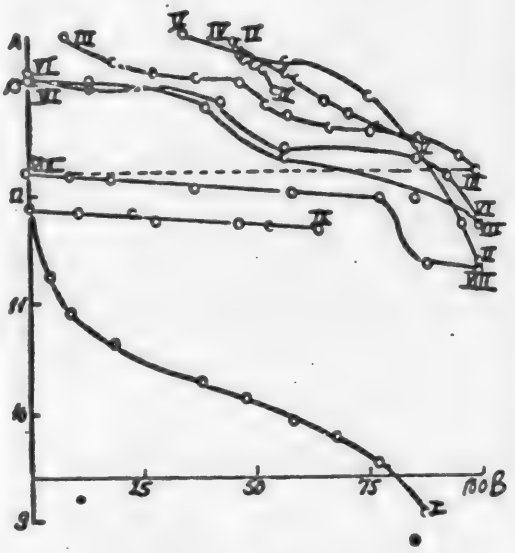

Fig. 2. Titration of ammonia and cuprammonium solutions with and without the addition of polyhydroxy compounds. A - Hydrogen ion concentration; B - per cent neutralization: Curve I - of ammonia; Curves II - IX of copper I - Aqueous NH_3 solution, NH_3 concentration = 53.55 grams/liter; II - VI - cuprammonium solutions with the following concentrations of NH_3 and Cu in grams/liter, respectively: II - 51.34 and 2.54; III - 49.42 and 2.54; IV - 46.75 and 2.67; V - 47.34 and 1.52; VI - 50.56 and 2.33; VII - cuprammonium solution of dulcitol, concentrations as follows: 50.56 grams NH_3 per liter; 2.33 grams Cu per liter; 0.02 mole dulcitol per liter; VIII - cuprammonium solution of sucrose, concentrations as follows: 49.42 grams NH_3 per liter, 2.54 grams Cu per liter; 0.10 mole sucrose per liter; IX - cuprammonium solution of celiulose, concentrations as follows: 48.40 grams NH_3 per liter; 4.13 grams Cu per liter; 0.07 basic mole per liter.

The cuprammonium solution of dulcitol thus prepared contained an ammonium base, a free cuprammonium base, a sulfate of the cuprammonium base, and a cuprammonium base combined with dulcitol.

The cuprammonium solutions that contained no added polyhydroxy compounds and the ammonia solutions were gradually neutralized in the same manner.

After the cuprammonium solutions containing no polyhydroxy compounds had been partially neutralized, part of the copper was present as the respective salt of the complex cuprammonium base, of the free cuprammonium base and of the ammonium base.

In the ammonia solution, after the NH_4OH had been partially neutralized, the solution contained $(NH_4)_2SO_4$, produced when the NH_4OH was neutralized by the H_2SO_4 solution, and the rest of the NH_4OH.

The results of our measuring the pH after neutralization of all these solutions are shown by the curves in Fig.2.

The titration curve of the ammonia solution exhibits that the pH drops sharply as the NH_3 is neutralized, as expressed in per cent of the original NH_3 content of the solution.

If we plot a curve showing the pH as a function of the concentration of the NH_3 left after the ammonia solution has been neutralized with the H_2SO_4 solution, it will occupy the position of and look like the Curve I' in Fig.1. As we see in Fig.1, this curve is much below Curve I.

Evaluation of Results.

Ammonia solutions. As the concentration of the NH_3 in the ammonia solution rises, the concentration of OH ions in the solution and the latter's pH also rise uninterruptedly (Curve I, Fig.1), faster at first, and then comparatively slowly, since the degree of dissociation of the NH_4OH apparently decreases as the concentration of NH_3 rises.

The curve showing the changes of pH resembles the curve showing the changes in conductance as a function of the concentration of NH_3 in the ammonia solution [5].

The degree of dissociation of the ammonia base, NH_4OH, is 0.4-0.5%, as calculated from the pH determinations of dilute solutions on the assumption that all the ammonia in the solution is in the form of NH_4OH. This figure agrees with the degree of dissociation of a dilute NH_3 solution, calculated from the conductance figures [6].

When ammonium sulfate is present in the ammonia solution, the pH drops sharply for a given concentration of NH_3 in the solution, as is shown in Fig.1 (Curve I'), which may be due to a substantial increase in the degree of dissociation of the NH_4OH due to the effect of the identical ion.

We must, therefore, make allowance for the appreciable influence of electrolytes and, especially, of similar ions upon the change of a solution's pH in potentiometric investigations of copper ammoniates and aminates. Some researchers, however, do not take this influence into account [7, 8] in their application of electrometric methods of research on copper ammoniate and aminate solutions. That is why their research findings and conclusions cannot be regarded as correct, but require serious corrections.

Cuprammonium solutions without any polyhydroxy compounds added. The concentration of OH ions in a cuprammonium solution is governed by the presence of two bases in the solution: the ammonium base NH_4OH and the complex cuprammonium base $[Cu(NH_3)m](OH)_2$.

The degree of dissociation of each of these bases differs, varying with the concentration of Cu and NH_3 in the solution and with other factors. Curves II and III in Fig.1 show that even at a low Cu concentration in a cuprammonium solution the solution pH is much higher than that of an ammonia solution for the same NH_3 concentration.

As the Cu concentration of a cuprammonium solution is raised, the concentration of OH ions rises, on the one hand, due to the cuprammonium base, while, on the other, the cuprammonium base, as the stronger base, greatly diminishes the degree of dissociation of the ammonia base.

An increase of the NH_3 concentration in a cuprammonium solution may, and probably does, influence changes in the physicochemical properties of the cuprammonium base, inasmuch as the increase in the concentration of NH_3 in the solution changes the degree of amination of the cuprammonium base.

The concentration of NH_3 in an ammonia solution must be substantially higher than that in a cuprammonium solution to attain the same pH in both solutions.

We worked up the curves of Fig. 1 graphically in order to get an approximate idea of the ratios of NH_3 and Cu concentrations that would ensure a rise in the pH of the cuprammonium solution to a given value and would therefore be equivalent in this respect.

We did this by drawing a series of straight lines parallel to the axis of abscissas, representing constant values of pH, until they intersected the pH-NH_3 concentration curves. Perpendiculars were dropped from these points of intersection, intercepting the axis of abscissas at points that indicated the NH_3 concentration of an ammonia or cuprammonium solution possessing the given pH.

The results of this graphical procedure are given in Table 2.

The last column in Table 2 gives the ratios of the differences between the NH_3 concentrations in ammonia and cuprammonium solutions (ΔNH_3) of the same pH to the Cu concentrations, both in moles. This ratio ranges from 100 to 400, depending upon the Cu concentration. The ratio of the equivalents will range, accordingly, from 50 to 200.

These ratios show that the cuprammonium base is tens of times as strong as the ammonia base. It proved to be impossible to make the same sort of calculation of the degree of dissociation of the cuprammonium base from the results of our potentiometric measurements, since the two bases jointly effected the degree of dissociation. The cuprammonium base, as the stronger of the two, exerts a very marked influence upon the degree of dissociation of the ammonia base.

Cuprammonium solutions of polyhydroxy compounds. The addition of dulcitol, sucrose, and cellulose to a cuprammonium solution always results in a more or less pronounced drop in the pH of the solutions, as is shown by the data in Table 1 and by the Curves VIII and IX in Fig.2.

Adding 0.10 mole of sucrose to one liter of a cuprammonium solution containing 49.42 grams of NH_3 per liter and 2.54 grams of Cu per liter lowered the solution pH to 12.20, i.e., by about one unit.

The pH continues to fall as more dulcitol is added (Table 1), even when the molar ratio dulcitol: Cu = 2-3, i.e., when the polyhydroxy compound is present in substantial excess.

TABLE 2

pH Values at Various Concentrations

pH	NH_3 concentration of an aqueous ammonia solution, moles/liter	Cu and NH_3 content at the same pH of the ammonia solution, moles/liter		Difference between the NH_3 concentrations of the ammonia and cuprammonium solutions at the same value of pH (ΔNH_3)	ΔNH_3. Cu ratio, moles per mole
		Cu	NH_3		
11.90	1.235	0.0042	0.360	0.875	207
12.00	1.559	0.0042	0.941	0.618	147
12.10	1.941	0.0042	1.500	0.441	105
12.20	2.441	0.0042	2.059	0.382	91
12.30	3.088	0.0042	2.647	0.441	105
12.20	2.441	0.0064	0.618	1.823	285
12.30	3.088	0.0064	0.706	3.382	372
12.40	4.049	0.0064	0.882	3.147	491

These results indicate that an equilibrium chemical reaction takes place between the cuprammonium base and polyhydroxy compounds, which may be represented as follows for the general case:

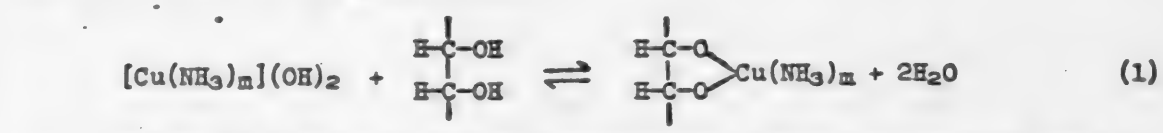

$$[Cu(NH_3)_m](OH)_2 + \text{H–C–OH / H–C–OH} \rightleftharpoons \text{H–C–O / H–C–O}\!>\!Cu(NH_3)_m + 2H_2O \qquad (1)$$

According to Reeves' recent conductometric investigations [9], this reaction takes place with those polyhydroxy compounds that possess a pair of OH groups in a cis position to each other or at an angle of no more than 120°.

This process causes the concentration of OH ions to fall, the more polyhydroxy compound being added and the lower the initial concentration of copper in the cuprammonium solution, the greater the extent of this decrease (Table 1). The solution pH does not drop much when a small amount of the polyhydroxy compound is added to a solution whose copper concentration is rather high (Curves V and VI, Fig. 2.)

This may be explained as follows: the combining of part of the cuprammonium base with the polyhydroxy compound shifts Reaction (1) to the right, but the concentration of OH ions in the solution does not drop or drops but slightly because the loss of OH ions due to the reaction is compensated by the additional dissociation into ions of the undissociated molecules of the cuprammonium base.

When large quantities of polyhydroxy compounds are added (Curves VIII and IX, Fig.2), the pH falls sharply, since the loss of a large proportion of the copper due to its combination with the polyhydroxy compound into an undissociated or slightly dissociated compound is evidently no longer able to be made up by dissociation of the undissociated part of the molecules of the cuprammonium base.

Another process that is theoretically possible is Reaction (2), which may likewise be an equilibrium reaction (giving rise to a molecular compound of the cuprammonium base and the polyhydroxy compound):

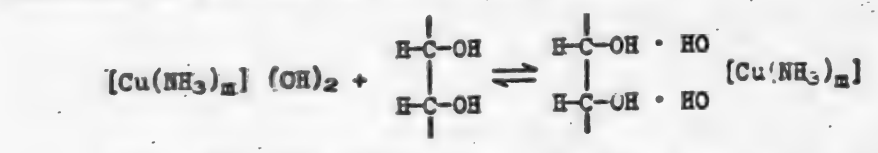

(2)

Here, too, the concentration of OH ions must fall as the cuprammonium base is combined with the polyhydroxy compound. Further research in this field is needed to indicate which of these two processes actually takes place. It seems to us, however, that the second process is hardly likely, since we know that a copper-cellulose compound is fairly stable chemically, which cannot be said of the compound produced in Reaction (2). One thing seems indisputable, however: judging from the results of potentiometric investigations, the bond between the cuprammonium base and the polyhydroxy compound cannot arise as a consequence of co-ordination bonds, with the formation of compounds of the following type, as some researchers have supposed [10]:

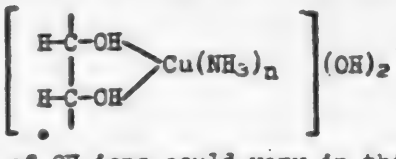

Even if the concentration of OH ions could vary in this case, it could only be as the result of a change in the composition of the complex cuprammonium base.

Potentiometric titration. As ammoniacal solutions are titrated (Curve I, Fig.1), the pH drops sharply, due to a decrease in the number of OH ions as a result of the conversion of part of the NH_4OH into $(NH_4)_2SO_4$, which in turn diminishes the concentration of OH ions by reducing the degree of dissociation of the NH_4OH as an electrolyte that contains the same NH_4^+ ion. The titration curves of cuprammonium solutions (Curves II and VI, Fig.2) lie much higher than the titration curves of an ammonia solution (Curve I, Fig.2) or the titration curves of cuprammonium solutions to which sucrose or cellulose had been added, and exhibit points of inflection at 50% of the back-titrated Cu (Curves III, IV, VI, VII). Whence it follows that there are two stages of dissociation for a cuprammonium base.

The first stage exhibits, as a rule, a higher degree of dissociation than the second one.

The titration curve of a cuprammonium solution of dulcitol, containing 0.020 mole of the latter per liter (Curve VII, Fig.2) and 2.35 grams of Cu per liter, the molar ratio of Cu: dulcitol being 1.83, is close to the titration curve for a solution containing the same percentages of Cu and NH_3, but without any dulcitol (Curve VI, Fig.2), and, like the latter curve, has a point of inflection at the neutralization point of approx 50% Cu.

This is apparently due to the fact that under these conditions only a small portion of the cuprammonium base combines with the polyhydroxy compound, which is insufficient to exert any appreciable influence upon a decrease in the pH at the start of titration or upon the nature of the titration curve.

The titration curves of cuprammonium solutions of sucrose and cellulose, containing 0.100 and 0.070 moles per liter, respectively, are located much lower and exhibit no point of inflection at the neutralization of 50% of the Cu

Obviously, in these instances most of the cuprammonium base is combined with the polyhydroxy compound, and the pH at the start of titration is 50% lower than the pH of the solution.

Titration curves of such shape may, we believe, be explained as due to the fact that as titration proceeds the reactions (1) or (2) are reversed.

As titration proceeds, the concentration of the free cuprammonium base that is not combined with the polyhydroxy compound gradually diminishes, while the sulfate of the cuprammonium base accumulates. The reaction proceeds from left to right. The pH gradually diminishes until all the cuprammonium base combined with the polyhydroxy compound has been freed from that compound.

As Curve VIII, Fig.2, indicates, the cuprammonium compound of sucrose is completely decomposed when more than 77.5% of the Cu is neutralized. The point of inflection of the curve, located at the point where the further neutralization of the Cu has progressed to about 87.5%, shows that when the cuprammonium polyhydroxy compound was completely decomposed, the solution contained about 25% of free cuprammonium base in terms of the total copper in the solution.

In conclusion we wish to express our warm gratitude to Prof.A.B.Pakshver for his invaluable counsel and guidance during the foregoing research.

SUMMARY

1. It has been shown that a cuprammonium base has a higher concentration of OH ions than an ammonia base, the concentration of OH ions of the ammonia base dropping sharply when a similar ion is present in the solution.

2. In titrating a cuprammonium solution a point of inflection is found to exist on the titration curve when about 50% of the Cu has been neutralized, which is an indication of two-stage dissociation of the cuprammonium base.

3. The addition of polyhydroxy compounds to a cuprammonium solution causes a more or less substantial drop in the solution pH, the lower the initial concentration of Cu in the solution and the more of the polyhydroxy compound added, the greater the pH drop, which may be due to a binding of part of the cuprammonium base in accordance with Equations (1) or (2).

LITERATURE CITED

[1] M.I.Arkhipov and V.P.Kharitonova, J.Appl.Chem.22, 761 (1949).
[2] P.P.Shorygin. The chemistry of cellulose, 140-150. Moscow: State Chemical Press (1939).
[3] A.B.Pakshver. The Technology of Cuprammonium fiber, 54-58. Moscow-Leningrad: State Light Industry Press.
[4] Treadwell and Hall. Treatise of analytical chemistry: Volumetric and gas analysis (Russ.ed.), 165 Moscow: United Scientific and Technical Press (1935).
[5] W.Bonsdorff, Z.allg.Anorg. Ch., 41, 132-192 (1904).
[6] O.Morgan, O.Maas, Canad. J.Research., 5, 190 (1931).
[7] F.Koch., J.Chem.Soc., London, 1418-1421 (1931).
[8] G.Carlson, J. McReynolds, .F.Verchoek, J.Am. Chem. Soc., 67, 8, 1334 (1945).
[9] R.Reeves, J.Am. Chem. Soc., 71, 209, 212, 215, 1737, 2117 (1949).
[10] K.Hess and E.Messmer, Ber., 55, 2432 (1922).

Received October 10, 1949.

BLANK
PAGE

COLORED FILMS BASED ON A SYNTHETIC BINDER

A. V. Pamfilov and E G. Ivancheva

Laboratory of Inorganic and Colloid Chemistry, University of Chernovtsy

The general trend in the technology of film-forming materials is more and more toward the use of synthetic products. This evolution, which has fairly well-known parallels in other branches of the chemical industry, is due to the short supply of drying oils and to an endeavor to produce coatings of higher quality. The most promising at the present time are combinations of polyatomic acids with polyhydric alcohols, the so-called alkyd resins, combined with vegetable oils or with the fatty acids derived from these oils-the modified alkyd resins [1,2].

Products of this sort remain, at least for the present, tied to vegetable oils as sources of the fatty acids and glycerol, though the range of oils available to the paint and lacquer industry has been extended considerably by the feasibility of using semidrying and nondrying oils; this also involves a substantial saving in oil.

The present report is a study of the time changes in the mechanical properties of pigmented films made by various film-forming materials under room and outdoor conditions and of the reactions of these film-forming materials with the pigments they contain. As we have pointed out previously [3], research of this type has as its objective a study of the mechanical properties of the films as such, disregarding the surface to which they are applied in their practical applications as protective coatings. Hence, the poor mechanical indexes of the film itself reported in this paper is no evidence of the uselessness of the given coating under operating conditions in general. (The problem of the anticorrosion qualities of a coating is not dealt with in this paper) The findings are, however, basic to a differentiated study of the processes occurring in films, which furnish material, we believe, for the evaluation of their properties and quality as a whole. The 'aging' of these films is itself of interest from the standpoint of applied colloid chemistry, to be sure, it also affects the operational qualities of the coating.

Samples of three types of resin alkyd glyptal, pentaphthal, and superbeckasite, were used in this research.

During the past two decades alkyd phthalic resins have secured for themselves a rather permanent place in the paint and dye industry The superiority of higher polyatomic alcohols than glycerol as constituents of film-forming materials of this type is stressed by Drinberg, who has investigated the effect of increasing the atomicity of the alcohol to be combined with the fatty acids upon the rate of film formation [4,5]. Resins based on pentaerythritol, a comparatively readily accessible alcohol from the manufacturing standpoint, have been special y recommended by that author and have been used industrially.

The Superbeckasite 1001 tested by us is one of the 100% phenolic resins for lacquers and consists of a combination of normal tert-butylphenol with formaldehyde. In view of the brittleness disclosed in preliminary tests, it was combined with the oil in ratios at least twice those called for in the literature [6].

We used three samples of modified glyptal resins: Alkydal T, Alkydal ST, the glyptal resin FL-39 (in the first and third preparations the resins were prepared by combining with linseed oil, and in the second, with castor oil), the pentaphthalic resin PFL-37, and Superbeckasite 100,. Some of the characteristics of these resins are given in Table 1.

TABLE 1

Characteristics of Resins

Resin composition, %	Acid Number	Saponification number	Hanus iodine number	Combustion residue, %
Alkydal T in linseed oil, 48% fat	14.5	360	86	0.06
Alkydal ST in castor oil, 58% fat.	20.0	312	75	0.03
FL-39 resin: 15.76% glycerol 28.38% phthalic anhydride, 45.86% linseed oil, 10.5% rosin.	13.2	290	91	0.05
PFL-37 resin: 11.0% pentaerythritol, 19.66% phthalic anhydride, 69.0% linseed oil, 0.34% lead lineolate.	9.8	270	110	0.14

EXPERIMENTAL

The resin sample was dissolved by heating it to 100° in its own weight of turpentine. The siccative used was a turpentine solution of lead and manganese resinates, containing 0.48% lead and 0.12% manganese, in terms of the resin. These solutions were given the following lacquer designations: Lacquer 1-T: a solution of the Alkyldal T resin in turpentine; Lacquer 2-ST: a solution of the Alkydal ST resin in turpentine; Lacquer 3-FL; a solution of the glyptal resin FL-39 in turpentine; Lacquer 4-PFL: a solution of the pentaphthalic resin PFL-37 in turpentine; Lacquer 6: 60 parts of tung oil, 10 parts of linseed oil, 30 parts of superbeckasite, and 60 parts of turpentine, with a lead-manganese siccative; and Lacquer 7: 20 parts of Superbeckasite, 40 parts of linseed oil, and 30 parts of turpentine, with a lead-manganese siccative.

Pigments were rubbed into these prepared lacquers. In addition to the two "active" pigments previously employed, red lead and zinc oxide, so-called because of their marked reaction with the oil and their accelerating effect upon the aging of the film, and the "inactive" pigments, red ocher and chromic oxide, we also employed lead chromate – a pigment widely used to produce greens, that has no harmful effect upon film-forming materials. Red lead is often employed in combination with a glyptal priming coat.

The rubbed paste was diluted with turpentine to paint consistency and then applied with a brush as rapidly as possible to amalgamated tinplate sheets. After the first coat had dried at ordinary temperature, a second coat was applied. The paint samples were kept out-of-doors and indoors and periodically tested in a Schopper apparatus for mechanical strength.

As the data in Figs. 1 – 12 indicate, nearly all the pigmented films that were kept out-of-doors soon became brittle and unsuitable for tensile tests. In the

more stable samples, this failure appeared after about four months of exposure. The unpigmented films became brittle out of doors in the same interval of time.

The films that contained zinc white and red lead broke down especially fast. Within one and a half to two months the surfaces painted with these pigments were covered with a network of cracks, reaching down to the priming coat in some areas of the painted surface. In order to eliminate any possible influence of the amalgamated surface, the paint paste was applied directly to iron sheets, which were

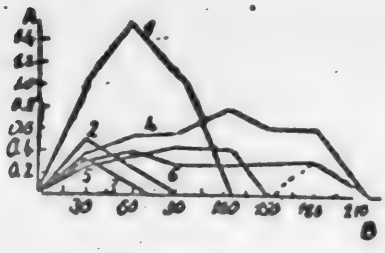

Fig. 1 Tensile strength (σ) of pigmented films of Lacquer 1-T; out-of-doors

A - σ, kg/sq mm; B - time, days. 1 - Lacquer without pigment; 2 - zinc oxide; 3 - red lead; 4 - iron ocher; 5 - chromic oxide; 6 - lead chromate.

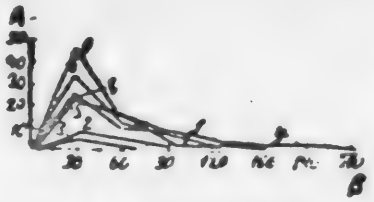

Fig. 2. % elongation (λ) of pigmented films of Lacquer 1-T; out-of-doors.

A - λ, %; B - Time, days. 1 - Lacquer without pigment; 2 - zinc oxide; 3 - red lead; 4 - iron ocher; 5 - chromic oxide; 6 - lead chromate.

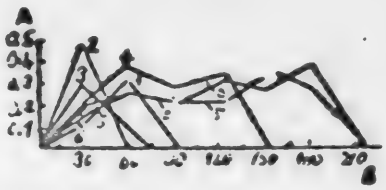

Fig. 3. Tensile strength (σ) of pigmented films of Lacquer 2-ST; out-of-doors

A - σ, kg/sq mm; B - time, days. 1 - Lacquer without pigment; 2 - zinc oxide; 3 - red lead; 4 - iron ocher; 5 - chromic oxide; 6 - lead chromate.

exposed out-of-doors. Here, too, cracks formed. The orange color of the red lead paint took on the typical whitish hue. We kept a roof that had been painted with red lead in a glyptal lacquer under observation for some time. Soon after painting, the presence of whitish free lead oxide and precipitated lead dioxide could be detected visually. The paint broke down badly fairly soon.

The pigmented and unpigmented films made of lacquer using the glyptal resin FL-39 were least resistant. The films of this lacquer, containing the specified pigments, became brittle after exposure out-of-doors for two or three months. Some films age rapidly even when kept indoors;[1] this is true, for instance, of the same Lacquer 3-FL. The brittleness of the films is evidently governed by the properties of the film-forming material.

Some films exhibited a complete loss of elasticity within brief intervals of time even when tested on the Lacquer and Paint Research Institute elasticity scale. The Alkydal T resin and the glyptal resin FL-39 were tested with a higher percentage of linseed oil, using equal parts of the oil of the resin, in order to find less brittle combinations. But even in this proportion, the films of both lacquers became brittle after two months of exposure out-of-doors, when pigmented with zinc oxide and red lead.

Superbeckasite is characterized by the low stability of films of the unpigmented lacquer out-of-doors. But indoors, when the slowly forming film has the chance to ripen completely, this resin exhibits high mechanical strength, distinguishing it from the other resins tested.

[1] We cite no data on the tests of films aged indoors in this paper.

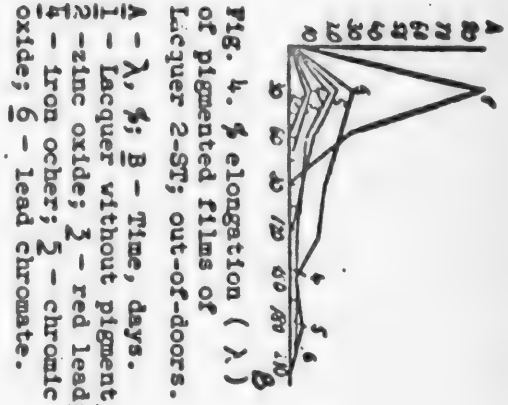

Fig. 4. % elongation (λ) of pigmented films of Lacquer 2-ST; out-of-doors.

A - λ, %; B - Time, days. 1 - Lacquer without pigment; 2 - zinc oxide; 3 - red lead; 4 - iron ocher; 5 - chromic oxide; 6 - lead chromate.

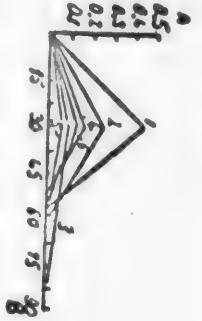

Fig. 5. Tensile strength (σ) of pigmented films of Lacquer 3-FL; out-of-doors.

A - σ, kg/sq mm; B - time, days. 1 - Lacquer without pigment; 2 - zinc oxide; 3 - red lead; 4 - iron ocher; 5 - chromic oxide; 6 - lead chromate.

Fig. 6. % elongation (λ) of pigmented films 3-FL; out-of-doors.

A - λ, %; B - Time, days. 1 - Lacquer without pigment; 2 - zinc oxide; 3 - red lead; 4 - iron ocher; 5 - chromic oxide; 6 - lead chromate.

TABLE 2

Reaction of the Resins with the Pigments in the Films

No.	Composition of the film		Metallic oxide in the soluble portion of the film as a percentage of the film-forming material (time in hours as the numerator; per cent of the metallic oxide as the denominator).								
	Per cent pigment	Per cent resin									
		FL-39									
1	Lead oxide, 69.2....	20.8	2/15.7	2/19.0	11/31.6	11/34.6	30/34	20/36	30/27	20/28.3	30/27.7
2	Red lead, 86.3	13.7	1/18.4	30/25.3	20/28.3	30/25.0	-	-	-	-	-
3	Zinc oxide, 74.8....	25.2	2/20.0	2/18.0	11/18.7	11/18.3	-	-	-	-	-
4	Zinc oxide, 66.6....	33.4	1/7.3	10/7.4	10/8.0	-	-	-	-	-	-
5	Red ocher, 69.6.....	30.4	1/3.2	10/3.8	10/3.8	-	-	-	-	-	-
6	Lead chromate, 68.1.	31.9	1/traces	30/2.7	30/1.8	-	-	-	-	-	-
7	Chrome oxide, 70.0..	30.0	1/traces	10/2.7	10/1.8	-	-	-	-	-	-
		PFL-37									
8	Red lead, 82.3.....	17.7	1/18.6	10/28.2	10/31.4	-	-	-	-	-	-
9	Zinc oxide, 74.0....	26.0	1/8.4	1/9.0	10/2.0	(The film dissolved sparingly in the dichloroethane after 10 days of exposure)					
10	Red ocher, 73.8.....	26.2	1/1.8	1/1.6	10	(The film did not dissolve)					

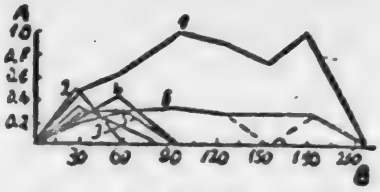

Fig. 7. Tensile strength (σ) of pigmented films of Lacquer 4-PFL; out-of-doors.

A - σ, kg/sq mm; B - time, days. 1 - Lacquer without pigment; 2 - zinc oxide; 3 - red lead; 4 - iron ocher; 5 - chromic oxide; 6 - lead chromate.

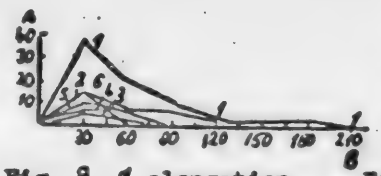

Fig. 8. % elongation (λ) of pigmented films of Lacquer 4-PFL; out-of-doors.

A - λ, %; B - Time, days. 1 - Lacquer without pigment; 2 - zinc oxide; 3 - red lead; 4 - iron ocher; 5 - chromic oxide; 6 - lead chromate.

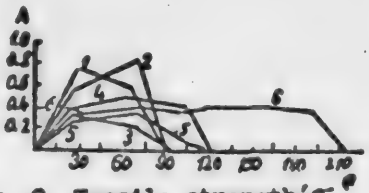

Fig. 9. Tensile strength (σ) of pigmented films of Lacquer 6; out-of-doors.

A - σ, kg/sq mm; B - time, days. 1 - Lacquer without pigment; 2 - zinc oxide; 3 - red lead; 4 - iron ocher; 5 - chromic oxide; 6 - lead chromate.

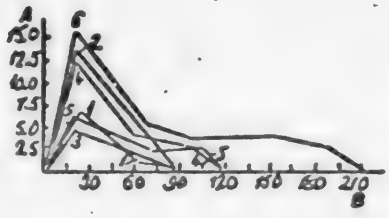

Fig. 10. % elongation (λ) of pigmented films of Lacquer 6; out-of-doors.

A - λ, %; B - Time, days. 1 - Lacquer without pigment; 2 - zinc oxide; 3 - red lead; 4 - iron ocher; 5 - chromic oxide; 6 - lead chromate.

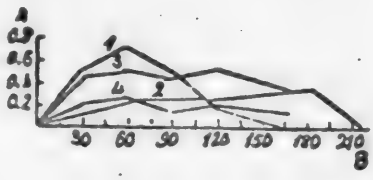

Fig. 11. Tensile strength (σ) of pigmented films of Lacquer 7; out-of-doors.

A - σ, kg/sq mm; B - time, days. 1 - Lacquer without pigment; 2 - zinc oxide; 3 - red lead; 4 - iron ocher

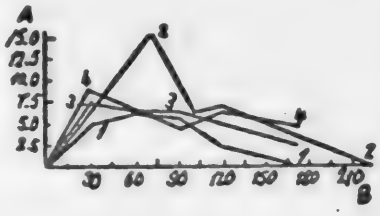

Fig. 12. % elongation (λ) of pigmented films of Lacquer 7; out-of-doors.

A - λ, %; B - Time, days. 1 - Lacquer without pigment; 2 - zinc oxide; 3 - red lead; 4 - iron ocher.

We have tested films made of Lacquer No.15, which proved to be unsatisfactory [7]. It may be that this is due to the presence of rosin in this lacquer. The low quality of rosin as a resin, especially its brittleness, is common knowledge. This negative quality is also exhibited by the synthetic resins we have tested, which therefore, cannot be regarded as satisfactory film-forming materials.

The rapid loss of elastic properties by the pigmented lacquer films is clearly shown in the graphs of per cent elongation (Figs. 2,4,6,8,10,12).

Interaction with pigments. We tested the interaction of the pigment with the binder for the glyptal resin FL-39 and the pentaphthalic resin PFL-37. The

pigmented films of the first of these resins break down rather rapidly, the second one being much stronger. The method of measurement has been described before [8]. Dichloroethane was used as the solvent this time. The pigments were rubbed into turpentine solutions of the resins, the pastes being applied to glass plates. A weighed sample of the resultant film was removed at regular intervals and dissolved by boiling it in dichloroethane.

Here, too, the lead oxides and red lead reacted most energetically with the alkyd resins (Table 2). The solutions of films of these resins containing these additives were yellowish, transparent, and separated very readily from the unreacted pigment, sometimes even in simple suction filtering, without centrifuging.

It was much harder to separate zinc oxide from similar solutions of pigmented films. The percentage of zinc oxide that reacted with the resin was likewise high, especially in Test 4, Table 2. The percentage of zinc oxide, as calculated from the resin's saponification number, was 21%, while a determination made for this combination after two days yielded as much as 20%. Small percentages of ferric oxide, chromic oxide, and lead chromate were found in the portion of the respective film that was soluble in dichloroethane. But these solutions were turbid even after prolonged centrifuging, so that there was a residue after calcining, due possibly to a highly disperse stabilized portion of the iron ocher and chromic oxide. The solubility of pigmented films of the alkyd resins decreases with time, so that the metallic oxide as a percentage of the amount of resin initially present in the paste decreases.

SUMMARY

1. The mechanical properties of the tested pigmented films of some synthetic film-forming materials grow worse fairly rapidly with time.

2. These films are inferior to films of prepared linseed oil in point of their rapid embrittlement.

3. The films in some samples age rapidly indoors as well as out of doors.

4. The resins react rather energetically with the pigments in the films.

5. The unsatisfactory qualities of the aged films, as far as their mechanical properties are concerned is not an unequivocal indication of the operational properties of coatings made from these film-forming materials.

LITERATURE CITED

[1] V. S. Kiselev. Paint Vehicles and lacquers, 3rd ed., 183. State Chemical Press (1940)

[2] A. Ya. Drinberg. The technology of film-forming substances, 410. State Chemical Press (1948).

[3] A. V. Pamfilov and E. G. Ivancheva, J.Appl.Chem. 20, 7, 676 (1947).

[4] A. Ya. Drinberg and A. A. Blagonravova, J.Gen.Chem 5, 126 (1935).

[5] A. Ya. Drinberg, Trans. Leningrad Inst. Tech. 14, 7 (1947).

[6] G. S. Petrov, B. N. Rutovsky and I. P. Losec. The technology of synthetic resins and plastics, 183. State Chemical Press (1946).

[7] A. V. Pamfilov, E. G. Ivancheva, and V. P. Granenova, J.Appl.Chem 22, 1, 87 (1949).

[8] A. V. Pamfilovand E. G. Ivancheva, J.Appl.Chem.21, 2, 104 (1948).

Received May 3, 1950.

THE VARIATION OF THE VISCOSITY OF PHOTOGRAPHIC EMULSIONS AND GELATIN SOLUTIONS WITH TEMPERATURE

M. I. Shor

Leningrad Institute of Motion-Picture Engineering

There is extremely little to be found in the technical literature on the variation of the viscosity of high-molecular compounds with temperature, despite the tremendous importance of this problem for various industries that use or process high-polymer compounds.

In one of our earlier papers [1] we managed to establish the temperature variation of viscosity of concentrated solutions of nitrocellulose in an alcohol-ether mixture.

We were interested in establishing the variation with temperature of the viscosity of solutions of gelatin and similar photographic emulsions, which are suspensions of a silver halide in water-gelatin medium.

Among the qualititative expressions for the viscosity of photographic emulsions as a function of temperature, only one is referred to: Bogomolov's [2], which has been put forward in the following empirical formula:

$$\eta = \frac{B}{\sqrt{t - t_{gel}}} \qquad (1)$$

where η is the emulsion viscosity in centipoises; t is the emulsion temperature in °C; t_{gel} is the gelling point of the emulsion in °C; and B is a constant that is a characteristic of each separate emulsion.

The gelling temperature, t_{gel}, is given approximately by the following temperature:

$$t_{gel} = 22.8 + 0.13\eta_{39} \qquad (2)$$

where η_{39} is the viscosity of the emulsion in centipoises at 39°C.

According to Fedorov [2], this formula works out rather well in practice; Deryagin also reports that it is satisfactory for practical purposes.

Kotova also checked the applicability of Bogomolov's empirical formula in the 30-40°C range, finding that there were no perceptible departures from the Bogomolov formula at temperatures above 35°C, while at temperatures below that point substantial deviations appear, apparently due to a change in the structure of the solution, which render the use of the formula impossible.

In addition to the limited applicability of the Bogomolov formula, another of its disadvantages is the fact that the constant B has to be determined anew for every emulsion and gelatin solution.

The present paper represents an effort to establish a different empirical relationship between viscosity and temperature that is free of the foregoing deficiencies.

Following the procedure employed in the plants of the photographic chemical industry, we measured viscosity in relative units, using the Zhimsky viscosimeter. The principle underlying the operation of this viscosimeter is the time that a tube of special design, fitted with a capillary (Fig.1), remains immersed in the test liquid, compared to its immersion time in water. The research laboratory of the Photo Paper Factory No.4 has calculated the equivalents of Zhimsky degrees (°Zh) in degrees Engler (°E) in centipoises. Their table has been checked by Deryagin and his co-works, using an Ubbelohde viscosimeter, and found to be suitable for use in practice.

Using this table, we have derived the equation $\eta_{centip} = \psi(\eta_{centip}: \eta_{Zh})$ (Fig.2) and derived the following empirical formula:

$$\eta_{centip} = \eta_{Zh}(1 - 0.014\,\eta_{Zh}), \qquad (3)$$

which we employed to convert viscosity from degrees Zhimsky to centipoises.

In the first series of test we measured the viscosity of photographic emulsions in the 30-40 °C range, the viscosity of the original emulsions being varied at intervals of 0.5° Zh by means of suitable dilution with water.

Fig.1 Zhimsky viscosimeter.

Fig.2. η_{centip} as a function of the $\frac{\eta_{centip}}{\eta_{Zh}}$ ratio.
A - viscosity (°Zh);
B - $\frac{\eta_{centip}}{\eta_{Zh}}$ ratio.

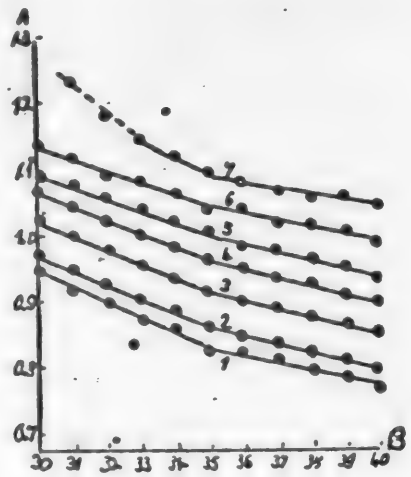

Fig. 3. The equation $\log\eta = \psi(t)$ for photographic emulsions of various dilution. A - logarithm of viscosity; B - temperature, °C. Initial emulsion viscosities, in centipoises: 1 - 5.8, 2 - 6.2, 3 - 7.0, 4 - 7.7, 5 - 8.5, 6 - 9.7, 7 - 11.0.

Figure 3 shows that the equation $\log\eta = \psi(t)$ is a straight line in the 35-40°C range, after which there is a discontinuity in each curve, followed by another straight line with a somewhat greater slope. The intersections of these straight-line sections are all located at 35-35.5°C. The slopes of most of the right-hand straight lines are given by tangent $\alpha = K_1 = 0.012$-0.013 (Table 1), with a tendency for the slope to drop to 0.009-0.011 for more highly viscous

emulsions. The left-hand sections of the curves have a slope of $K_2 = 0.020$, and they, too, exhibit a tendency for the slope to diminish as the viscosity of the initial emulsions rises. The left-hand branch of the curve for $\eta_{40} = 11.0$ is considerably distorted, possibly owing to the extremely high viscosities involved ($\eta > 14$ centipoises or $>18.5°$ Engler), which parenthetically, are of no practical importance in the technology of photographical chemical manufacture.

We may conclude from the foregoing that in the cases considered the possible occurrence of structural phenomena involves no fundamental violation of the temperature variation of viscosity, but merely introduces a correction, involving a greater slope of the curve.

The analytical interpretation of the curves in Fig. 3 makes it possible to formulate the following equation for each individual branch:

$$\log \eta_1 - \log \eta_2 = K(t_2 - t_1) \tag{4}$$

or

$$\eta_1 = \eta_2 \cdot 10^{K(t_2 - t_1)} \tag{5}$$

where η_1 and η_2 are the respective viscosities at the temperatures t_1 and t_2, and K is the slope.

TABLE 1

Slope Coefficient of the $\log \eta = \Psi(t)$ Curves

No.	Initial emulsion viscosity, centipoises.	Slope coefficients	
		K_1 in the 35-40°C range.	K_2 in the 30-35°C range.
1	5.8	0.011	0.023
2	6.2	0.012	0.022
3	7.0	0.013	0.021
4	7.7	0.013	0.020
5	8.5	0.012	0.012
6	8.7	0.011	0.017
7	11.0	0.009	0.025

Taking t_2 as 40°C (the standard temperature at which viscosity is measured), the corresponding viscosity $\eta_2 = \eta_{40}$ is as follows for the right-hand branch of the curve:

$$\eta t = \eta_{40} \cdot 10^{K_1 (40 - t)}. \tag{6}$$

while the viscosity for the left-hand branch is:

$$\eta t = \eta_{35} \cdot 10^{K_2 (35 - t)}. \tag{7}$$

After recomputing η_{35} in terms of η_{40}, we get the following equation for the left-hand branch:

$$\eta t = \eta_{40} \cdot 10^{5K_1 + K_2 (35 - t)} \tag{8}$$

which may be used to calculated the viscosity at any temperature once we know the viscosity at 40° (if we are to caculate the viscosity at $t > 35°$, we can set $K_1 = K_2$).

Taking the mean values of K_1 and K_2 from the curves in Fig. 3 (0.012 and 0.020, respectively, we get Equations (6) and (8) in the following forms:

$$\eta t(t > 35) = \eta_{40} \cdot 10^{0.48 - 0.012t} \tag{9}$$

$$\eta t(t < 35) = \eta_{40} \cdot 10^{0.76 - 0.02t} \tag{10}$$

Differentiating Equation (9) yields the temperature coefficient of viscosity:

$$\alpha \eta t = \frac{- \eta_{40} \cdot 10^{0.48 - 0.012t} \cdot 0.012 \, dt}{\log e}$$

but since

$$\eta_{40} \cdot 10^{0.48 - 0.012t} = \eta_t,$$

we get

$$\frac{d\eta_t}{dt} = -\frac{0.012}{0.43}\eta_t = -0.028\ \eta_t, \qquad (11)$$

i.e., the temperature coefficient of viscosity is a function of the viscosity itself, a change of 1° in temperature causing an inverse change of 2.8% in viscosity. For temperatures below 35°, the corresponding figure is 4.6%.

This problem was developed still further in research undertaken by the author in conjunction with Kapinos. The objective of the research was to make a study of the temperature variation of viscosity over a wider temperature range, and to define the factors affecting the value of K.

The research was done on gelatin solutions in the 35-71°C range. Of all the factors that may affect the value of K, we chose the chromium number as an index of the extent to which the gelatin is hydrolyzed, and the concentration of the gelatin solution.

The characteristics of gelatin solutions are given in Table 2 as affected by the initial variables.

TABLE 2

Characteristics of Gelatin Solutions

Gelatin Chromium number	Solution Concentration %					
	5		7		9	
	Zh	Centip.	Zh	Centip.	Zh	Centip.
3.4	3.5	3.3	6.4	5.8	10.5	9.0
2.4	4.1	3.9	7.6	6.8	12.8	10.5
1.0	5.9	5.4	11.1	9.4	17.4	14.0

TABLE 3

Values of K for Various Gelatin Solutions

Gelatin chromium number	Values of K, Solution concentration, %		
	5	7	9
3.4	0.0098	0.0092	0.0090
2.4	0.0093	0.009	0.009
1.0	0.0098	0.0092	0.0092

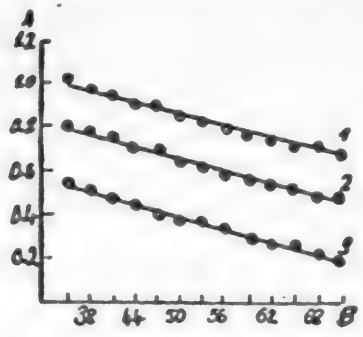

Fig. 4. $\log\eta = \psi(t)$ for gelatin solutions of various concentrations. Gelatin chromium number = 3.4
A - Logarithm of viscosity; B - temperature, °C. Solution concentrations, per cent: 1 - 9; 2 - 7; 3 - 5.

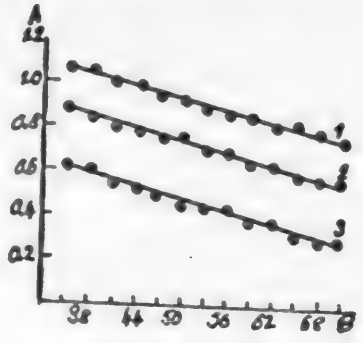

Fig. 5. $\log\eta = \psi(t)$ for gelatin solutions of various concentrations. Gelatin chromium number = 2.4
A - Logarithm of viscosity; B - temperature, °C. Solution concentrations, per cent: 1 - 9; 2 - 7; 3 - 5.

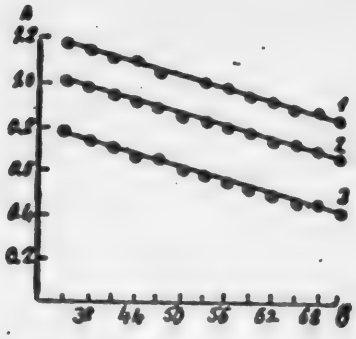

Fig. 6. $\log \eta = \psi(t)$ for gelation soiutions of various concentrations. Gelatin chromium number = 1.0. A - Logarithm of viscosity; B - temperature, °C. solution concentrations, per cent: 1 - 9; 2 - 7; 3 - 5.

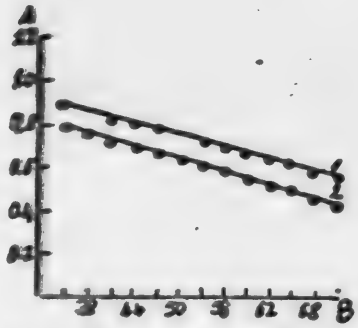

Fig. 7. $\log \eta = \psi(t)$ for gelatin solutions hardened with chrome alum. A - Logarithm of viscosity; B - temperature, °C. 1 - Chromium number 2.4, C 5%, K 0.01; 2 - Chromium number 3.4, C 7%, K 0.01.

We see from Figs. 4, 5, and 6 that the linearity of the function $\log \eta = \psi(t)$ previously established for the 35-40° range also applies to the 35-71° range. As for the values of the constant K, it exhibits a slight tendency to fall with rising concentration of the gelatine solution, as is seen in Table 3.

On the whole, the value of K is close to 0.01 in every case, or somewhat lower than the previously established value of 0.012.

The following discussion tells us whether it is allowable to employ mean values of K and the precision of computation required in calculating this coefficient to satisfy the practical demands of the technology of applying the emulsion to a flexible backing.

In the equation derived by Deryagin for the thickness of applied emulsion coatings as a function of its governing factors [3], viscosity figures as a factor with an exponent of 2/3, so that the coating thickness is

$$H = \psi(\eta)^{\frac{2}{3}}.$$

Thickness deviations of the order of ±5% are quite tolerable in the operational application of emulsion coatings. This yields the following allowable viscosity deviation:

$$\frac{H'}{H''} = \left(\frac{\eta'}{\eta''}\right)^{\frac{2}{3}} = 1.05,$$

whence:

$$\frac{\eta'}{\eta''} = 1.05^{\frac{3}{2}} = 1.08,$$

or 8%,

On the other hand, from Equation (6):

$$\frac{(\eta t)'}{(\eta t)''} = 10^{(K_1' - K_1'')(40 - t)}$$

Computing the viscosity for a temperature that differs from the initial figure by 5°, we get $40 - t = 5$, and

$$5(K_1' - K_1'') = \log 1.08 = 0.034$$

or

$$K_1' - K_1'' = 0.007$$

Hence, even if we take the extreme values of K secured in the first series of tests (Fig. 3) and in the second series (Figs, 4, 5 and 6), 0.013 and 0.009, we get a $\Delta K = 0.004$, or a deviation that fully satisfies the practical requirements. In general, K may be calculated to two significant figures.

Since hardened emulsions are employed in practice, we also tested the effect of chrome alum in the gelatin solution upon the value of K. No change in K was observed (Fig. 7).

SUMMARY

1. The variation of the viscosity of gelatin solutions (photographic emulsions) with temperature is linear within the temperature range investigated (30-71°C), with a discontinuity at a temperature approximating 35°C.

2. The analytical function $\eta = \psi(t)$ for each branch of the curve may be expressed by the exponential formula:

$$\eta_{t_1} = \eta_{t_2} \cdot 10^{(t_2 - t_1)},$$

resembling the one previously derived for solutions of nitrocellulose.

3. The values of the constant K may be taken to be 0.01 and 0.20, respectively, for temperatures above and below 35°. On the basis of the standard measurement of viscosity at 40°C, we can recommend the use of the following equations for practical purposes:

$$\eta t(t > 35) = \eta_{40°} \cdot 10^{0.40 - 0.01t}$$

and

$$\eta t(t < 35) = \eta_{40°} \cdot 10^{0.75 - 0.02t}$$

or the following numerical values of the temperature coefficient of viscosity.

$$\frac{d\eta}{dt}_{(t > 35)} = -0.025\eta$$

and

$$\frac{d\eta}{dt}_{(t < 35)} = -0.05\eta$$

LITERATURE CITED

[1] M.I.Shor, Cinema and Photographic Chemical Industry. 3, 4, 32-36 (1937).

[2] I.M.Fedorov. Principles of Calculating the processes and apparatus of photographic chemical technology, Vol.II, 3 Moscow (1947).

[3] B.V.Deryagin, Dokl. USSR Acad. Sci.39, 1, 11-14 (1943).

THE THERMAL AND THERMOHYDROLYTIC DECOMPOSITION OF CELLULOSE ACETATE AND FILMS MADE THEREOF

A.A.Freiman and V.A.Shcherbakova

Chair of the Technology of Motion-Picture Film Bases, Leningrad Institute of Motion-Picture Engineering.

Investigating the processes involved in the decomposition of cellulose acetate by high temperatures and atmospheric moisture is of considerable interest from the practical standpoint. Once we know the extent to which these factors operate on cellulose acetate, and how they do, we can probe more deeply into the reasons behind the changes in the mechanical and other properties of cellulose acetate articles during use and can work out a rational plan for the employment and storage of these articles.

There is extremely little to be found in the literature at the present time on the decomposition of cellulose acetate, most of the papers dealing with acetone-soluble, so-called secondary cellulose acetate [1].

It has been found that cellulose acetate, like all the other cellulose esters, undergoes thermal and hydrolytic decomposition.

It is decomposed thermally at high temperature, as the result of a redistribution of the static energy among the molecules. This redistribution causes some of the molecules to acquire the reserve of energy necessary for decomposition. The number of such molecules increases as the temperature is raised, thus increasing the rate of thermal decomposition.

Hydrolytic decomposition occurs in the presence of moisture, being the result of saponification of the cellulose ester. Both of these processes lead to destruction of the cellulose ester and a change in the degree of its esterification.

The present paper deals with an investigation into the changes of molecular weight and the acetyl number of cellulose acetate during its thermal, hydrolytic, and thermo-hydrolytic decomposition.

EXPERIMENTAL

Characteristics of the original products. We investigated cellulose triacetate and secondary cellulose acetate, the properties of which were as follows:

	Acetyl Number	Molecular Weight	Per cent Ash
Cellulose Triacetate	62.2	82,000	0.0328
Secondary cellulose acetate	55.2	48,000	0.195

We also tested films of cellulose triacetate and secondary cellulose acetate. The formulas employed in fabricating the films were:

I.	Cellulose triacetate	8.9%	II.	Secondary cellulose acetate	12.4%
	Methylene chloride	85.4%		Acetone	73.8%
	Methanol	5.7%		Ethyl alcohol	13.8%

The cellulose triacetate and the secondary cellulose acetate were dried in a thermostat at 100-105° for 6 hours to remove their residual moisture. The residues of solvents were removed from the films by washing them for 48 hours in distilled water and then drying them at 100-105° before the start of the test.

Research procedure. The molecular weight of the cellulose acetate was measured viscosimetrically, using a capillary viscosimeter. We determined the specific viscosity of 0.1% solutions of cellulose acetate in m-cresol, and then calculated the molecular weight from the following formula [2]:

$$M = \frac{\eta sp}{K_m \cdot C_m}$$

where ηsp is the specific viscosity of the solution; K_m is a constant depending upon the solvent and the solute, being $6.3 \cdot 10^{-4}$ for cellulose triacetate dissolved in m-cresol, and $8 \cdot 10^{-4}$ for secondary cellulose acetate dissolved in m-cresol; and C_m is the solution concentration in moles per liter, in terms of the basic high-polymer molecule (the chain link). C_m was $3.58 \cdot 10^{-3}$ for the 0.1% solutions of cellulose triacetate we employed and $3.88 \cdot 10^{-3}$ for the corresponding solutions of secondary cellulose acetate.

Before determining the molecular weight of decomposed samples, we eliminated the acetic acid and other soluble decomposition products by washing the cellulose acetate with warm distilled water and alcohol, followed by drying to constant weight at 100-105°. Films that had undergone decomposition were washed for 24 hours in cold distilled water and then dried to constant weight at 100-105°.

The acetyl number was determined by the usual alkaline saponification method. Before the acetyl number was determined, the cellulose acetate was subjected to the same preliminary treatment as that used prior to the determination of the molecular weight. In determining the acetyl number, the cellulose triacetate and the secondary cellulose acetate were dissolved out of the film and precipitated, the cellulose triacetate being precipitated with boiling water from a 1-2% solution in methylene chloride, and the secondary cellulose acetate being precipitated with cold water from a 3-4% acetone solution. This method of precipitation yields the loosest and most readily saponifiable products.

Thermal decomposition. We made a study of the changes in the molecular weight and acetyl number of cellulose triacetate and secondary cellulose acetate after they had been subjected to high temperature with air and moisture excluded.

Separate test samples, consisting of the fibrous triacetate, the powdery cellulose acetate, and films made of both, were placed in glass tubes from which the air was evacuated until the residual pressure was 10^{-4} mm Hg. Then the tubes were sealed, suspended in thermostats at 80 and 160°, and kept there for 100, 200, 300, and 600 hours, with the exception of some of the samples of the acetone-soluble cellulose acetate, which were kept at 160°C for 50, 100, 150, and 200 hrs. The secondary cellulose acetate was not heated to 160° for a longer period, since its outward appearance after 200 hours indicated that it had already undergone extremely severe decomposition (browning and brittleness). The molecular weight and the acetyl number of the triacetate and of the acetone-soluble cellulose acetate were measured after each of the foregoing intervals of time.

The results of our investigations are shown in Figures 1, 2, 3, and 4.

Fig.1. Change in the molecular weight of cellulose triacetate as the result of thermal action.
A) Molecular weight, per cent of the initial figure; B) time, hours. 1) Initial cellulose triacetate, $\underline{t}$ = 80°C; 2) initial cellulose triacetate, $\underline{t}$ = 160°C; 3) film, $\underline{t}$ = 80°C; 4) film, $\underline{t}$ = 160°C.

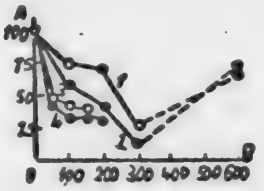

Fig.2. Change in the molecular weight of secondary cellulose acetate as the result of thermal action.
A) Molecular weight, per cent of the initial figure; B) time, hours. 1) Initial cellulose acetate, $\underline{t}$ = 80°C; 2) film, 80°C; 3) initial cellulose acetate, $\underline{t}$ = 160°; 4) film, $\underline{t}$ = 160°C.

As we see in Figures 1 and 3, the molecular weight and the acetyl number of cellulose triacetate both fall as the result of its thermal decomposition. As might have been expected, the temperature affects the rate of thermal decomposition greatly.

The molecular weight of the cellulose triacetate precipitated from a film drops faster than that of the fibrous cellulose triacetate. In measuring the molecular weight we found that the viscosity of a 0.1% solution of the cellulose triacetate film that had been heated to 160°C for 500 hours was higher than that of a solution of the same film after 300 hours of heating. Inasmuch as the molecular weight cannot rise during the course of decomposition, the increase in viscosity was probably due to a change in the solubility of the cellulose ester as a result of the latter's decomposition; we therefore have drawn this section of the curve (Fig.1.) as a dotted line.

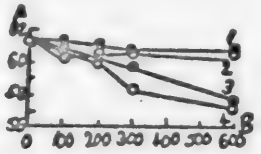

Fig.3. Change in the acetyl number of cellulose triacetate as the result of thermal action.
A) Acetyl number; B) time, hours. 1) film at 80°C; 2) initial cellulose triacetate at 80°C; 3) film at 160°C; 4) initial cellulose triacetate at 160°C.

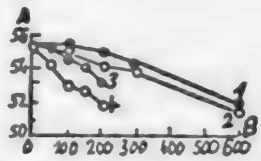

Fig.4. Change in the acetyl number of secondary cellulose acetate as the result of thermal action.
A) Acetyl number; B) time, hours. 1) film at 80°C; 2) initial secondary cellulose acetate at 80°C; 3) film at 160°C; 4) initial secondary cellulose acetate at 160°C.

Figure 3 shows that acetic acid is split off very slowly during the thermal decomposition of cellulose triacetate.

It is apparent from the curves in Figures 2 and 4 that the thermal decomposition of secondary cellulose acetate involves a decrease in its molecular weight and acetyl number. The rate of thermal decomposition of secondary cellulose acetate rises with rising temperature. As in the thermal decomposition of the triacetate, the molecular weight of the powdery secondary cellulose acetate drops less than does the molecular weight of the secondary cellulose acetate in film form. After 600 hours of heating secondary cellulose acetate with air excluded, we again found that the viscosity of a 0.1% solution

in m-cresol is higher than the viscosity after 300 hours of heating. Acetic acid is split off from the powdery secondary cellulose acetate at a faster rate than from the secondary cellulose acetate in the shape of film.

Hydrolytic decomposition. The hydrolytic decomposition of the triacetate was effected at room temperature by the action of air with a relative humidity of 95%. Samples were taken at 200, 400, 800, 1000, and 1200 hours after the start of the test to determine the molecular weight and the acetyl number.

The acetone-soluble (secondary) cellulose acetate and films made from it were likewise subjected to the action of air with a relative humidity of 95%, the test samples being taken after 200, 400, 800, 1000, and 1200 hours. The results of our determinations of the molecular weight and acetyl number after hydrolytic decomposition are shown in the curves of Figures 5, 6, 7, and 8.

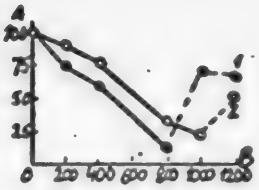

Fig.5. Change in the molecular weight of cellulose triacetate during hydrolytic decomposition. Relative humidity of the air: 95% at 20°C. A) Molecular weight, per cent of the initial figure; B) time, hours. 1) Film; 2) initial cellulose triacetate.

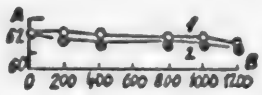

Fig.6. Change in the acetyl number of cellulose triacetate during hydrolytic decomposition. Relative humidity of the air: 95% at 20°C. A) Acetyl number; B) time, hours. 1) Initial cellulose triacetate; 2) film.

As we see in Figures 5 and 6, the molecular weight of cellulose triacetate falls as the result of hydrolytic decomposition. As in thermal decomposition, the molecular weight of fibrous cellulose triacetate drops more slowly than that of the cellulose triacetate in the shape of film. The viscosity is increased after 1000 hours of heating. The acetyl number of cellulose triacetate is practically unaffected by hydrolytic decomposition.

As we see in Figures 7 and 8, the molecular weight and the acetyl number of secondary cellulose acetate are diminished as the result of hydrolytic decomposition.

The secondary cellulose acetate in powder form is saponified somewhat faster than when it is in film form.

Thermohydrolytic decomposition Samples of cellulose triacetate, secondary cellulose acetate, and of films made from them were kept at 80°C and at relative humidities of 18, 58, and 95% to determine the effect of high temperature at different values of relative humidity. Samples were taken at 100, 200, 300, and 400 hours.

The results of our determinations of molecular weight and acetyl number are shown in the curves of Figures 9, 10, 11, and 12.

As we see in Figures 9, 10, 11, and 12, there is no clearly marked variation of the molecular weight and acetyl number with the relative humidity of the air, though, as we see in Figure 5, the molecular weight drops somewhat more slowly at a relative humidity of 95% than at the relative humidities of 18 and 58%. As in thermal and hydrolytic decomposition, the viscosity of 0.1% solutions of cellulose triacetate in m-cresol was increased after 300 hours of thermohydrolytical decomposition at relative humidities of 18 and 58%.

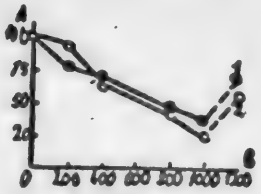

Fig.7. Change in the molecular weight of secondary cellulose acetate during hydrolytic decomposition. Relative humidity of the air: 95% at 20°C. A) Molecular weight, per cent of the initial figure; B) time, hours. 1) film; 2) initial secondary cellulose acetate.

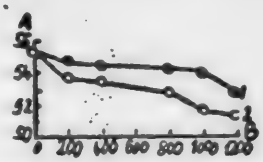

Fig.8. Change in the acetyl number of secondary cellulose acetate during hydrolytic decomposition. Relative humidity of the air: 95% at 20°C. A) Acetyl number; B) time, hours. 1) film; 2) initial secondary cellulose acetate.

The greatest saponification of the secondary cellulose acetate occurred at a relative humidity of 95%, the cellulose acetate in powder form being saponified faster than that in the shape of film. When cellulose triacetate, secondary cellulose acetate, and the films made of these cellulose esters were heated with air excluded, they were decomposed thermally, the rate of decomposition rising with the temperature.

The molecular weight and the acetyl number of cellulose triacetate and of secondary cellulose acetate fell during thermal decomposition. The destruction of the cellulose triacetate and the secondary cellulose acetate in a film was faster than that of the fibrous cellulose triacetate or of the powdery secondary cellulose acetate.

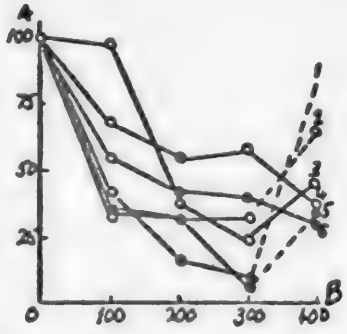

Fig.9. Change in the molecular weight of cellulose triacetate during thermohydrolytic decomposition. Temperature: 80°C. A) Molecular weight, per cent of the initial figure; B) time, hours. 2, 3, and 4 — Initial cellulose triacetate; 1, 5, and 6 — film. Relative humidity, per cent: 1 - 18; 2 - 58; 3 - 18; 4 - 95; 5 - 58; 6 - 95.

Cellulose esters decompose very fast in solutions, and since the films are solid solutions [2], the destruction of cellulose acetate is greater in the films than in the initial products.

The fact that cellulose acetate in films is saponified more slowly than the initial cellulose acetate is likewise due to the greater ability of solid solutions, i.e., the films, to absorb and retain acetic acid than is exhibited by fibrous solid products.

The rate of thermal decomposition of cellulose acetate drops off as the degree of its acetylation rises, the triacetate proving to be much more stable than the acetone-soluble cellulose acetate.

The investigation of the hydrolytic decomposition of cellulose triacetate and of secondary cellulose acetate has shown that the action of highly moist air at room temperature causes a reduction in the molecular weight of cellulose triacetate and of secondary cellulose acetate and a saponification of the secondary cellulose acetate. As was the case in thermal decomposition, the destruction of the cellulose triacetate is more rapid in film form than in the fibrous cellulose triacetate. The same behavior pattern was not found in the hydrolytic decomposition of secondary cellulose acetate.

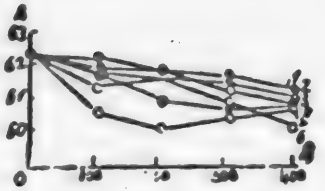

Fig.10. Change in the acetyl number of cellulose triacetate during thermohydrolytic decomposition. Temperature: 80°C. A) Acetyl number; B) time, hours. 1, 2, and 4 - Initial cellulose triacetate, 3, 5, and 6 - film. Relative humidity, per cent: 1 - 18, 2 - 58, 3 - 18, 4 and 5 - 95, 6 - 58.

Here, too, the film of secondary cellulose acetate is saponified more slowly than the powdery secondary cellulose acetate.

The action of air containing various percentages of relative humidity at 80°C results in the thermohydrolytic decomposition of cellulose acetate. We did not find any distinct influence of the relative humidity of the air upon the molecular weight of cellulose acetate. But it is true that the destruction was greatest at relative humidities of 18 and 58%. The slower rate of destruction at a relative humidity of 95% may be due to an increase in the hygroscopicity of the cellulose acetate as the air's relative humidity rises, resulting in a dilution of the acetic acid produced during decomposition and a diminution in its destructive action.[1] Humidity was observed to affect the rate of saponification only in our investigation of the decomposition of secondary cellulose acetate. We found that secondary cellulose acetate was saponified most at a relative humidity of 95%, secondary cellulose acetate being most readily saponified in powder form.

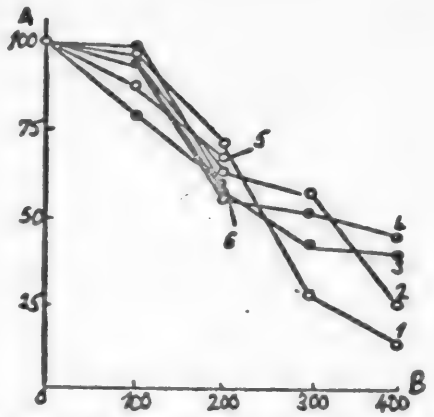

Fig.11. Change in the molecular weight of secondary cellulose acetate during thermohydrolytic decomposition. Temperature: 80°C. A) Molecular weight, per cent of the initial value; B) time, hours. 1, 2, and 5 - Initial secondary cellulose acetate; 3, 4, and 6 - film. Relative humidity, per cent: 1 - 18; 2 - 58; 3 - 18; 4 - 58; 5 and 6 - 95.

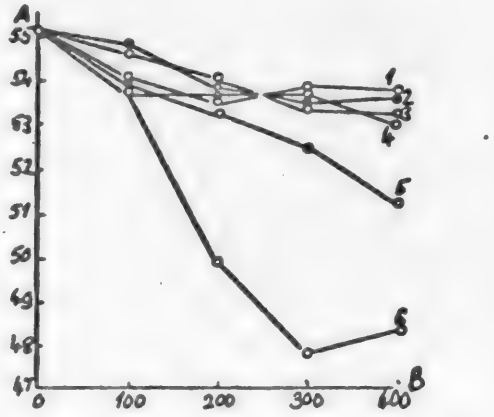

Fig.12. Change in the acetyl number of secondary cellulose acetate during thermohydrolytic decomposition. Temperature: 80°C. A) Acetyl number; B) time, hours. 1, 4, 5, and 6 - Initial secondary cellulose acetate; 2 and 3 - film. Relative humidity, per cent: 1 and 2 - 58; 3 and 4 - 18; 5 and 6 - 95.

[1]) The decrease in the rate of destruction of a cellulose ester as the atmospheric humidity is raised may also be due to a decrease in the partial pressure of oxygen when water vapor is present.

The secondary cellulose acetate was much more saponified than the cellulose triacetate, while the molecular weight of cellulose triacetate dropped faster than that of the secondary cellulose acetate.

Prolonged thermal, hydrolytic, and thermohydrolytic decomposition of cellulose triacetate and of secondary cellulose acetate caused an increase in the viscosity of 0.1% solutions of the test samples in m-cresol. Inasmuch as the actual molecular weight cannot rise during decomposition, the rise in viscosity may be due to a change in the solubility of cellulose acetate in m-cresol as the result of a change in its chemical properties during decomposition, so that we may assume that the formula employed in calculating molecular weight cannot be employed in this case.

SUMMARY

1. Thermal decomposition involves a decrease in the molecular weight and the acetyl number of cellulose triacetate. The destruction of cellulose triacetate and of secondary cellulose acetate is faster in the shape of film than when the cellulose triacetate was in fibrous form and the secondary cellulose acetate was a powder. The acetyl number of fibrous cellulose triacetate and powdery secondary cellulose acetate drops off much faster than the acetyl number of these substances in the shape of film. Secondary cellulose acetate was decomposed more by thermal action than was cellulose triacetate.

2. Hydrolytic decomposition involves the destruction of cellulose triacetate and of secondary cellulose acetate and the saponification of secondary cellulose acetate. Cellulose triacetate is destroyed more rapidly in film form than in fibrous form. Secondary cellulose acetate is saponified more readily than secondary cellulose acetate in the shape of a film. Cellulose triacetate is not saponified during hydrolytic decomposition, which is evidence that is has higher chemical stability than secondary cellulose acetate.

3. Cellulose triacetate and secondary cellulose acetate are destroyed and saponified during thermohydrolytic decomposition. The greatest destruction of cellulose triacetate occurred at relative humidities of 18 and 58%. The effect of atmospheric humidity upon the saponification rate is manifested in the decomposition of secondary cellulose acetate. Secondary cellulose acetate is saponified most at a relative humidity of 95%. Secondary cellulose acetate is saponified more rapidly in powder form than in film form.

LITERATURE CITED

[1] N. V. Kozlov. Physical chemistry of cellulose ester films. State Cinema Press (1948). — [2] H. Staudinger. High-molecular organic compounds. United Scientific and Technical Press (1935).

Received January 15, 1950.

BLANK
PAGE

IMPREGNATING FABRICS WITH INDIVIDUAL LIQUIDS AND SOLUTIONS OF EMULSIFIERS[1]

S. S. Voyutsky and Ya. M. Yabko

At the present time, impregnating fabrics with aqueous dispersions of hydrophobic substances is widely employed in the textile industry to render fabrics waterproof, in the synthetic-leather industry to produce artificial leather, linings, and the like, in rubber technology to impregnate cord, and so forth. Despite the tremendous practical importance of impregnation with aqueous dispersions, little research has been done on the mechanism involved. There are only a few papers, chiefly by Soviet researchers, dealing with the phenomena that occur when a dispersion penetrates into a fabric [1, 2, 3, 4, 5, 6, 7].

One of the reasons why so little research has been done on the mechanism of impregnation is the fact that aqueous dispersions of hydrophobic substances are complicated colloidal or microheterogeneous systems. It is quite obvious that numerous factors must affect the impregnation process: particle size, the viscosity of the impregnating fluid, the aggregation and sorption instability of the dispersion, the surface tension and the wetting power with respect to the fabric, etc., which greatly complicate the analysis of the picture we see in the penetration of the fabric by a dispersion.

The present paper reports on an attempt to explore the mechanism involved in the impregnation of fabrics by the simpler systems: individual liquids and solutions of comparatively low viscosity. There is no reason to expect a plugging of the capillaries, retarding or altogether stopping the penetration of the liquid into the fabric, because of the molecular dispersion and high aggregation stability of these systems. The viscosities are also far from great and are not far from one another, so that the viscosities cannot be the reason for the different impregnating properties of the individual liquids and solutions.

Hence, the impregnating ability of individual liquids and solutions is evidently determined by purely thermodynamic factors alone, which are governed in turn by the free energies of the various interphase surfaces present within the system.

The importance of surface tension as a controlling factor in impregnating properties is a matter of common knowledge. The surface tension at the surface-air boundary has been long considered in practice the basic index of the impregnating and wetting properties of liquids. [8]

Yet the widely held notion that surface tension is the sole factor controlling wetting is found to be wrong when the problem is gone into more deeply.

Genin [9] and Flint [10] have pointed out that there is no complete agreement between the wetting power and surface tension of latexes (rubber dispersions), widely employed in impregnating fabrics. The inadequacy of

---

1) Report 1 of a series on the impregnation of fabrics with aqueous dispersions of hydrophobic substances.

surface tension as the sole criterion of impregnating properties is demonstrable from purely theoretical considerations.

As a matter of fact, the surface tension of the impregnating liquid at the liquid–air boundary is only one of the three forces operative in the well-known equation for the contact angle and, hence, the wettability of the given substance:

$$\cos\theta = \frac{\sigma_{23} - \sigma_{13}}{\sigma_{12}},$$

where σ_{23} is the surface tension at the air–solid boundary, σ_{13} the surface tension at the liquid–solid boundary, and σ_{12} that at the air–liquid boundary.

But if this is so, then the ability of the liquid to be absorbed by the fabric does not depend upon σ_{12} alone, but σ_{13} and σ_{23} as well, since in the usual conditions of impregnation a liquid can penetrate only into those capillaries whose walls are wetted, more or less, by the liquid.

The foregoing would lead one to suppose that the index of the impregnating ability of latexes is the wetting, defined as the cosine of the angle of contact formed by a drop of the liquid upon the material [11]. There was even more reason to assume that the impregnating ability of a latex was related to the wetting work: the work of immersion $W_T = \sigma_{23} - \sigma_{13} = \sigma_{12}\cos\theta$; the work of spreading $W_{sp} = W_T - \sigma_{12} = \sigma_{12}(\cos\theta - 1)$; and the work of adhesion $W_A = W_T + \sigma_{12} = \sigma_{12}(\cos\theta + 1)$. These varieties of work, though they may not be characteristic of the kinetics of wetting or impregnating processes, may reflect the general trend or direction of these processes. As a matter of fact, our previous investigations, made with synthetic latexes, have shown that the angle of contact and the work of wetting are fair indexes of impregnating ability.

In the present research we have endeavored to determine the extent to which the impregnating properties of liquids correspond to their surface tensions, wetting and work of wetting with respect to fabrics, testing in a large number of examples of systems that obey the laws of thermodynamics.

EXPERIMENTAL

Research objects and procedures. The impregnating liquids used were water–alcohol mixtures and various nonviscous organic liquids, as well as aqueous solutions of the emulsifiers most often employed in preparing impregnating dispersions; sodium oleate, Nekal (the sodium salt of an alkylnaphthalenesulfonic acid), and ammonium caseinate. Solutions containing 0.05, 0.15, 0.4, and 1.5% of the given emulsifier were used in the research. It was impossible, unfortunately, to use equimolecular solutions of the emulsifiers for impregnating, as we did not know the molecular weight of the Nekal or of the ammonium caseinate.

The material to be impregnated was a three-ply cotton fabric, kersey, whose tightness of weave made it a particularly suitable material for investigating the liquid's penetration into the fabric.

The impregnating ability was determined by the so-called "wet gain in weight" method, described at length by us elsewhere [12], which involves the determination of the added weight of the sample after standing in the impregnating bath for a given length of time.

The surface tension at the air–liquid interface was measured with a

tensiometer, involving the detaching of a ring from the surface.

The angle of contact was determined by placing a drop of the test liquid on the surface and projecting the drop on a screen as described in the papers by Rebinder [13] and Kazarovitsky [14]. It was impossible to measure the contact angle on the fabric directly because of the fabric's roughness, resulting in high hysteresis and in capillary rise, distorting the results of measurement. We therefore had to employ a conventional surface the properties of which resembled that of cellulose.

The researches carried out in our laboratory indicated that nitrocellulose film was the most suitable surface for this purpose. The contact angles of the liquids at the nitro film are close to the contact angles formed on native cellulose. Moreover, it is extremely easy to prepare this film from ordinary collodion, and it possesses a perfectly smooth surface

Notwithstanding the closeness of the contact angles formed by the liquids on the nitrocellulose film and on cellulose, we must stress the nominal nature of the wetting values and of the work of immersion, spreading, and adhesion cited below. We believe, however, the use of these figures is fully permissible in the present research, the purpose of which is solely to find qualitative regularities. There is no reason to believe that if the drops were applied to the fabric, the wetting ability of the liquids would lie in a different sequence than that found when the drops were applied to the nitrocellulose film.

Tests of individual liquids. The figures on the impregnating ability of different liquids, together with data on their surface tension, wetting ability, and wetting work, are given in Table 1. The figures are arranged in the order of increasing impregnating ability. Since liquids of different specific gravity were employed in this series of tests, the added-weight results have been recalculated as volumetric relationships, expressing the ratio of the volumes of liquid and water absorbed during impregnation.

TABLE 1

Properties of Impregnating Liquids

Impregnating liquid	Wet gain in weight, recalculated as volumetric relationships	Surface tension, ergs per cm^2	Wetting	Work of wetting[1], ergs per cm^2.		
				W_T	W_{sp}	W_A
Water.....	1.0	72.75	0.309	+22.5	-50.6	+95.3
Alcohol:water = 1:6.....	3.8	48.6	0.559	+27.0	-21.5	+75.8
Methyl methacrylate	7.3	28.1	0.989	+27.8	- 0.3	+56.0
Acetic acid....	8.0	29.5	0.872	+25.7	- 3.7	+55.2
Alcohol:water = 1:2.....	8.4	37.0	0.832	+30.8	- 6.2	+67.9
Acetone.....	8.7	25.8	0.920	+23.7	- 2.1	+49.5
Xylene.....	9.0	29.3	0.990	+29.0	- 0.3	+58.3
Oleic acid.....	9.4	34.7	0.966	+33.6	- 1.2	+68.2
Alcohol.....	9.5	25.6	0.974	+24.9	- 0.7	+60.5

[1]) In this table, as in the subsequent ones, the plus sign (+) denotes work done by the system, while the minus sign (-) denotes work that has to be done on the system to create the surface in question.

We see in Table 1 that no one characteristic corresponds to impregnating ability. Nevertheless, we do see that there is a distinct tendency for the impregnating properties of a liquid to improve as the surface tension diminishes, the wetting increases, and the absolute values of the negative work of spreading diminish.

Tests of emulsifier solutions. The findings on the impregnating ability, the surface tension, the wetting, and the work of wettting of solutions of Nekal, sodium oleate, and ammonium caseinate are tabulated in Table 2.

TABLE 2

Properties of Aqueous Solutions of Emulsifiers

Impregnating liquid		Wet gain in weight recalculated as volumetric relationships	Surface tension, ergs per cm^2	Wetting	Work of wetting, ergs per cm^2		
					W_T	W_{sp}	W_A
Water		1	72.75	0.309	+22.5	-50.6	+95.3
Nekal Solution, %	0.5%	1.6	46.0	0.431	+19.8	-26.3	+65.8
	0.15	4.3	40.9	0.616	+25.2	-15.7	+66.1
	0.40	7.7	38.5	0.879	+33.8	- 4.6	+72.4
	1.50	8.3	35.9	1.000	+35.9	0	+71.8
Sodium oleate solution, %	0.05	2.7	37.5	0.500	+18.7	-18.7	+56.3
	0 15	4.4	34.1	0.653	+22.7	-11.8	+56.9
	0.40	5.2	33.3	0.866	+28.8	- 4.5	+62.1
	1.50	8.4	32.3	0.875	+28.2	- 4.0	+60.5
Caseinate solution, %	0.05	1 4	48.0	0.391	+18.8	-29.3	+66.7
	0.15	1.5	46.8	0.500	+23.4	-23.4	+70.2
	0.40	1.6	46.0	0.533	+24.5	-21.5	+70.5
	1.50	2.1	43.8	0.612	+26.8	-17.4	+70.6

Table 2 indicates that there is complete correlation between the impregnating ability, on the one hand, and the surface tensions, the wetting, and the work of spreading, W_{sp}, on the other for all three emulsifiers.

The correlation between the impregnating ability and the work of immersion and the work of adhesion is poor.

Table 2 likewise enables us to infer the surface activity of various emulsifiers. As might have been expected, amonium caseinate, which is a colloidal emulsifier, exhibits the least activity.

Tests of solutions of two emulsifiers In addition to the tests of solutions of individual emulsifiers, we also ran tests of solutions of two emulsifiers, the concentration of one being held constant while that of the other was varied.

The data on the variation of the impregnating properties, the surface tension, the wetting, and the work of wetting of two-emulsifier solutions with the concentration of one of them are given in the shape of curves in Figs. 1, 2, and 3.

As the figures indicate, there is often no correlation between surface tension and impregnating ability when fabrics are impregnated with solutions of two emulsifiers. When small amounts of Nekal are added to a solution of ammonium oleate, for instance, there is practically no change in the surface tension, while the impregnating properties of the solution are improved considerably. The same thing happens when ammoinum caseinate is added to a solution of sodium oleate. In this latter case the surface tension is even increased somewhat.

There is poor correlation between the impregnating ability of solutions and the work of immersion or of adhesion (*cf*, for example, the curves for the tests in which Nekal and sodium oleate were added to a caseinate solution).

The best correlation is observed between impregnating ability and wetting or the work of spreading.

Evaluation of Results

As has been stated above, although some correlation has been found between surface tension, wetting, and the work of wetting, on the one hand, and the impregnating properties, on the other, in our tests of impregnation with individual organic substances, this correlation was incomplete. The reason for this is that wholly different liquids were used in these tests. Some of these liquids are undoubtedly able to dissolve the incrusting substances and fats on the surface of a natural fiber, while others can act upon cellulose, causing it to swell. Last the viscosity of the liquids used in impregnating differed. Thus, there is no doubt that extraneous factors affected the thermodynamical picture of impregnation in these instances.

A much better correlation between impregnation and the indexes we are interested in was observed in the experiments using emulsifier solutions. We found that a diminution of surface tension and an increase in wetting always corresponded to an improvement in impregnation in each series of tests. The most striking correlation with the impregnating properties of these solutions was exhibited by the work of spreading.

The problem of the correltaion of the indexes is more complicated when we are dealing with impregnation with solutions of two emulsifiers. As we have seen, the only instance in which correlation was satisfactory was that between the impregnating properties and the work of spreading. The reason for this is obviously that the two emulsifiers may differ in their ability to be adsorbed at the air - liquid or liquid - solid surface. Naturally enough, the values of the surface energies at the interfaces and, hence, the impregnating properties may vary when the quantitive ratio between the emulsifiers in the solution are changed. When this is so, the only indexes that will exhibit any correlation with the impregnating properties will be those which directly control the liquid s impregnating properties.

We calculated the respective correlation coefficients, using the methods of elementary statistics,to find the indexes of the individual liquids of the emulsifier solutions, and of their combinations that exhibited the best correlation with impregnating ability. Our calculations indicated that the work of spreading exhibits the best correlation. Good correlations likewise exist between impregnating properties and wetting. The coefficient of correlation between impregnating properties and surface tension is much poorer, not exceeding 0.5 in some instances. The worst correlation with impregnating ability is displayed by the work of immersion and the work of adhesion.

This conclusion that the work of spreading exhibits the best correlation with

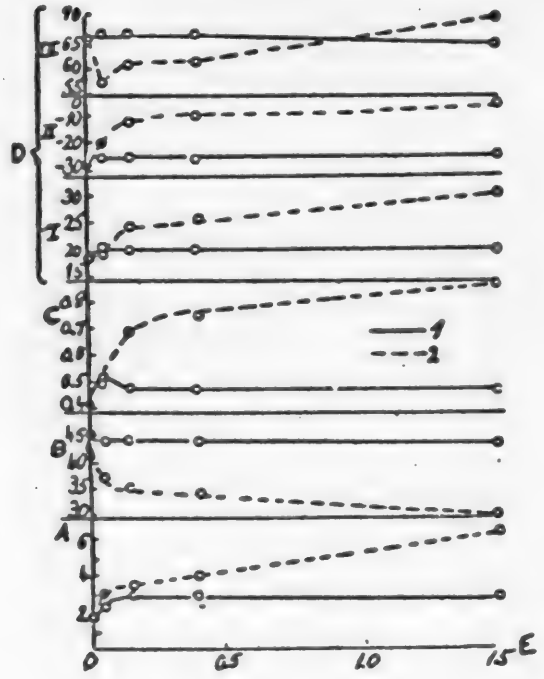

Fig. 1. Effect of sodium oleate and ammonium caseinate upon the impregnating properties, the $\sigma\cos\theta$, the W_T, the W_{sp}, and the W_A of a 0.05% Nekal solution.

A - Wet gain in weight, recalculated as volumetric ratios; B - surface tension, ergs per sq cm; C - wetting, $\cos\theta$; D - work of wetting, ergs per sq cm: I - W_T; II - W_{sp}; III - W_A; E Concentration, %. 1 - ammonium caseinate; 2 - sodium oleate.

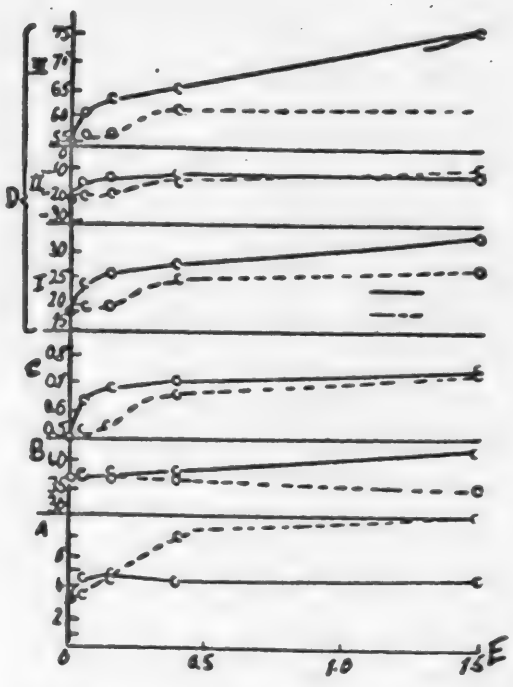

Fig. 2. Effect of Nekl and ammonium caseinate upon the impregnating properties, the $\sigma\cos\theta$, the W_T, the W_{sp}, and the W_A of a 0.05% solution of sodium oleate.

A - Wet gain in weight, recalculated as volumetric ratios; B - surface tension, ergs per sq cm; C - wetting, $\cos\theta$; D - work of wetting, ergs per sq cm: I - W_T; II - W_{sp}; III - W_A; E - Concentration, % 1 - ammonium caseinate; 2 - Nekal.

impregnating properties is at variance with the findings previously secured by one of the present authors which indicated a correlation between impregnating ability and the work of immersion. The conclusion reached in the present research seems to us to be more probable, since it is based upon a large number of observations to begin with, and, second, the work of spreading corresponds essentially to the phenomena observed during impregnation. In actuality, the work of spreading is determined by the spreading of the liquid over the surface, i.e., by the substitution of the air-liquid interface for the air-fiber interface. All this also takes place during impregnation. The liquid enters the fabric displacing a certain volume of air from the fabric and wetting the fiber, so that

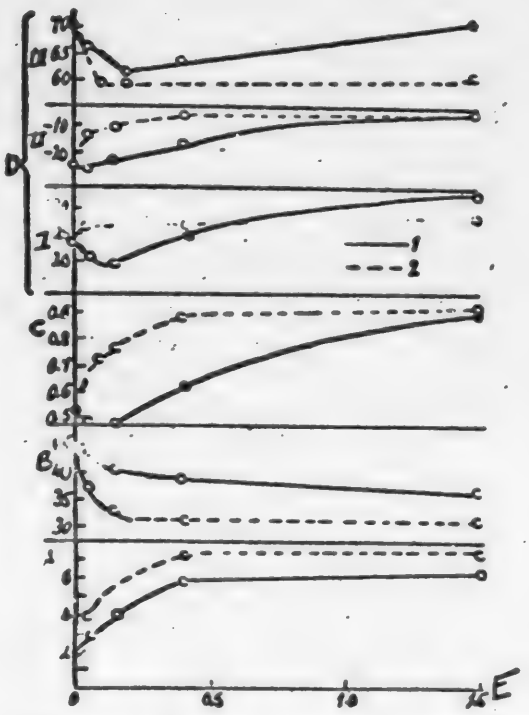

Fig. 3. Effect of sodium oleate and Nekal upon the impregnating properties, the $\sigma \cos \Theta$, the W_T, the W_{sp}, and the W_A of a 0.4% solution of ammonium caseinate.

A - wet gain in weight, recalculated as volumetric ratios; B - surface tension, ergs per sq cm; C - wetting, $\cos \Theta$; D - work of wetting, ergs per sq cm: I - W_T; II - W_{sp}; III - W_A; E - Concentration, %. 1 - Nekal; 2 - sodium oleate.

a fiber - liquid interface replaces the fiber - air interface. Under ordinary conditions, however, only part of the air is displaced from the fabric under the usual impregnation conditions. As one of the present authors has shown [15], the narrowest capillaries in the fabric always contain an appreciable amount of air, even after the fabric has been impregnated with aqueous solutions possessing extremely good wetting properties. As a result, a new liquid - air interface may be constituted within the fabric after impregnation.

Consideration of Figs.1, 2, and 3 from the standpoint of the effect of one emulsifier upon the activity of the other yields interesting conclusions.

We see from the drawings that adding continuously increasing percentages of ammonium oleate to a solution of Nekal results - as might have been expected - in a diminution of the surface tension, an improvement of wetting, a diminution in the absolute values of the work of spreading, and an improvement in the impregnating properties.

On the other hand, adding ammonium caseinate to a Nekal solution produces hardly any change in the specified indexes, except when extremely munute amounts are added. This is evidently due to the fact that the caseinate is not a surface - active substance.

The addition of small amounts of Nekal to a solution of sodium oleate causes no decrease in surface tension, but does produce some improvement in wetting and, hence, a diminution of the absolute value of the work of spreading. This results, of course, in a corresponding improvement in the impregnating ability. This is further confirmation of the inadequacy of surface tension as a criterion of the impregnating properties of a liquid.

Adding ammonium caseinate to a solution of sodium oleate has about the same effect as adding Nekal, though these emulsifiers are not alike. Mention should also be made of the increase in surface tension as the caseinate is added. This may be caused by a decrease in the concentration of sodium oleate in the solution, due to its adsorption on the particles of ammonium caseinate.

The introduction of ever-increasing percentages of Nekal into a 0.4 % solution of ammonium caseinate results in a marked improvement of impregnating properties, a comparatively slight decrease in the surface tension, and a very

gradual decrease in the absolute value of the work of spreading. Wetting is even diminished somewhat when small amounts of Nekal are added. The comparatively slow diminution of the surface tension of a caseinate solution when small percentages of Nekal are added to it may likewise be attributed to the adsorption of the latter upon the albuminous particles and to the absence of an adequate amount of surface - active substance in the solution to give the liquid a low surface tension and high wetting ability. The ability of small percentages of this emulsifier to be completely adsorbed on particles of the disperse phase is borne out by the existence of dispersions that are stabilized by small percentages of Nekal and possess a surface tension equivalent to that of pure water.

The improvement in wetting caused by an increase in the precentage of Nekal added may be attributed to the fact that at a certain percentage of Nekal the amount of the latter in the solution exceeds the amount required to saturate the surface of the ammonium caseinate particles.

The addition of sodium oleate, which does not possess the specific properties of Nekal, to a solution of ammonium caseinate, diminishes the surface tension appreciably and causes no impairment of wetting. Accordingly, sodium oleate greatly improves the work of spreading and the impregnating properties of the mixture.

SUMMARY

1. It has been shown that, contrary to widely held opinion, surface tension cannot serve as a criterion for the evaluation of the impregnating properties of liquids.

2. It has been found that of all the thermodynamic factors the best criterion for assessing the impregnating properties of liquids is the work of spreading.

3. It has been established that the penetration of fabric by a solution of two emulsifiers, one of which is surface active, and the other colloidal, is possibly a case of antagonistic action. The cause of this, probably, lies in the in the adsorption of the surface active substance by the colloidal particles of the second emulsifying agent.

LITERATURE CITED

[1] S. S. Voyutsky and E. M. Dzyadel, Bast Fiber Industry 1940, 11-12, 26.

[2] S. S. Voyutsky and E. M. Dzyadel, Colloid Jour. 1941, 7, 3,

[3] S. S. Voyutskv and E. M. Dzyadel, Symposium on "Problems of the technology of leather substitutes." State Light Industry Press (1941).

[4] Chwala, Koll. Zeit., 102, 1, 69 (1943).

[5] N. Zotova, K. Bernshtein, and S. Voyutsky, Textile Industry (1944) 5-6,18.

[6] L. E. Fedorova and S. S. Voyutsky, Light Industry 1944, 9, 15.

[7] I. V. Plotnikov, Light Industry 1947, 3, 36.
[8] Noble, Latex in Industry (1930).
[9] G.Genin. Chemie et Technologie du Latex de caoutchouc. Paris (1934).
[10] C. F. Flint. The Chemistry and Technology of Rubber Latex. London (1938).
[11] P. A. Rebinder, Jour.Phys.Chem. 1, 4-5,553 (1930).
[12] S. S. Voyutsky, Light Industry 1944, 3, 26.
[1] P. A. Rebinder. The physical chemistry of flotation processes.Metallurgy Press (1933).
[14] Kazarovitsky, Fact.Lab 1938, 8,6.
[15] S. S. Voyutsky and L. E. Fedorova, Light Industry 1945, 12, 12.

Received July 23, 1949.

NOTES ON THE DESIGN OF AN INSTRUMENT FOR DETERMINING THE MOISTURE IN STARCH

S. N. Beketovsky

In addition to perfecting several analytical methods [1-6], we have improved a method for determining the moisture content of starch.

The Soviet dielcometer has been widely employed for all sorts of purposes (determining the moisture content of tea, of macaroni, etc.). We have used it to determine the moisture in starch. The specific properties of the test product required modifications in the design of the instrument: we substituted a special part, a sort of wide flat box, for the usual container for the product under test.

In our determinations of the moisture in starch with this instrument, we found that the accuracy of analysis is principally affected by two factors: one, the method employed in filling the box with starch (the different kinds of rapping used in filling the box yielded differing results), and two, the dimensions of the box, since even when no tamping of the box was employed, the accuracy of anaylsis was improved, up to a certain limit, by increasing the size of the starch container used.

In analyzing the moisture in starch we adopted a box 1 cm high with a bottom 10 X 10 cm in size. The bottom of the box and its sliding cover were fitted with metallic plates to which electric wires were soldered. The starch was poured in through a sieve without any tamping or rapping of any objects against the box or of the box itself.

The excess flour was always removed by the same rotating motion of the sliding cover. After the cover had been refastened and the box containing the starch connected to the instrument, the analysis was made as usual.

The results of the measurements made with the foregoing special device as part of the instrument were compared with the results of moisture measurements made in the usual manner (drying cabinet), no perceptible discrepancies being observed in parallel determinations.

LITERATURE CITED

[1] S. N. Beketovsky, Proc. Stavropol State Pedagogical Inst. 2, 74 (1948).

[2] S. N. Beketovsky, J. Appl. Chem. 22, 2, 179 (1949).

[3] S. N. Beketovsky, Textile Industry 1949, 9, 33.

[4] S. N. Beketovsky, J. Appl. Chem. 23, 4, 444 (1950). [1)]

[5] S. N. Beketovsky, Textile Industry 1950, 5, 35.

[6] S. N. Beketovsky. Abstracts of speeches delivered at the All-Union Conference on Colloid Chemistry, June 13-18, 1950, p. 113. Kiev (1950).

Received July 3, 1950.

1) See Consultants Bureau English translation, p. 463.

BLANK
PAGE

THE SCIENTIFIC PRINCIPLES UNDERLYING THE DESIGN OF CHEMICAL ENGINEERING PROCESSES [1)]

D. A. Epshtein

In our preceding report [1] we showed that chemical reactions employed in technology may be classified into six basic types, according to their physico-chemical characteristics, each reaction type being characterised by its own kind of functions:

$$\eta = f(\tau, t^\circ, P, C \ldots.)$$

and

$$I = \varphi(\tau, t^\circ, P, C \ldots.),$$

where η and I are the yield and the intensity, respectively; and τ, t°, P, and C are the process variables. length of reaction, temperature, pressure, reagent concentration, and so forth.

These equations may be employed to determine the optimum conditions and best procedures for realizing the chemical reactions technically. The appropriate technological outlines, methods of computation and, to a certain extent, the reaction equipment are projected for each type of reaction.

The first report was reviewed in the press [2,3] and was also discussed in several scientific meetings. Vinogradov [3] and others have expressed a desire for quantitative characteristics based on a thermodynamical criterion of the types of chemical reactions used in technology. The present paper is an attempt to deal with that problem.

Let us consider simple reactions, to begin with [1]. The given values of the parameters – temperature, pressure, ratios of the reagent concentrations – correspond to a definite state of equilibrium of the system on question. Of the factors listed, temperature plays a special part because of the well-known relationships that link together the velocities of chemical reactions, equilibrium, and temperature. In many instances it is possible to state the temperature of the so-called onset of the reaction, i.e., the temperature below which the reaction practically does not take place at all. The special importance of temperature as against the other factors is seen most clearly in the case of the reactions that involve solid catalysts. Many of these reactions proceed at measurable velocities only within a very narrow temperature range. At the present time the synthesis of ammonia can be effected, for example, only in the 350-700° range, ultrahigh pressures being required for the synthesis to be carried out at 850-900°. The upper limit is fixed by the catalyst's loss of activity as a result of changes in its surface. Inasmuch as many reactions employed in manufacturing are exothermic, we are often involved in a contradiction between the desirability of lowering the temperature in order to shift the state of equilibrium in the favorable direction and the necessity of raising the temperature to achieve the necessary reaction rate.

If the reaction does not entail a change in volume, the state of equilibrium cannot be shifted by changing the pressure (within the applicability of the laws governing the ideal state of gases). In many cases it is inadvisable to increase the utilization factor of one reagent by using an excess of another reagent. Hence,

---

[1)] Report II of a series on this topic.

the possibilities of shifting the equilibrium in the desired direction are often found to be limited. The engineer is often compelled to carry out reactions under conditions that are unfavorable as far as the state of chemical equilibrium is concerned.

In this connection, all reactions are divided into three grpups in technology, according to their state of equilibrium: the first group covers irreversible reactions, the second, reversible reactions, and the third, reversible unshifted reactions. Typical reactions in each group are listed in the table.

TABLE

Characteristics of the Principal Types of Chemical Reactions in Technology

Name of reaction	Quantitative characteristic	Typical representative
1. Simple irreversible	$\eta = 1$	$S_2 + 2O_2 = 2SO_2$
2. Simple reversible	$\eta = 0,1$	$2SO_2 + O_2 = 2SO_3$
3. Simple reversible unshifted	$\eta \ll 1$	$N_2 + 3H_2 = 2NH_3$
4. Composite irreversible	$\eta_{NO} \to 1$	$4NH_3 + 5O_2 = 4NO + 6H_2O$ $4NH_3 + 3O_2 = 2N_2 + 6H_2O$
5. Composite reversible	$\eta_{CO} = 0\text{-}1$	$C + H_2O = CO + H_2$ $CO + H_2O = CO_2 + H_2$
6. Composite reversible unshifted	$\eta_{CH_3OH} \ll$	$CO + 2H_2 = CH_3OH$ $CO + 3H_2 = CH_4 + H_2O$

Irreversible reactions are those in which the equilibrium product yield is practically $\eta = 1$ within the realisable range of variability of experimental conditions. The equilibrium constants $\underline{K}$ are extremely small throughout the range of variable conditions (the numerator being the partial pressures of the initial substances, and the denominator containing the reaction products). In selecting the optimum conditions for these equations we are guided by the kinetic data, the equations cited above being derived by integrating the differential equations for the reaction rates.

Reversible reactions are those in which the equilibrium product yields range from 0 to 1 ($\eta = 0 - 1$). The essential difference between this group of reactions and the preceding one is that the yield approaches unity only under rigidly determined conditions. In selecting the optimum conditions for securing a high yield, the first thing to bear in mind is the effect of a change in the conditions upon the state of chemical equilibrium. The equations for yield and intensity are derived from the kinetic equations, which contain the equilibrium constant in either the explicit or implicit form.

Reversible unshifted reactions are characterized, within the realizable region of changes in the experimental conditions, by equilibrium product yields that are much below unity, $\eta \ll 1$. The yield is much below unity even with the most favorable conditions that can be possibly achieved. When these reactions are carried out industrially, technological plans are used that make it possible to achieve high process yields in spite of this, a typical operational

plan being a circulatory one. Technical developments, such as the discovery of new low-temperature catalysts, may expand the boundaries of these changes in reaction conditions, as a result of which the reaction would be shifted from this group to the preceding one.

The composite reactions are classified thermodynamically like the simple ones. In each case, we determine which of the partial reactions controls the assignment of the composite reaction in question to one group or another.

The table lists typical examples of the six fundamental reaction types occurring in technology.

SUMMARY

The quantitative characteristics of the types of chemical reactions employed in technology are set forth, based on a thermodynamical criterion

LITERATURE CITED

[1] D.A.Epshtein, J.Appl.Chem 19, 1125 (1946).
[2] K.V.Astakhov, Chem. Prog. 15, 655 (1946).
[3] G.V.Vinogradov, Petroleum Economy 1946, 12, 62.

BLANK
PAGE

THE VARIATION OF THE VISCOSITY OF LINSEED OIL WITH ITS OXIDATION

V.G.Georgievsky and B.N. Shakheldyan

Moscow Polygraphic Institute

In our first report [1] we described a method we used for the simultaneous observation of the oxidation and the related thickening of vegetable oils and also cited some data secured in a study of the oxidation of linoleates.

The present paper deals with the variation of the viscosity of linseed oil with oxidation. Three samples of linseed oil were tested; their constants are given in the table.

TABLE

Constants of Tested Samples of Linseed Oil

Sample No.	Acid number	Saponification Number	Hübl iodine Number	d^{20}_4	Viscosity, centipoises
1	3.6	190.2	178.6	0.931	30.8
2	4.2	181.3	172.6	0.924	29.1
3	4.0	189.6	177.1	0.929	27.0

This is Report II of a series on the oxidation and viscosity of film-forming vegetable oils. The results secured with different oil samples proved to be quite similar, differing only in the magnitude of the initial viscosity and in the length of the induction period during oxidation. In this paper we shall cite the findings secured for Sample 1 of the oil.

Like the linoleates, linseed oil does not thicken when heated for a long time to 100° in an oxygen-free medium, the viscosity rising only with oxidation. The general course of the oxidation of linseed oil under various conditions and the resulting rise in its viscosity are shown in Fig. 1.

It is significant that the induction period of oxidation is reduced to zero when benzoyl peroxide is present, though a perceptible induction period persists when the oil is oxidized in pure oxygen, despite the much greater acceleration of oxidation. It is usually asserted that the causes of the induction period are: first, the presence of natural inhibitors in the oil, which retard oxidation, and second, the autocatalytic nature of the oxidation process. But the absence of an induction period in the oxidation of synthetic esters, repeatedly noted in the literature [2, 3] as well as in our own research, compels us to think that autocatalysis has a minor influence upon the kinetics of oxidation and, in any event, does not control the prolonged induction period encountered in the oxidation of vegetable oils. We ran a series of tests involving the combined oxidation of linseed oil, first in oxidation and then in air, to check this (Fig. 2).

If catalysts were accumulated during the induction period, our substitution of air for oxygen ought to result in a higher oxidation rate than in the ordinary oxidation in air alone, inasmuch as oxidation is more intensive in an oxygen atmosphere. The respective curves exhibit the same slope, however. Thus, we were unable to observe any formation of oxidation catalysts during the induction period. Still, catalysts are formed during the oxidation proper, as is witnessed by the rise in the oxidation rate in the tests represented by Curves 3 and 4 in Fig. 2, where the air replaced the oxygen after the conclusion of the

induction period.

We ran tests in which the oxidation of the oil by oxygen was combined with a processing of the oil in a nitrogen atmosphere in order to ascertain the effect of a preliminary oxidation upon a subsequent increase of viscosity in an oxygen-free medium.

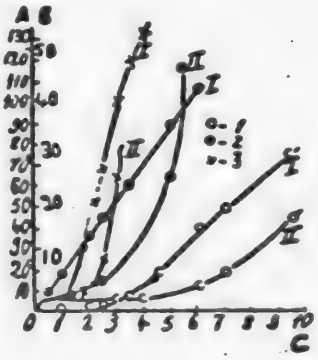

Fig. 1. Oxidation and rise of viscosity of linseed oil under various conditions. A - Amount of oxygen absorbed, ml O_2/gram; B - outflow time, seconds; C - time, hours. I - Oxidation; II - viscosity. Oxidation conditions: 1 - in air; 2 - in air containing 1.6% of benzoyl peroxide; 3 - in oxygen.

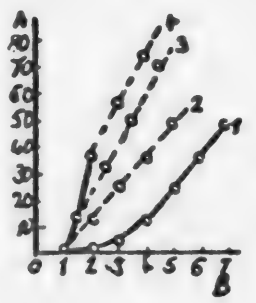

Fig. 2. Effect of oxidation in oxygen upon the rate of subsequent oxidation in air. A - Amount of oxygen absorbed, ml O_2/gram; B - time, hours. Oxidation conditions: 1 - in air; 2, 3 and 4 - in oxygen, later replaced by air.

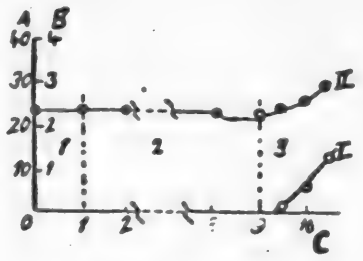

Fig. 3. Effect of oxidation in oxygen upon a subsequent rise of viscosity in nitrogen. A - Amount of oxygen absorbed, ml O_2/gram; B - outflow time, seconds; C - time, hours. I - oxidation; II - viscosity. Oxidation conditions: 1 - in oxygen; 2 - in nitrogen; 3 - in air.

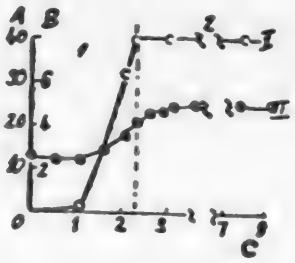

Fig. 4. Effect of oxidation in oxygen upon a subsequent rise of viscosity in nitrogen. A - Amount of oxygen absorbed, ml O_2/gram; B - outflow time, seconds; C - time, hours. I - Oxidation; II - viscosity. Oxidation conditions: 1 - in oxygen; 2 - in nitrogen.

We see in Fig. 3 that when the oxygen is replaced by nitrogen at the end of the induction period, the preliminary oxidation involves no changes that could produce a rise of viscosity in the absence of the oxygen. But when the nitrogen was replaced by air after 8 hours of heating, the same rise of viscosity set in as was observed in simple oxidation of the oil in air after the conclusion of the induction period.

When the oxygen is replaced by nitrogen after the end of the induction period, the viscosity rise that has begun soon comes to a stop, the viscosity becoming constant (Fig. 4). But when oxidation is continued to a higher stage, perceptible thickening is found to occur even in the absence of oxygen (Figs. 5 and 6).

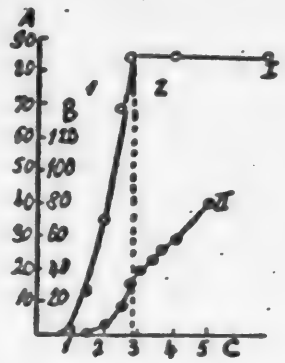

Fig. 5. Effect of oxidation in oxygen upon a subsequent viscosity rise in nitrogen. A - Amount of oxygen absorbed, ml O_2/gram; B - outflow time, seconds; C - time, hours. I - Oxidation; II - viscosity. Oxidation conditions: 1 - in oxygen; 2 - in nitrogen.

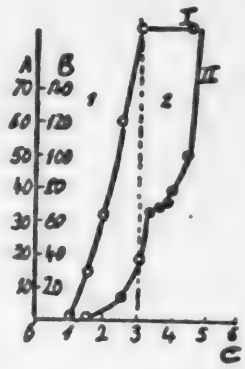

Fig. 6. Effect of oxidation in oxygen upon a subsequent viscosity rise in nitrogen. A - Amount of oxygen absorbed, ml O_2/gram; B - outflow time, seconds; C - time, hours. I - Oxidation; II - viscosity. Oxidation conditions: 1 - in oxygen; 2 - in nitrogen

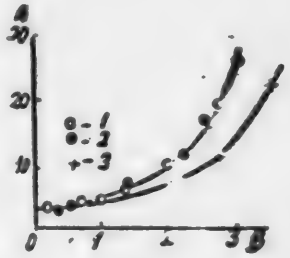

Fig. 7. Variation of the viscosity of linseed oil with oxidation. A - Viscosity, centipoises; B - amount of oxygen absorbed, moles of O_2 per mole of oil. Oxidation conditions: 1 - in air; 2 - in air containing 1.6% of benzoyl peroxide; 3 - in oxygen.

Two periods, therefore, exist in the thickening of linseed oil during oxidation.

At first, the viscosity rise is related directly to oxidation, depending entirely upon it, but as the oxidation products accumulate, the rise of viscosity not directly related to oxidation and undoubtedly due to secondary conversions of the oxidation products becomes significant. During the initial period there is a well-defined variation of viscosity with the amount of oxygen absorbed. Repetitions of our experiments have shown that the relationship between viscosity and the amount of oxygen absorbed remains a constant, despite any change in the rate of air circulation or interruptions in heating or in the passage of air.

As we see from the curves reproduced in Fig. 7, the addition of benzoyl perioxide likewise has no effect upon the relationship between viscosity and the

degree of oxidation. Still, the absorption of a given amount of oxygen results in the formation of more highly viscous products when the oil is oxidized in air than when it is oxidized in pure oxygen.

It is significant that this regularity of the variation of the viscosity of linseed oil with the extent of its oxidation is quite like the pattern we had observed for the lineolates.

SUMMARY

1. The application of the method we have evolved has enabled us to establish the presence of two periods during the rise in viscosity of linseed oil: a) an increase of viscosity due to oxidation; and b) an increase in viscosity not directly related to oxidation, which is observed at a higher degree of oxidation.

2. No oxidation catalysts are formed during the induction period.

3. Natural linseed oil exhibits the same pattern of variation of viscosity with the extent of oxidation as synthetic esters of linoleic acid.

LITERATURE CITED

[1] V.G.Georgievsky and B.N.Shakheldyan, J.Appl.Chem 24, 6, 593 (1951).[1)]

[2] A.A.Blagonravova and A.M.Lazarev, J.Appl.Chem 13, 883 (1940).

[3] W.Treibs. Ber., 75, 203 (1942).

Received June 28, 1950.

---

1) See Consultants Bureau translation, p. 661.

VARIATION OF THE VISCOSITY OF BOILED LINSEED OILS WITH OXIDATION[1]

V.G.Georgievsky and B.N.Shakheldyan

Moscow Polygraphic Institute

1) Report III of a series on the oxidation and viscosity of film-forming vegetable oils.

In our preceding reports [1, 2] we pointed out that the thickening of linoleates and of natural linseed oil follows the same pattern, which is quite understandable when we remember that the properties of linseed oil are determined by its high content of linoleic and linolenic acids. The latter differs in that it is an unsaturated acid, but has a similar chemical structure, as is indicated by the similarity of the activation energies of their esters: 17.2 cal for ethyl linoleate and 17.5 cal for ethyl linolenate [3].

We were interested in determining how viscosity varied with oxidation for the polymerized and oxidized linseed oil used as a paint vehicle.

The samples of oxidized and polymerized oils were prepared by heating linseed oil to 280° in a current of CO_2 to get a polymerized oil and to 150° in a current of air to get an oxidized oil, i.e., the conditions customarily employed for producing polymerized and oxidized paint vehicles.

The constants of the samples are given in the table.

TABLE

Constants of the Samples Tested

Constants of the oils	Oxidized oil		Polymerized oil	
	No.1	No.2	No.1	No.2
Acid number.....	8.2	7.5	7.4	6.9
Saponification number.....	198.6	199.5	198	194.6
Iodine number.....	138	161	125	141.5
d^{20}_4	0.967	0.952	0.952	0.942
Viscosity, centipoises at 20°	163	142.2	276	100.5

Our tests indicated that the oxidized oils exhibited the same pattern of the variation of viscosity with oxidation as previously found for natural linseed oil. In particular, adding benzoyl perioxide, which accelerated oxidation and thickening, did not affect the relationship between viscosity and the amount of oxygen absorbed. The results obtained with sample 1 are shown in Fig. 1.

A polymerized linseed oil is distinguished by the fact that a higher viscosity is obtained for the same amount of oxygen absorbed when benzoyl peroxide is present (Fig. 2). This is related to transformations undergone by the linseed oil during thermal processing.

One of these transformations that changes the chemical nature of the linseed oil fundamentally is the isomerization of the isolated double bonds of the linoleic and linolenic acid to conjugated bonds [4].

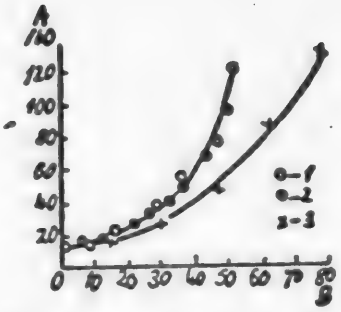

Fig. 1. Variation of the viscosity of an oxidized oil with oxidation. A - Viscosity, centipoises; B - amount of oxygen absorbed, ml O_2/gram. Oxidation conditions: 1 - in a current of air; 2 - in a current of air containing 1.2% of benzoyl peroxide; 3 - in a current of oxygen.

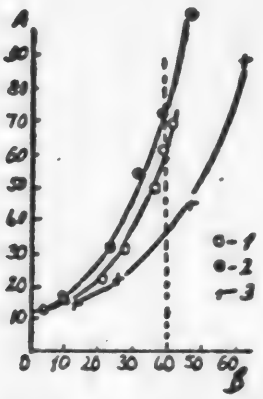

Fig. 2. Variation of the viscosity of a polymerized oil with oxidation. A - viscosity, centipoises; B - amount of oxygen absorbed, ml O_2/gram. Oxidation conditions: 1 - in a current of air; 2 - in a current of air containing 1.2% of benzoyl peroxide. 3 - in a current of oxygen.

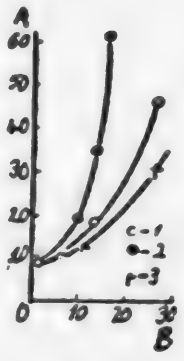

Fig. 3. Variation of the viscosity of tung oil with oxidation. A - Viscosity, centipoises; B - amount of oxygen absorbed, ml O_2/gram. Oxidation conditions: 1 - in a current of air; 2 - in a current of air containing 1.2% of benzoyl peroxide; 3 - in a current of oxygen.

That the formation of conjugated double bonds is the reason for this singularity in the action of benzoyl perioxide is also supported by the circumstance that a similar and even more pronounced effect is observed when benzoyl peroxide is added to tung oil (Fig. 3).

In all the cases we have studied we find the characteristic effect of an increase in the oxygen concentration upon the variation of viscosity with oxidation, namely that as the oxygen concentration is raised, the relationship between viscosity and the amount of oxygen absorbed shifts toward the formation of less viscous oxidation products.

Slansky [5] oxidized films of linseed oil at room temperature and observed a similar phenomenon. He attributed it to the fact that, for molecules excited by the energy of the initial oxidation act, the probability of purely oxidative transformations rises at the expense of the probability of polymerization reactions as the oxygen concentration is increased. This explanation may be adopted provided the term polymerization is taken to mean the reaction of particle aggregation, involving the indispensable participation of oxygen, since our experiments have shown that when no oxygen is present the viscosity does not rise, notwithstanding the addition of so active an initiator as benzoyl peroxide.

SUMMARY

1. The variation of viscosity with oxidation in an oxidized linseed oil resembles that of natural linseed oil.

2. The addition of benzoyl peroxide to polymerized linseed oil or to tung oil changes the variation of viscosity with oxidation in the direction of the formation of more viscous products for the same degree of oxidation.

LITERATURE CITED

[1] Georgievsky and Shakheldyan, J.Appl.Chem. 24, 6, (1951). [1)]

[2] Georgievsky and Shakheldyan, J.Appl.Chem 1951, 7. [2)]

[3] J.L.Bolland, G. Gee, Trans. Far. Soc., 3 - 4 236 (1946).

[4] V.S.Kiselev and M.F.Sorokin, Jour.Chem. Ind.1946, 6, 14.

[5] P.Slansky, J. Oil and Colour Chem.Association, 31, 161 (1948).

Received June 28, 1950.

---

1) See Consultants Bureau English translation, p. 661.

2) See Consultants Bureau English translation, p. 875, this issue.

BLANK
PAGE

THE MUTUAL SOLUBILITY OF CYCLOHEXANOL AND WATER [1)]

E.N.Zilberman

In calculating the separation of a mixture of cyclohexanol and water we found it necessary to determine the mutual solubility of these substances. Our results are set forth in this report.

The literature contains only fragmentary data on this problem. Markovnikov [1] found that cyclohexanol dissolves in 28 times its volume of water at room temperature and that the warmth of one s hand turned a saturated solution turbid. De Forcrand [2] found 11.27 g of water dissolved in 100 g of cyclohexanol at 11°C, with 5.67 g of cyclohexanol dissolving in 100 g of water. We find the following data on the solubility of cyclohexanol in a cyclohexanol-water mixture (in per cent by weight) in the D'Ans and Lax handbook [3]: 5.00 at 7.2°; 5.14 at 121.95°; 15.00 at 174.3°; and 32.3 at 184.7°.

In our experiments we used commercial cyclohexanol, which was redistilled into our laboratory rectifying column. The constants of the resulting product were as follows:

Freezing point: 24.95°C, d_4^{25} 0.9437; n_D^{25} 1.4669; 0.02% phenol.

Markovnikov [1] secured cyclohexanol with a freezing point of + 25°C. The figures given in the literature for the specific gravity and refractive index are also close to our findings [4, 5].

We determined solubility by the classical method of Alekseyev [6]. A mixture of calculated quantities of cyclohexanol and water was slowly heated in a sealed thick-walled test tube (10mm in diameter and 80mm long) on a paraffin bath until turbidity appeared or disappeared completely. Then the test tube was slowly cooled until turbidity appeared or disappeared. This operation was repeated several times in order to bring the temperatures at which turbidity appeared and disappeared as close together as possible. The mean of the two closest readings was taking as the layering temperature. This temperature difference did not exceed 1° up to 100°C, rising to 2° at higher temperatures. The temperature was measured with tested thermometers graduated to 0.2° (up to 100°) and to 1° (above 100°C). A correction was applied for the emergent mercury column.

A total of 50 tests was run, from which we plotted the curves in Figs. 1 and 2, graphical interpolation yielding the data listed in Tables 1 and 2.

We found that the solubility of cyclohexanol in the mixture is a minimum (3.1%) at 54-62°C, the solubility of the cyclohexanol rising at lower or higher temperatures than this.

We checked whether our test mixture obeyed Alekseyev's rule of linear diameter [7], according to which the equation of the line drawn through the midpoints of the isothermal straight lines is very close to a linear equation. As we see in Fig. 2, this line is fairly close to a straight line in the interval from 0 to 150°C. The rule does not hold at temperatures in excess of 150°C. In view of the slight curvature of the solubility curve at temperatures in the vicinity of the critical value (184°C), we were frequently unable to determine the corresponding critical composition by the usual method. We therefore found it by

1) Report I of a series on the physico-chemical properties of a cyclohexanol-water mixture.

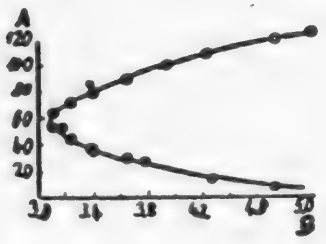

Fig. 1. Solubility of cyclohexanol and water from 0 to 120°

A – Temperature, °C; B – Cyclohexanol in the cyclohexanol-water mixture, wt.%

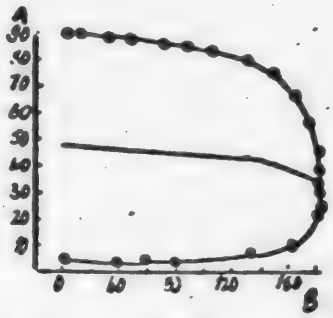

Fig. 2. Mutual solubility of cyclohexanol and water.

A – Cyclohexanol in the cyclohexanol-water mixture, wt %; B – temperature, °C.

TABLE 1
Solubility of Water in Cyclohexanol

Temperature (°C)	Water in the mixture, wt,%	Temperature, (°C)	Water in the mixture, wt, %.
0	10.03	100	17.04
10	10.54	110	18.1
20	11.07	120	19.3
30	11.63	130	20.7
40	12.23	140	23.6
50	12.89	150	25.3
60	13.58	160	29.5
70	14.34	170	36.2
80	15.17	180	47.7
90	16.07	184 (Critical temperature °C).	66.1 (Critical composition, wt. %)

TABLE 2
Solubility of Cyclohexanol in Water

Temperature (°C)	Cyclohexanol in the mixture wt.%	Temperature (°C).	Cyclohexanol in the mixture wt.%.
0	5.35	100	3.93
10	4.57	110	4.28
20	4.00	120	4.7
30	3.60	130	5.3
40	3.33	140	6.1
50	3.14	150	7.2
54–62 (minimum solubility)	3.1	160	8.8
70	3.19	170	11.5
80	3.41	180	17.8
90	3.65	184 (Critical temperature °C)	33.9 (Critical composition wt. %)

graphical extrapolation, prolonging the line joining the midpoints of the isothermal conoids until it intersected the solubility curve. The intersection lay at the critical composition: 33.9% of cyclohexanol by weight.

These figures on solubility agree rather well with the figures in the literature cited above. The slight deviation from the figures given by De Forcrand

[2] is evidently due to the fact that he did not employ a cyclohexanol of adequate purity (freezing point 22.5°C).

We also ran several tests at temperatures below 0°C. We were unable to detect any increase in the solubility of water in the mixture as the temperature fell, i.e., a downward turn of the upper portion of the curve in Fig. 2. The solid phase settled out before we reached the critical point. Thus, the cyclohexanol-water mixture has only an upper critical temperature.

SUMMARY

1. The temperature and the composition of "minimum dissolution" of cyclohexanol in water have been found to be 54-62°C and [illegible]% by weight of the mixture, respectively.

2. The critical temperature of a cyclohexanol-water mixture has been found to be 184°C.

LITERATURE CITED

[1] V. V. Markovnikov, Jour. Russ. Phys. Chem. Soc. 30, 167 (1898).

[2] De Forcrand, Comptes rend. 154, 1380 (1912).

[3] J. D'Ans and E. Lax, Taschenbuch f. Chem. u. Phys., Berlin, Springer-Verlag, 959 (1943).

[4] N. D. Zelinsky, Ber., 34, 2800 (1901).

[5] Timmermans, Hennaut-Roland, J. chim. Phys., 34, 718 (1937).

[6] V. Ya. Anosov and S. A. Pogodin, Principles of Physicochemical analysis, 122. USSR Acad. Sci. Press: Moscow-Leningrad (1947).

[7] V. F. Alekseyev, Mining Jour. 2, 385 (1894).

Received August 6, 1950.

Re-submitted February 13th, 1951.

BLANK
PAGE

THE SOLUBILITY OF IRON SULFATES IN CONCENTRATED SULFURIC ACID AT HIGH TEMPERATURES

G. A. Zakharchenko

A. P. Belopolsky and S. Ya. Shpunt have made a critical review of our paper, on the basis of their own researches [1,2].

A paper by these authors [3] gives the results of their investigations of the solubility isotherms of ferrous sulfate in sulfuric acid of various concentrations at temperatures of 50, 60, 70 and 90 deg. At low acidities (below 1% H_2SO_4) the authors observed a perceptible oxidation of the $FeSO_4$ by atmospheric oxygen, and to prevent this oxidation they employed "distilled water boiled for a long time and saturated with nitrogen". In a second paper on the oxidation of ferrous sulfate in a solution of free oxygen [4], one of these authors arrives at the indisputable conclusion that the rate of oxidation falls substantialy as the concentration of the sulfuric acid is raised. These observations were made at 40, 60, and 80°.

In our paper [1], we investigated the solubility of ferrous sulfate in 91.25% sulfuric acid in the temperature range of 100-243°. We attribute the decrease in the solubility of ferrous sulfate with rising temperature to the gradual oxidation of this salt to the less soluble ferric sulfate, which seems incomprehensible to Belopolsky and Shpunt. These author's observations, made at maximum temperatures of 80 and 90° in their investigations, cannot be regarded as a rigorous criterion of our conclusions.

The oxidation of ferrous sulfate in concentrated H_2SO_4 at temperatures in excess of 100° is not caused by atmospheric oxygen, but by the sulfuric acid, as follows:

$$2FeSO_4 + 2H_2SO_4 = Fe_2(SO_4)_3 + 2H_2O .$$

It is easy to check this by performing the experiment in a test tube fitted with a gas outlet tube and determining the SO_2 evolved, the latter being readily detected by passing it through a $KMnO_4$ solution: the higher the heating of the test tube, the more SO_2 is evolved, which agrees perfectly with our quantitative findings on the increase in the oxidizability of ferrous sulfate with rising temperature. In this respect, our conclusions rest upon an adequate experimental foundation.

We were unable to follow the advice of the authors mentioned: to prevent the oxidation of the ferrous sulfate as they had done, for reasons that require no explanation. Moreover, this was not the question that interested us in our research project.

The second conclusion in our paper [1] on ferrous and ferric sulfate is inaccurate. Instead of stating the conclusion that followed directly from the experimental data: "The smoothness of the solubility curves indicates the absence of sharp transformations in the systems investigated," our formulation was erroneous: "The smoothness of the solubility curves indicates the absence of new compounds in the systems investigated."

The inaccuracy of the conclusion's formulation gave Belopolsky and Shpunt a legitimate occasion for their far-reaching critical comment, in which they state that "The authors have concluded that at a sulfuric acid concentration of approx-

imately 91% the saturated solid phase is copperas, i.e., $FeSO_4 \cdot 7H_2O$, in the 100-243°C range."

Belopolsky and Shpunt must, no doubt, have read not merely the summary of our paper but the article as a whole, from which it clearly follows that Zakharchenko and Tsitsorin make no such assertion, but emphasize the contrary. In discussing the experimental data, we write: "The nearly smooth course of the $FeSO_4 \cdot 7H_2O$ solubility curves indicates that there are no sharp transformations of compounds. As the temperature is raised, the salt is evidently gradually dehydrated. No hydrates containing smaller percentage of water and more or less stable under the specified conditions were found." As for the ferric sulfate, we write: "The smoothness of the curve excludes any possibility of the formation of any stable compounds of ferric sulfate with the solvent." Our conclusion does not contradict the conclusion reached by Bolopsky and Shpunt in their paper [2]: "The 90° isotherm, plotted up to a 91.93% concentration of sulfuric acid, also consists of $FeSO_4 \cdot H_2O$ and $FeSO_4$ branches"; on the contrary; it corroborates their conclusion.

To be sure, the shape of the temperature curve of solubility cannot always serve as a rigorous criterion of the transformation of compounds; if the sclubilities of different compounds are very close together and moreover not high, the solubility curve will not exhibit the transformation points distinctly.

In this respect, our conclusion is an approximate one.

The main objective of our research was determining the percentage of iron that is dissolved by concentrated H_2SO_4 from ferrous and ferric sulfates at high temperatures, irrespective of how the valency of the iron changes.

In this respect our paper' conclusions are valuable for workers in industry.

LITERATURE CITED

[1] G. A. Zakharchenko and V. A. Tsitsorin, J.Appl.Chem.22, 7, 703 (1949).

[2] A. P. Belopolsky and S. Ya. Shpunt, J.Appl.Chem.23, 2, 220 (1950). [1)]

[3] A. P. Belopolsky and S. Ya. Shpunt, J.Appl.Chem. 14, 6, 716 (1941).

[4] A. P. Belopolsky and V. V. Urusov, J. Appl.Chem. 21, 9, 903 (1948).

Received June 3, 1950.

[1)] See Consultants Bureau English translation, p. 225.

13,000